UNIVERSIDAD NACIONAL AUTÓNOMA DE MÉXICO

POSGRADO EN CIENCIAS DE LA TIERRA

CENTRO DE GEOCIENCIAS UNAM CAMPUS JURIQUILLA

Paleoclimatic and paleoenvironmental history of the Northern Mesoamerican Frontier

TESIS

Para optar por el grado de:

DOCTOR EN CIENCIAS DE LA TIERRA

Presenta

Kurt Heinrich Wogau Chong

Tutor

Dr. Harald Norbert Böhnel, Centro de Geociencias UNAM,Campus Juriquilla

Comité tutorial

Prof. Dr. Helge Wolfgang Arz, Leibniz Institute for Baltic Sea Research Warnemünde

Dra. Sarah Metcalfe, School of Geography, University of Nottingham

Dr. Juan Pablo Bernal Uruchurtu, Centro de Geociencias UNAM,Campus Juriquilla

Dr. Alexander Correa Metrio, Instituto de Geología UNAM

Juriquilla, Querétaro, México. Enero, 2020

Universidad Nacional Autónoma de México
UNAM
Biblioteca Central
Dirección General de Bibliotecas de la UNAM

UNAM – Dirección General de Bibliotecas
Tesis Digitales
Restricciones de uso

DERECHOS RESERVADOS ©
PROHIBIDA SU REPRODUCCIÓN TOTAL O PARCIAL

Todo el material contenido en esta tesis esta protegido por la Ley Federal del Derecho de Autor (LFDA) de los Estados Unidos Mexicanos (México).

El uso de imágenes, fragmentos de videos, y demás material que sea objeto de protección de los derechos de autor, será exclusivamente para fines educativos e informativos y deberá citar la fuente donde la obtuvo mencionando el autor o autores. Cualquier uso distinto como el lucro, reproducción, edición o modificación, será perseguido y sancionado por el respectivo titular de los Derechos de Autor.

Paleoclimatic and paleoenvironmental history of the Northern Mesoamerican Frontier

La Alberca maar lake by Kurt Wogau

Kurt Heinrich Wogau Chong
Junio-2019

UNAM – Dirección General de Bibliotecas
Tesis Digitales
Restricciones de uso

DERECHOS RESERVADOS ©
PROHIBIDA SU REPRODUCCIÓN TOTAL O PARCIAL

Todo el material contenido en esta tesis esta protegido por la Ley Federal del Derecho de Autor (LFDA) de los Estados Unidos Mexicanos (México).

El uso de imágenes, fragmentos de videos, y demás material que sea objeto de protección de los derechos de autor, será exclusivamente para fines educativos e informativos y deberá citar la fuente donde la obtuvo mencionando el autor o autores. Cualquier uso distinto como el lucro, reproducción, edición o modificación, será perseguido y sancionado por el respectivo titular de los Derechos de Autor.

Declaratoria ética

Declaro conocer el Código de Ética de la Universidad Nacional Autónoma de México, plasmado en la Legislación Universitaria. Con base en las definiciones de integridad y honestidad ahí especificadas, aseguro mediante mi firma al calce que el presente trabajo es original y enteramente de mi autoría. Todas las citas de, o referencias a, la obra de otros autores aparece debida y adecuadamente señaladas, así como acreditadas mediante los recursos editoriales convencionales.

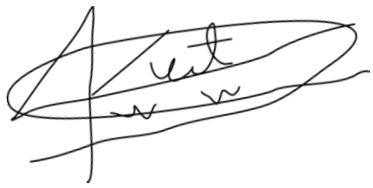

Kurt Heinrich Wogau Chong

Agradecimientos

Quiero agradecer al Dr. Harald Norbert Böhnel, Dr. Norbert Nowaczyk, Dr. Helge W. Arz, Dra. Sarah Metcalfe, Dr. Juan Pablo Bernal Uruchurtu y Dr. Alex Correa por su asesoría, interesantes discusiones científicas, por guiarme en mi trabajo de campo-laboratorio y enriquecer mi conocimiento. Gracias por todo su esfuerzo, dedicación y paciencia.

También quiero agradecer al Dr. Tim Lawton y Dra. Katrin Sieron por guiarme durante todo mi doctorado, por aportar ideas y sugerencias a este trabajo. A la arqueóloga Fiorella Fenoglio por guiarme en el conocimiento sobre la historia de la Frontera Norte de Mesoamérica. Al Dr. Roberto Molina Garza por apoyarme desde el primer día que llegué al CGEO, por las interesantes discusiones científicas y amistad.

A todo el personal académico, técnico y amigos del Centro de Geociencias UNAM, Campus Jurquilla, del Deutsches GeoForschungsZentrum GFZ, sección 5.2 y Leibniz-Institut für Ostseeforschung Warnemünde que directa o indirectamente contribuyeron a esta investigación, desde el arduo trabajo de campo o trabajo de laboratorio.

Al proyecto PAPIIT “Sedimentos de lago como registros paleoambientales” código 1N1101117, por financiar esta investigación.

A todos mis amigos que compartieron conmigo una o varias cervezas, una cena, una plática o un té durante todo este gran viaje. A mi familia, que siempre ha creído en mi y me ha brindado su apoyo incondicional. Por último, a la persona especial que llegó a mi vida y empezó a escribir una nueva historia a mi lado.

A todos ustedes, gracias.

Dedicatoria

Esta tesis esta dedicada a todos los investigadores pioneros, que han contribuido al estudio de paleoclimas, paleoambientes y su relación con las culturas prehispánicas, en la Frontera Norte de Mesoamérica.

Abstract

The relationship between climatic-environmental changes and the cultural implications in the Northern Mesoamerican Frontier is poorly understood, because of the lack of high-resolution well-dated paleoclimatic-paleoenvironmental records. In this work I present high-resolution paleoclimate and paleoenvironmental reconstructions of the Northern Mesoamerican Frontier for the last 6700 yr BP, using laminated sediments from La Alberca maar lake, Guanajuato. Besides, I study the possible correlation between dramatic climatic-environmental changes and social oscillations associated with the Northern Mesoamerican Frontier. For these objectives, I used different techniques such as X-ray fluorescence, microfacies analysis, magnetic parameters, bulk sedimentary $\delta^{18}O$, $\delta^{13}C$ records and radiocarbon dating. The results of these techniques are compared with archeological evidence of Northern Mesoamerican Frontier. My results document relevant climatic and environmental changes. At around 5600 yr BP, the Early Holocene peak insolation period and a subsequent decline of monsoon strength are described. Variable hydrological conditions start to dominate around ~4400 yr BP consistent with the rise of latitudinal variations of the Intertropical Convergence Zone. This hydrological variability is linked with the late establishment of agricultural activities, low social developments during the early Pre-Classic. A rise in sedimentation rate and increase of *Amaranthaceae* pollen percent occurred between ~ 225 BCE- 600 CE and is related with the beginning of agricultural activities by the Chupicuaro pre-Hispanic culture. Microfacies analysis allows the identification of two periods of increase of soil degradation by ancient agriculture practices, around 137 BCE- 37 CE and 155-220 CE. During the Epiclassic period, two drought events around ~700-790 CE and ~810-880 are interpreted, supporting the Armillas' theory that drastic climate events motivated the social changes and shift in the geographic position of Northern Mesoamerican Frontier. In the final part of the Postclassic period a pluvial interval is associated with the rise of Tarascan culture in the area. I propose that droughts and pluvial periods between 1500-600 yr CE are connected with SSTs variability of Tropical Atlantic Basin.

Keywords:
Paleoclimate, Laminated maar lake sediments, Northern Mesoamerican Frontier, Drought, Epiclassic.

Resumen

La relación entre cambios climáticos-ambientales y sus implicaciones culturales en la frontera norte de Mesoamérica es poco comprendida, debido a la ausencia de registros paleoclimáticos y paleoambientales de alta resolución. En este trabajo, presentamos un registro paleoclimático-paleoambiental de alta resolución de la frontera norte de Mesoamérica, para los últimos 6700 años AP utilizando sedimentos lacustres laminados del cráter maar La Alberca. También estudiamos la posible relación entre cambios climáticos-ambientales y las oscilaciones sociales de la frontera norte Mesoamericana. Para estos objetivos, se emplearon diversas técnicas como fluorescencia de rayos X, análisis de microfacies, magnetismo ambiental, isotopos de $\delta^{18}O$, $\delta^{13}C$ y un modelo de edades con doce fechamientos carbono catorce. Nuestros resultados fueron comparados con evidencia arqueológica de la frontera norte de Mesoamérica. El registro lacustre muestra cambios climáticos y ambientales relevantes. Alrededor de los 5600 años AP, nuestro record muestra la finalización del Máximo Termal del Holoceno y el debilitamiento del monzón mesoamericano. Condiciones climáticas variables son interpretadas a partir de los 4400 años AP, debido a las oscilaciones latitudinales de la Zona Intertropical de Convergencia. A esta variabilidad climática se le atribuye la expansión tardía de la agricultura, el bajo desarrollo social durante el inicio del periodo Pre-Clásico. Entre el periodo de 225 a.C.- 600 d.C. el incremento en la tasa de erosión y contenido de polen de *Amaranthaceae* se asocia con el comienzo de actividades agrícolas por la cultura Chupicuaro. Los resultados del análisis de microfacies muestran dos periodos de degradación del suelo por actividades agrícolas entre 137 a.C.- 37 d.C. y 155-220 d.C. En el periodo Epiclásico se interpretan dos periodos de sequía entre el 700-790 d.C. y 810-880 d.C. Estos datos apoyan la teoría de Armillas, que relaciona los cambios geográficos y sociales de la frontera norte de Mesoamérica con sequías extremas. En la parte final del Postclásico se interpreta un periodo pluvial que es relacionado con el establecimiento de la cultura Tarasca en la región. Se propone a la variabilidad de la SSTs del Atlántico Tropical como el principal factor oceánico que generó las oscilaciones climáticas en la región de la frontera norte de Mesoamérica.

Table of contens

Chapter I **1**

Introduction 1

1-General introduction 2

Chapter 2 ..... **7**

Study region 7

2.1-Local and geological settings 8

2.2-La Alberca limnology 13

2.3-Present climatic factors in the study area 14

2.4-High resolution paleoclimatic studies in the Central and Northern Mesoamerican region 18

2.5-Archeology of the Northern Mesoamerican Frontier 22

2.6-The possible effect of 4.2 ka event in the paleoclimate conditions and Mesoamerican societies. 29

Chapter 3 ..... **31**

Methodology 31

3.1-Introduction 32

3.2-Fieldwork, sampling and lithostratigraphic descriptions 32

3.3-Laboratory methods 33

3.3.1-Radiocarbon dating 33

3.3.2-XRF 34

3.3.3-XRD 34

3.3.4-Pollen identification 34

3.3.5-Rock magnetism measurements 34

3.3.6-SEM observations 35

3.3.7-Organic carbon content 36

3.3.8-Microfacies analysis 36

3.4-Statistics 36

Chapter 4 ..... **38**

Results 38

4.1-Results 39

4.2-Lithostratigraphic 40

4.3- Sediment chemistry 42

4.4-Organic C 43

4.5-Stable isotopes $\delta^{18}O$ and $\delta^{13}C$ 44

4.6-Pollen 44
4.7-Microfacies results 46
4.7.1- Sediment profile 46
4.7.2- Sedimentary textures of laminations 47
4.7.3- Laminate characteristics 47
4.7.4- XRF element scanning 49
4.7.5- Magnetic susceptibility 49
4.8-Magnetic mineralogy 52
4.8.1- Concentration dependent magnetic parameters 52
4.8.2-Grain size dependent magnetic particles ratios 52
4.8.3-Type of magnetic minerals 53
4.8.4-Hysteresis curves 53
4.8.5-FORC Diagrams 53
4.8.6-Thermomagnetic curves 55
4.8.7-IRM coercivity spectrum analysis 55
4.9-SEM description 58
4.10-Magnetic properties of catchment area samples 62
4.11-^{14}C ages 64
Chapter 5 67
***Discussion* 67**
5.1-High resolution paleoclimate and paleoenvironmental reconstruction in the Northern Mesoamerican Frontier for Prehistory to Historical times 67
5.1.1-Introduction 68
5.1.2-Paleoclimate and paleoenvironmental reconstruction for the Prehistory period. 69
Stage VI (~ 6700-5600 yr BP) 69
Stage V (~ 5600-4400 yr BP) 70
Stage IV (~ 4400-2200 yr BP) 71
5.1.3-Paleoclimate and paleoenvironmental reconstruction in Historical times 73
Stage III (~ 250 BCE-225 CE) 73
Stage II (~ 225 CE- 1500 CE) 74
Stage I (~ 1500 CE- 2000 CE) 76
5.1.4-Climate forcing of La Alberca paleolimnological changes 78
5.1.5-Summary and conclusions 82
5.2-Paleoclimate and paleoenvironmental magnetism study during the Mid-Holocene and its cultural implications in Mesoamerica. 83
5.2.1-Sources and genesis of magnetic minerals and its relationship with the NAM oscillations during the Mid-Holocene. 84
5.2.2-Anthropogenic imprint in the magnetic fraction and social implications of the hydrological variability during the Mid-Holocene in Mesoamerica. 89
5.2.3-Concluding Remarks 90

5.3-Paleoenvironmental and paleoclimatic study of the Late Preclassic period in the Northern Mesoamerican frontier 91

5.3.1-Varve formation 92

Type 1(DOL-AL) 92

Type 2 (DOL-OL-AL) 93

5.3.2-Human and paleoclimate imprint in La Alberca sedimentary sequence during the Late Pre-Classical period 97

5.3.3-The record of human dynamics in Northern Mesoamerican Frontier and its relationship with climatic oscillations 99

5.3.4-Concluding remarks 102

Chapter 6 103

General conclusions 104

Outlook 107

References 109

Appendix 128

Figure List

Figure 2.1- A) Location of La Alberca maar lake and paleoclimatic records discussed in this thesis. (1) La Alberca, Parangueo, San Nicolas maar lakes, Zirahuen and Yuriria (Park et al., 2010; Lozano-García et al., 2013 and Holmes et al., 2016); (2) Juanacatlan (Davies et al., 2018); (3) Aljojuca maar lake (Bhattacharya et al., 2015); (4) Juxtlahuaca speleothem (Lachniet et al., 2017); (5) Cueva del Diablo speleothem (Bernal et al., 2011); (6) Cariaco Basin (Haug et al., 2001; Wurtzel et al.,2013); (7) El Junco lake (Conroy et al., 2008); **B)** Geographical location of the Northern Mesoamerican Frontier, study area, and archeological sites referred to in this thesis;(A) La Quemada, (B) El Coporo, (C) Cañada de la Virgen, (D) Peralta, (E) Cerro Barajas, (F) El Opeño, (G) Tarascan empire, (H) El Cerrito, (I) El Colorado, (J) El Rosario, (K) La Trinidad, (L) Santa Rosa Xalay, (M) Tula, (N) Teotihuacan, (O) Tenochtitlan, (P) Cuicuilco, (Q) Teotenango, (R) Xochicalco, (S) Cantona. **C)** Location of La Alberca maar lake in the Valle de Santiago and drilled cores.

Fig 2.2- Photogeological map of Valle the Santiago Region (Modified from Aranda-Gómez et al., 2013)

Fig 2.3- Schematic NE-SW cross section thru La Alberca maar (modified from Rincon, 2005)

Figure 2.4- (A) Mean monthly temperature and (B) daily rainfall average on Valle de Santiago, Guanajuato, between 1922 to 2016 (Modified from Servicio Meteorologico Nacional)

Figure 2.5- A) Total precipitation levels in the Mesoamerican region between 1979-2016 during August-April B) Sea levels pressure levels in the Mesoamerican region between 1979-2016 during August-April C) Sea surface temperature levels in the Mesoamerican region between 1979-2016 during August-April (Images from EarthNow Team. National Oceanic and Atmospheric Administration https://sphere.ssec.wisc.edu/).

Figure 2.6-High resolution paleoclimatic records of Cueva del Diablo, Juanacatlan, Aljojuca and Juxtlahuca. The orange shadow areas represent relevant climatic dry events and blue bars wetter periods during the Holocene.

Figure 2.7- A) Geographic distribution of Mesoamerica regions. (A) Occident;(B) Northern Mesoamerican Frontier (NMF), (C) Basin of Mesoamerica, (D) Gulf, (E) Guerrero, (F)Oaxaca, (G) South Coast (H)Maya. Principal sectors of Northern Mesoamerican Frontier. (B.1) Occident, (B.2) Center and (B.3) Oriental (Zamora, 2017). **B)** Map of distribution of principal archeological sites of Northern Mesoamerican Frontier. ;(A) La Quemada, (B) El Coporo, (C) Cañada de la Virgen, (D) Peralta, (E) Cerro Barajas, (F) El Opeño, (G) Tarascan empire, (H) El Cerrito, (I) El Colorado, (J) El Rosario, (K) La Trinidad, (L) Santa Rosa Xalay, (M) Tula, (N) Teotihuacan, (O) Tenochtitlan, (P) Cuicuilco, (Q) Teotenango, (R) Xochicalco, (S) Cantona.The shadow light-dark green areas represent oscillations of Northern Mesoamerican Frontier. The study zone is represented by yellow circle.

Figure 2.8- From left to the right, graphic representation of occupation periods to diverse Mesoamerican cultures in the Northern Mesoamerican Frontier, periods of influence of principal Mesoamerican cultures in the region and principal oscillations of the frontier (Gorenstein, 1985; Braniff, 1998; Florance, 2000).

Figure 2.9- A) Chupicuaro figurines of maternity cult; B) Typical polychromatic ceramics of Chupicuaro tradition; C) Schematic representation of shaft tombs of Capacha and El Opeño traditions (Modified image from Willians, 1979).

Figure 3.1- Location of drilling sites of cores Alberca Rojo and Alberca Azul.

Figure 4.1- A) Correlation between Alberca Azul (master core) and Alberca Rojo cores using high resolution magnetic susceptibility curves and stratigraphic characteristics. B) Correlation between Alberca Azul (master core) and Hoya Alberca core, using high resolution magnetic susceptibility curves, Ca/Ti ratio from

Alberca Azul and $\delta^{18}O$ from Hoya Alberca. The correlation was performed using independent ages model for both cores

Figure 4.2-A) Stratigraphic column from AZ core, symbology and high-resolution images of the five lithostratigraphic units. The light green shadow area, displays the interval where thin sections were produced; B) Thin section photos of laminated sediments; C) Microscopic photo showing the two different type of laminations; D) From top to bottom: microscopic images of detrital lamination, displaying different characteristics like rounded carbonate crystals highlighted in a yellow shadow and organic matter. SEM image of aragonite crystals. E) Symbology of sedimentary facies. Massive organic strata (Facies A), laminated section (Facies B), massive strata (Facies C), turbidites (Facies D) and tephras (Facies E).

Figure 4.3- Alberca Azul Stratigraphic column and downcore, magnetic properties and X-ray fluorescence. From Hoya Alberca core, isotopes and pollen data. Magnetic susceptibility (*k)*, S-ratio, Fe and Ti are parameters sensitive to detrital input, Sr and Ca/Ti indicate the concentrations of carbonates. The Mn/Fe displays the redox conditions of the lake. Hoya Alberca record of $\delta^{18}O$ and $\delta^{13}C$ are representative of E/P ratios, and *Amaranthaceae*, *Zea mays* pollen are indicators of anthropogenic landscape disturbance. Using the variability on detrital, magnetics parameters and facies distribution, the master core is dived in six main stages. Turbidites facies are indicated by red numbers.

Figure 4.4-A) High resolution X-ray fluorescence data of Ti and Ca/Ti between 146-226 cm. B) PCA reveals three groups of elements: Ca, Sr, sensitive to carbonate presence Zr, Ti, Fe, Ba, Si, Al; indicative of detrital fraction; Mn, sensitive to redox conditions C) Broken stick of PCA.

Figure 4.5-Stratigraphic column of La Alberca lake between 170 to 230 cm. Thickness of detrital-organic, aragonite, organic, turbidite and massive layers. Measured thickness of Type 1 and Type 2 varves and its pre magnetic susceptibility, XRF data such as PCA1, Ca/Ti and Mn/Fe ratios.

Figure 4.6- (A, B) Thin section photos, SEM images and layer arrangement of varve type 1 and varve type 2. (A.1) From left to right: SEM images of aragonite crystals, organic mud and detrital lithic. (B.1) From left to right: SEM picture of diatom bloom and the principal diatom species (*Cymbella murelli and Nitzschia palea*).

Figure 4.7-A) Thin section photos of massive layers with parallel and crossed Nichols. These layers comprise a mix of detrital, calcium carbonate and organic components. B) Thin section photos of turbidites layers with parallel and crossed nichols. These layers display normal gradation, erosive contacts and high content of organic material.

Figure 4.8- Down core variations of magnetic properties and stratigraphic column of “La Alberca” maar lake. Red numbers on the stratigraphic column represent turbidites. Magnetic parameters with blue lines(k, SIRM, and ARM) are sensitive to the concentration of ferromagnetic fraction, parameters with purple lines (kARM ,ARM/SIRM and kARM/klf) are sensitive to grain size of ferrimagnetic minerals and parameters with red lines (MDF, ARM and S-ratio) are sensitive to the presence of ferrimagnetic minerals. Solid black lines indicate the division of the six main stages.

Figure 4.9- FORC diagrams and hysteresis loops for representative samples of the “La Alberca” lacustrine sequence, soil located around the lake, crater walls and pre-maar lava. Dark blue solid line represents the hysteresis loop curve after the subtraction of dia-and paramagnetic contribution.

Figure 4.10- Normalized temperature-dependent magnetic susceptibility and spectral analysis of isothermal remanent magnetization acquisition curves of selected samples. Red arrows on normalized temperature-dependent curves indicate heating process and blue arrows indicate the cooling process. Black dots on coercivity spectrum represents the coercivity distribution, blue and purple lines, indicates the number of magnetic components and shaded area represents error envelopes of 95% confidence interval. Coercivity (Bh) and dispersion parameter of every (DP) component is also displayed.

Figure 4.11- Representative SEM images of stages VI, IV and III. High concentration with diverse grain size and shapes of (titano-) magnetites (A), close view of (titano-) magnetites with octahedral shapes (B) (C), (titano-) magnetites with shrinkage-cracks indicative of mahemitazation process and small crystals of (titano-) magnetites inside of a volcanic glass shard (E). Blue circles indicate locations of X-ray spot element analysis.

Figure 4.12- Ilmenite crystal (A), framboidal pyrite (B) and rare (titano-) magnetites bubbles observed on background stages (V,II,I).Comparison between typical magnetic crystals found it in background stages (V,II,I) and peaks stages (VI,IV,III) (D, E). Background zones are dominated by the presence of ilmenite crystals or (titano-) magnetites affected by dissolution and peak stages (VI, IV, III) by mostly well-preserved (titano-) magnetites with octahedral shapes. Blue circles indicate X-ray spot element analysis.

Figure 4.13- Some other typical crystals found it on background stages (V, II, I). Irregular shaped borders (A) and etching features (B) indicate the dissolution process (B) of (titano-)magnetites crystals. Iron carbonates like siderite (C) and cubic pyrite (D) are also common.

Figure 4.14- Magnetic crystals of crater wall (CWA) and soil samples (SA). Well preserved (titano-) magnetite crystal in soil sample and high concentration of (titano-) magnetite crystals with diverse shapes and sizes (B). Intergrows of hematite on (titano-) magnetite surfaces (C, D) observed on crater wall samples. Octahedral (titano-) magnetite crystal (E).

Figure 4.15-Age-depth model of “La Alberca” maar lake. Light blue and purple shading represent the accumulated error of the data; black marks represent the included data in the model; data with the red mark are excluded from the model.

Figure 5.1- Comparison between selected magnetics (k, S-ratio), chemistry (PCA1, Ca/Ti, Mn/Fe), oxygen isotopes and pollen records from “La Alberca” with local and regional records. A) Paleoclimate and paleoenvironmental Interpretation of local records of San Nicolas and Parangueo, based on pollen counts and geochemistry of the sediments. Blue columns are interpreted as wet periods, brown columns as represents dry periods, and the purple columns indicates anthropogenic disruptions (Park et al., 2010); B) $\delta^{18}O$ record of speleothem “Cueva del Diablo” located in the western part of Mesoamerica, influenced by moisture form North Atlantic basin until 4300 yr BP (Bernal et al., 2011); C) Ti record from Juanacatlan Basin sensitive to NAM variations (Metcalfe et al., 2010); D) Ti record of “Cariaco Basin”. This record is influenced by the position of ITCZ (Haug et al., 2001). E) Percent of sand of “El Junco” sensitive record of ENSO frequency (Conroy et al.,2008); F) June summer insulation curve for 30ºN (Berger and Loutre, 1991).

Figure 5.2- Comparison between La Alberca maar lake record, local-regional paleoclimatic records and archeological data. A) Mesoamerican monsoon rainfall reconstruction over the last 500 BCE obtained from Juxtlahuaca record (Lachniet et al., 2017); B) Ti record of “Cariaco Basin” sensitive to ITCZ variability (Haug et al., 2001); C) SST reconstruction of tropical Atlantic (Wurtzel et al., 2013); D) North Atlantic oscillation index (Trouet et al., 2009); E) Percent of sand of “El Junco” sensitive record of ENSO frequency (Conroy et al.,2008). At the bottom of the image, principal historical events from Central Mesoamerica and Northern Mesoamerican Frontier (Sanders et al., 1979; Darras and Faugère, 2007)**.** Blue bars represent pluvial period, orange bars mark drought interval and purple bar displays anthropogenic activity. Remarkable correlation between the study record and Juxtlahuaca paleo rainfall reconstruction is observed between 400 to 1500 CE.

Figure 5.3- Wavelets analysis and its respective detrended Ti values of stages VI, V, IV and II.

Figure 5.4- Periodogram analysis of stages VI, V, IV, and II. The solid purple lines indicate significative periods with more of 99% confidential limit.

Figure 5.5- Comparison between selected magnetics (SIRM, kARM, S-ratio), chemistry (PCA 1, Ca/Ti, Mn/Fe), % C , pollen and δ18O parameters with regional and global paleoclimate records. Black arrows on magnetics parameters indicate the increase in oxic conditions. Ti record from Juanacatlan Basin sensitive to NAM variations (Metcalfe et al., 2010). Ti record of Cariaco Basin. This record is influenced by the position of ITCZ (Haug et al., 2001). Percent of sand of El Junco record sensitive of ENSO frequency (Conroy et al.,2008). δ18O record on G. ruber on Red Sea is sensitive to increase or reduction of monsoon strength (Arz et al., 2006). Mawmluh δ18O speleothem record provides information about the tropical monsoon strength (Berkelhammer et al.,2015). Dust history from Kilimanjaro ice core sensitive to dry conditions (Thompson et al., 2002). Grey and blue bars represent the principal archeological subdivision of the Mesoamerica history.

Fig 5.6- A) Detail core section of stage IV. Chemistry parameters and ratios sensitive to detrital input (Ti) carbonate precipitation (Ca/Ti) and redox conditions (Fe/Mn). Their respective interpretation is indicated at the top. The blue shading areas represent wet events with its respective thickness B) Wavelet analysis of stage IV displaying significative periods of 256, 32 and 20 years C) Redfit analysis of stage IV revealing significative periods of 10, 7,6,5,3 and 3 years.

Figure 5.7- Thin section photos with crossed and parallel nichols, layer distribution and interpretation of varve Type 1 and Type 2. Daily rainfall average and monthly temperature from Valle the Santiago region between 1922 to 2016.

Figure 5.8-A) ^{14}C age model of la Alberca lake B) Chronology of study section anchored by two calibrate ^{14}C ages and one interpolated age. The solid purple line represents varve counts and the black solid line displays varve count after calculation of estimated age of massive layers, inferring sedimentation rates from neighboring varve.

Figure 5.9- A) Comparison between stratigraphic section and Ti, $\delta^{18}O$ and *Amaranthaceae* records of La Alberca lake. B) Detailed varve analysis of stage III for the late Pre-Classic period. I compare varve results, with XRF results, sedimentation rates, pollen samples and archeological evidence (Darras and Faugere 2007). Orange bars represents interpreted as drought periods and purple bars represent periods with intensification in anthropogenic land use

List of tables

Table 5.1- AMS ^{14}C data acquired from terrestrial plant, fragments of wood and organic sediment, calibrated with Clam software (Blaauw, 2010) using the IntCall 13.14 calibration curve (Remier et al. 2013). AMS ^{14}C analyses were carried out by Beta Analytics.

Table 5.2- Mean thickness and of detrital organic layers, aragonite layers and varves. Percent of distribution of varve Type 1, varve Type 2 and massive layers

Chapter I

Introduction

Cañada de la Virgen,Guanajuato,México. Image taken from National Institute of Culture, Guanajuato, Mexico.

1-General introduction

The first ideas about the Northern Mesoamerican Frontier (NMF) described a striking cultural contrast between pre-Hispanic cultures from central Mesoamerica and Northern Mesoamerican regions. In other words, the NMF separated the sedentary civilized farmers in Central Mesoamerica from the bands of roaming hunter-gatherers in the north. Armillas (1969) called this hypothesis as a “Hard Frontier model.” A number of scholars tried to emphasize the cultural disparity between both Mesoamerican regions. In the Florentine Codex, the northern Mesoamerican region is described as follows: “It is a place of misery, pain, suffering, fatigue, poverty and torment. It is a place of dry rocks, of failure; a place of lamentations; a place of death from thirst; a place of starvation. It is a place of much hunger, of much death. It is to the north” (Bernardino et al.,2012).

Recent archeological studies, however, describe the NMF as a much more complex and interesting Mesoamerican regions than was thought previously (Dueñas, 2017). The pluricultural character, inhabited by hunter-gatherers and stratified societies describe this region (Saint-Charles et al., 2010). Additionally, the NMF is also now described as a flexible frontier with diverse episodes of geographic and social fluctuations. The principal NMF oscillation took place between 600-900 CE. During this period a continuous northward expansion of pre-Hispanic cities and evolution into more complex stratified societies occurred. After 900 CE, many towns were abandoned, and diverse societies returned to the hunter-gathering lifestyle. Armillas (1964,1969) argued that the geographical and social shift in the NMF was ruled by dramatic climatic changes, such as prolonged drought periods. However, many scholars disagree with this hypothesis.

Sauer (1941) argued: “The position of the frontier was determined by cultural, not environmental reasons, and it is to be regarded as the meeting of two different ways of aboriginal life”. Other authors (Brown, 1984; Elliot et al., 2010; 2012) argue that the principal mechanism that triggered the NMF oscillations was environmental degradation by the intensification in agricultural practices, deforestation and exhaustion of mines.

On the other hand, recent paleoclimatic research correlates dramatic climatic oscillations with the collapse of pre-Hispanic societies especially in the Maya area (Hodell et al., 2005) and Central Mesoamerica (O'Hara et al., 1994; Hodell et al., 2005; Stahle et al., 2011; Bhattacharya et al., 2015; Lachniet et al., 2012,2017; Park et al.,2019). This pattern has been also linked with the rise and fall of ancient societies around the world (deMenocal, 2001). Arid conditions during the 4.2 ka climatic event are related in Mesopotamia with the fall of the Akkadian Empire and in Egypt with the collapse of the Old Kingdom after a series of lower Nile floods (Weiss et al.,1993; Stanley et al., 2003).

The Holocene spans from 11.7 ka until the present day (Rasmussen, et al., 2014). In general, this period marks the end of the last glacial, the begin of warm global conditions and the start of human societies. Diverse climatic anomalies, such as cold episodes at 9.5 and 8.2 ka, the stablish of warm climatic phase in the monsoon regions during the Holocene Thermal Maximum(HTM) (11-5 ka), the 4.2 ka dry event, the Medieval Warm Period and the Little Ice Age describe a complex climatic period. These climatic anomalies respond to the diverse atmospheric and oceanic mechanisms. In the Mesoamerica region, the North American Monsoon system (NAM), is an essential precipitation source and plays an important role in the modulation of climatic patterns during the Holocene. This system is considered to be one of primary monsoons on earth (Lachniet et al., 2017) and produces up to 60 % of annual precipitation in the Mesoamerican area (Jones et al., 2015; Metcalfe et al., 2015; Weiss, 2016).

The paleoprecipitations conditions during the start of the Holocene in Mesoamerica seems to be strongly influenced by the insolation forcing and sporadic pulses of meltwaters from the remains of Laurentide ice Sheet (Bernal et al., 2011; Metcalfe et al., 2015). After this, diverse decadal or multidecadal forces start to affect the monsoon strength, especially the Pacific Decadal Oscillation (PDO), El Niño Southern Oscillation (ENSO) from the Pacific Basin and Atlantic Multidecadal Oscillation, North Atlantic Oscillation from the Tropical Atlantic Basin. Several other factors can influence the tropical circulation in the Mesoamerican region, such as the position of Intertropical Convergence Zone (ITCZ), easterly flows, low-level jets, tropical cyclones and the displacement of the Bermuda High. Precipitation distribution is also shaped by diverse orographic conditions in the Mesoamerican region, producing areas with major convection and areas with constraining flows.

Diverse paleoclimatic records suggest coherent evidence of a drying event during the final part of the Classical Period, also known as the Epiclassic (Hodell et al., 2005; Bhattacharya et al., 2015). Although the rise of interest in the study of this climatic event, clarification of the atmospheric-ocean mechanism is needed, another interesting dry event during the Holocene is the 4.2 ka event. Little is known about the effects of this dry event in the Mesoamerican area.

To stablish a comprehensive framework of paleoclimate conditions natural high-resolution archives are need it. Recently, high-resolution natural archives such as stalagmites and lake sediments have been used in the Mesoamerican region, combining diverse analytical techniques. These studies are powerful tools for helping to clarify and increase the comprehension of climatic events with centennial, decadal or subdecadal. Nevertheless, the small number of this type of studies still hinders our understanding of how Mesoamerican societies were affected or benefited by these climatic oscillations.

Laminated sediments of maar lakes provide some of the most complete paleoclimate and paleoenvironmental natural archives on the continental regions. This type of lake is sensitive to high-frequency climatic modulation and responds to the change of the environmental and anthropogenic process (Marchetto et al., 2015).

This thesis aims to reconstruct past climate-environmental conditions, and the possible social implications, especially in the Northern Mesoamerican Frontier, using laminated lake sediments as a high-resolution natural archive over the last 6700 yrs. I retrieved two cores from the central part of La Alberca crater maar lake located in Valle de Santiago, Guanajuato, within the Northern Mesoamerican Frontier. A comprehensive understanding climatic-environmental changes and its relationship with cultural development requires the combination of diverse analytic techniques. X-ray fluorescence, environmental magnetism, microsedimentology, ^{14}C radiometric ages, X-ray diffraction, archeological data, among others techniques were used.

As I mentioned above, the primary objective of this research is to investigate paleoclimatic variability during the last 6700 yr BP and the possible connection between paleoclimatic conditions and social evolution or disruptions along the Northern Mesoamerican Frontier. For reaching these objectives three main scientific questions were formalized:

1- What were the climatic and environmental conditions during the last 6700 yrs along the Northern Mesoamerica Frontier, especially in the Epiclassic archaeological period?

2- Did the 4.2 ka BP global dry event alter Mesoamerican paleoclimate? Did this dry event affect the development of Mesoamerican societies?

3-Is there any relation between climatic-environmental changes and cultural oscillations during the Late Pre-Classic period in the NMF?

To answer these scientific questions, the following specific objectives have to be achieved:

1- Retrieve of at least two cores of the central part of Alberca crater maar lake.
2- Study the principal microstratigraphic characteristics of the lake sequence.
3- Produce a age model using radiocarbon ages of ^{14}C ages.
4- X-ray fluorescence measurements for studying the geochemical variability of the sediments have to be performed.
5- Measurement of rock magnetic properties to describe the concentration, grain size of primary and secondary magnetic minerals.

6- Microfacies studies will be carried out in a selected core section, in order to understand the main limnological process of the lake and this is influenced by climatic.
7- Comparsone geochemical, rock magnetic, and microsedimentological variations with other paleoclimatic archives of Mesoamerica to help understand the main climatic forces that shaped climate variability during the last 6700 yrs in the study zone.
8- Comparison of geochemical, rock magnetic, and microsedimentological records with archeological information of Mesoamerica and Northern Mesoamerican Frontier allows to study the possible influence of climatic variability with Mesoamerican societies evolution.

The thesis is divided into five chapters and the discussion chapter (5) is subdivided into three main topics, which represent distinct papers, which are either published or in preparation.

Chapter 1 resumes the scientific background, compiles the general objectives, specific objectives and the scientific questions to solve.

Chapter 2 is dedicated to reviews diverse general aspects of the study area like its demographic history, information about land escape modification by agricultural activities, principal vegetation type, geomorphological and geological characteristics of Valle de Santiago, Guanajuato. A general limnological description is presented, the description of the actual climate regimes in the NMF, and a brief review of previous paleoclimate studies. The last part of the chapter illustrates the main archeology data of the study and the surrounding areas.

Chapter 3 gives an overview of the principal methodologies employed in this work.

Chapter 4 summarizes the sedimentary characteristics of the records, principal geochemical patterns observed with XRF and XRD techniques, describes the principal magnetic fraction of the record, isotopic analysis, pollen analysis, varve counting results and the age model construction.

The chapter 5.1 discuss the high-resolution paleoclimate and paleoclimate reconstruction int the NMF region. This objective was achieved using diverse techniques such as: X-ray fluorescence, microfacies analysis, magnetic parameters, bulk sedimentary $\delta^{18}O$, $\delta^{13}C$ records and twelve AMS 14C ages. The discussion is divided into two main sections: Prehistory times and Historical times. During Prehistory times, relevant climatic features being like the end of Early-Holocene peak insolation period (EHPIP), the decrease of summer monsoon precipitation around 5.5 cal yr BP was interpreted. In historical times (2500 cal yr BP-present). I analyzed the transformation of the by human activities during

the Classical period by the Chupicuaro culture, the occurrence of punctual dry events during the Epiclassic and its relationship with social disruptions in the MNF.

The chapter 5.2 particularly concentrates on the time window around the 4.2 ka event and test the existence of this climactic event in Mesoamerican and its social implications. The variations in the preservation of the magnetic fraction of the record document a gradual rise of oxic conditions in the lake, possibly motivated by the enhanced mixing states between 4400-2200 cal yr BP. This change in the paleolimnological conditions of the lake correlates with the start of the strong variability of ITCZ and the rise of ENSO activity during the Mid-Holocene.

Chapter 5.3 present the results of the microfacies analysis. This chapter centers the discussion in the study of human landscape modification, due to the ancient agricultural practices and its possible relationship with paleoclimate change during the Late Preclassic in the Valle de Santiago area. Multiple occupation periods are interpreted based on the increase of anthropogenic erosion and the presence of *Nitzschia paleacea* around 137 +/- 171 BCE to 37+/- 168 CE and 155 +/- 172 to 220 +/- 183 CE. This idea describes a social dynamic NMF during the Pre-Classic to Classical period.

Chapter 2

Study region

Valle de Santiago, Guanajuato, by Santiago Arau.

2.1-Local and geological settings

The La Alberca maar is located in the Valle de Santiago volcanic region (VSVR) (Fig. 2.1). It comprises a series of east-west trending valleys covered by alluvial and lacustrine sediments (Aranda-Gómez et al.,2013). The valley depression is filled by vertisolic soils that developed in poorly drained areas after the Late Tertiary and Quaternary volcanism modifying the original drainage system (Butzer and Butzer, 1997). According to Murphy (1986), the volcanic structures in the VSVR are younger than 0.07 Ma. The VSVR is part of the Mexican Volcanic Belt which is related to the subduction of the Cocos/Rivera plate during the last 17 Ma (e.g., Ferrari et al., 2000). The chemical composition varies from calci-alkaline rocks, typical for subduction zones to alkaline magmas (Luhr et al., 2006; Aranda-Gómez, 2014). The VSVR comprises diverse volcanic structures such as cinder cones, maars and calc-alkaline shields, older than 6.8 Ma (Murphy, 1986). The North and East of VSVR are covered by alluvium, which was probably part of a paleolake (Aranda-Gómez et al., 2013) (Fig. 2.2).

The literature describes seven principal maar craters in the study area: La Alberca, Cintora, Rincon de Parangueo, San Nicolas, Solis, Hoya Estrada and Hoya Blanca (Fig. 2.1C). These phreatomagmatic volcanoes define a N 25 W structural trend. La Alberca and Rincon de Parangueo were excavated in lava shields with andesitic composition (Aranda-Gómez et al., 2013) and its lakes were fed by the Salamanca aquifer.

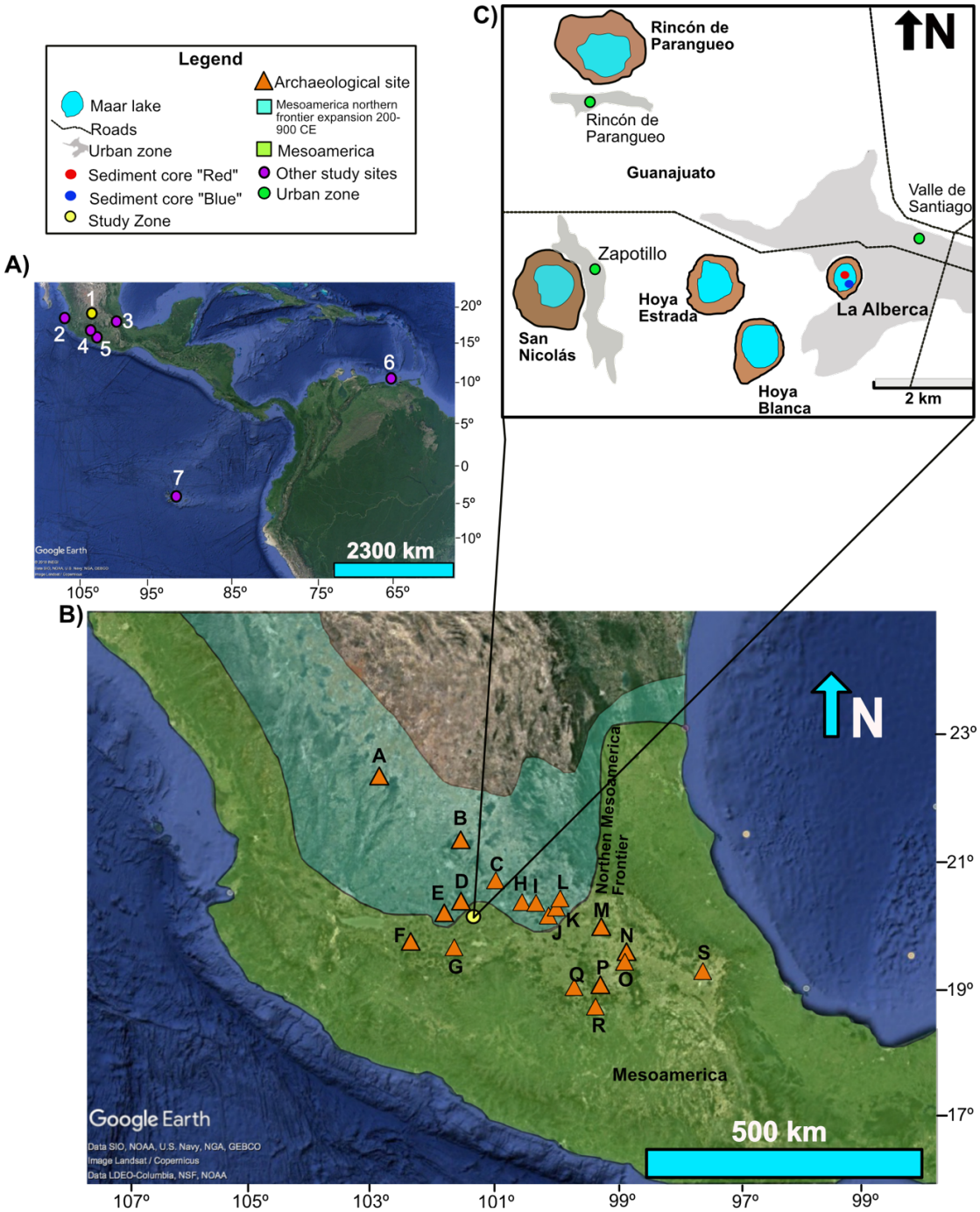

Figure 2.1- A) Location of La Alberca maar lake and paleoclimatic records discussed in this thesis. (1) La Alberca, Parangueo, San Nicolas maar lakes, Zirahuen and Yuriria (Park et al., 2010; Lozano-García et al., 2013 and Holmes et al., 2016); (2) Juanacatlan (Davies et al., 2018); (3) Aljojuca maar lake (Bhattacharya et al., 2015); (4) Juxtlahuaca speleothem (Lachniet et al., 2017); (5) Cueva del Diablo speleothem (Bernal et al., 2011); (6) Cariaco Basin (Haug et al., 2001; Wurtzel et al.,2013); (7) El Junco lake (Conroy et al., 2008); **B)** Geographical location of the Northern Mesoamerican Frontier, study area, and archeological sites referred to in this thesis;(A) La Quemada, (B) El Coporo, (C) Cañada de la Virgen, (D) Peralta, (E) Cerro Barajas, (F) El Opeño, (G) Tarascan empire, (H) El Cerrito, (I) El Colorado, (J) El Rosario, (K) La Trinidad, (L) Santa Rosa Xalay, (M) Tula, (N) Teotihuacan, (O) Tenochtitlan, (P) Cuicuilco, (Q) Teotenango, (R) Xochicalco, (S) Cantona. **C)** Location of La Alberca maar lake in the Valle de Santiago and drilled cores.

La Alberca maar has a quasi-circular shape with a crater diameter of 700 m and a surface area of 0.15 to 0.69 km^2. Four five units compound the stratigraphic column of the Alberca crater. The pre-maar rock is an andesite lava flow that is not related to the phreatomagmatic activity of the maar. Using Ar/Ar method this unit was dated to 0.24 +/- 0.02 Ma (Rincón, 2005) (Fig. 2.3). Colonies of Stromatolites grew attached to this lava flow unit on the NE wall. The next unit is a paleosol which separates the pre-maar unit, with the pyroclastic products of the phreatomagmatic eruptions. This unit represents a lack of volcanic activity. Above the paleosol, a scoria cone was formed, indicating a dry magma eruption. The final unit is a pyroclastic deposit, directly related to phreatomagmatic activity.

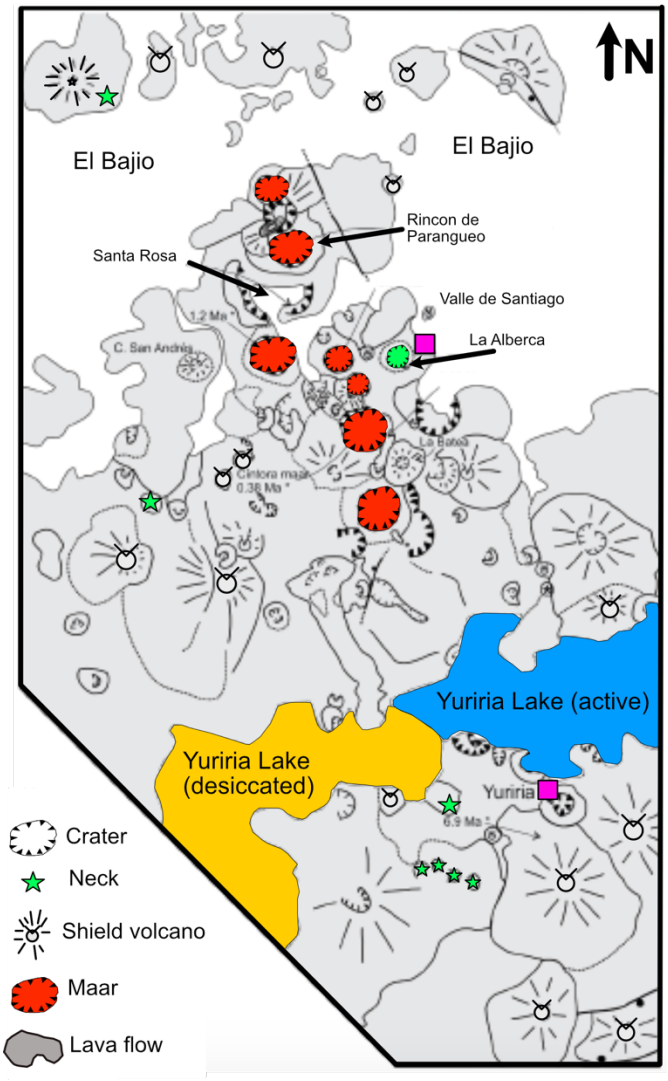

Fig 2.2- Photogeological map of Valle the Santiago Region (Modified from Aranda-Gómez et al., 2013)

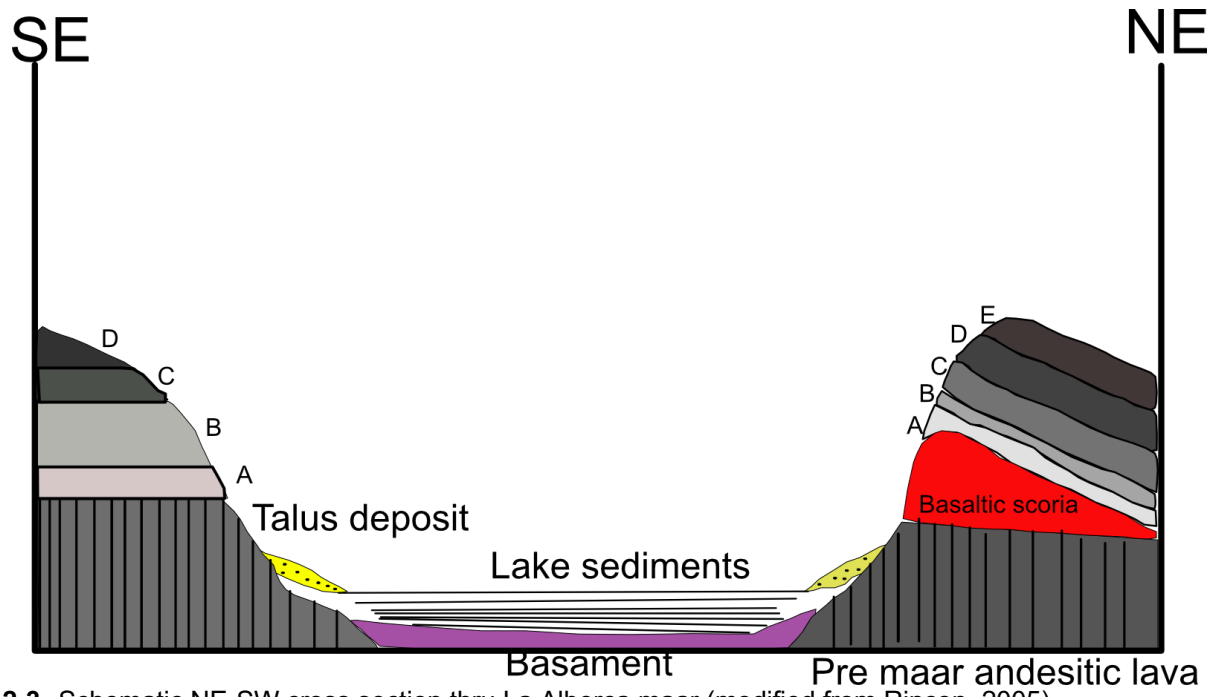

Fig 2.3- Schematic NE-SW cross section thru La Alberca maar (modified from Rincon, 2005)

The present vegetation in the region prior to the development of actual agriculture was *bosque tropical caducifolio* and *matorral subtropical.* The relatively unmodified vegetation of La Alberca is formed by relic *bosque tropica cadufilo* (Conserva, 2003). The volcanic soils and irrigation potential in Valle de Santiago region, generate one of the most productive agricultural areas of Mexico. A wide range of crops can be found in the region including, wheat, broccoli, watermelon and corn. Graze livestock is obtained in piedmonts areas (Conserva, 2003). Actually, the lake is surrounded by the Valle the Santiago city, founded in 1607 by Spanish conquerors.

The present climate conditions in Valle de Santiago are: average annual temperature of 19–20°C, average annual precipitation of 715-737 mm with maximum precipitation of 962–1192 mm between May-October and minimum precipitation of 369–452 mm between November-April (Fig. 2.4). Another important characteristic regarding the climate are: A) The actual climate is marginal for rain-fed agriculture; B) The evaporation exceeds precipitation and the rain quantity may vary from year to year. These conditions may trigger the possibility of drought seasons; C) The region of Valle the Santiago is located in the northern margin of the tropical summer rain belt, named the arid frontier of Mesoamerica (Alcocer et al., 2000; Kienel et al., 2009).

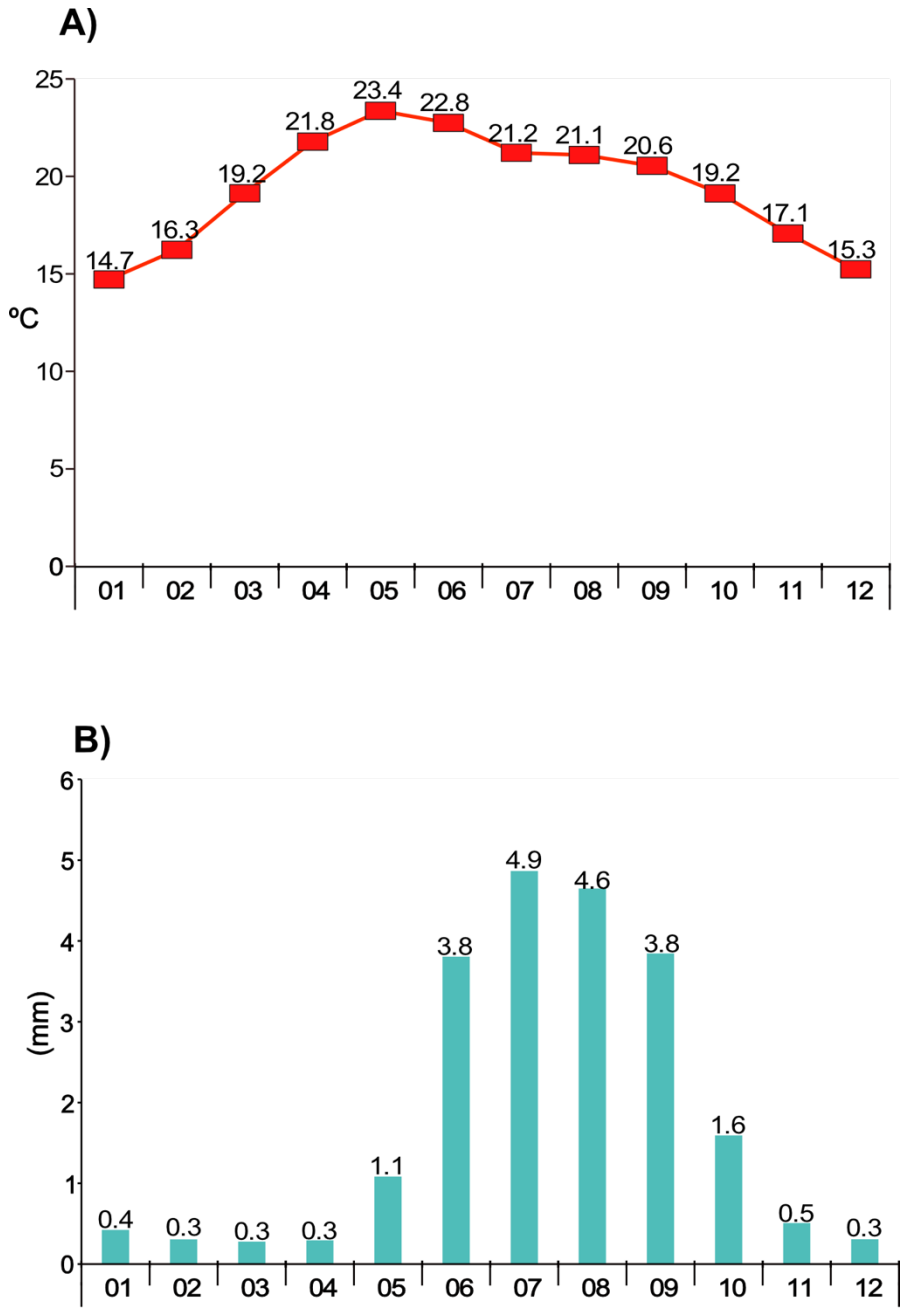

Figure 2.4- (A) Mean monthly temperature and (B) daily rainfall average on Valle de Santiago, Guanajuato, between 1922 to 2016 (Modified from Servicio Meteorologico Nacional).

2.2-La Alberca limnology

The classification of lakes can depend on several factors, such as geological formation process, mixing states, or water chemistry. La Alberca lake is a crater maar, and its genesis is related to phreatomagmatic activity and it was classified as a monomictic based on its mixing state (Alcocer personal communication). In this type of lake, mixing occurs once per year and they are stably stratified during the rest of the year (Lewis, 1983).

La Alberca maar lake was classified as a hyposaline lake with conductivity values up to 2300 μScm^{-1} and the principal salt content is $NaHCO_4$ followed by Na_2CO_3>NaCl>NA_2SO_4 (Alcocer and Hammer, 1998). Reported pH values are between 9.6-9.7. These pH and conductivity values were measured in October 1999 (Armienta et al., 2008). The presence of HCO_3 and SO_4 are derived from CO_2 and H_2S, respectively; Cl is leached from the volcanic rocks and NO_3 proceed from pollutants related from the intensive pasture (Orozco and Mendinaveitia, 1941). The low concentration of Ca^{2+} and Mg^{2+} is due to their precipitation as carbonates.

The low precipitation levels in the study area, around 715-737 mm/per year, and the high evaporation levels, around 1935 mm/per year, show that evaporation-precipitation (E/P) ratio plays an important role in the dilution/concentration of diverse dissolved components in Alberca Maar lake. Alberca lake was classified as hypereutrophic (highly productive) (Armienta et al., 2008).In the past, the perennial lake at the bottom of the crater was fed it by the Salamanca aquifer, but today, the lake is completely dried out, due to the over-pumping of water wells for intensive irrigation and water supplies to the villages (Alcocer et al., 2000).

Kienel et al. (2009) reported that the desiccation of the lake was progressive. In 1996 the water level was still 15 m below the top of the tuff ring, and the maximum water depth was 8 meters, in 2001 less than 1 meter, and in January 2006 the lake was mostly dry with only a shallow pond during the rainy season. In August 2010 the pond had a deep red watercolor, probably produced by a bloom of cyanobacteria (Aranda, 2014). More characteristics about the water chemistry, primary productivity and phytoplankton and zooplankton composition, the benthic macroinvertebrates, and the fish fauna are listed in Appendix 1-6.

2.3-Present climatic factors in the study area

Mohtadi et al. (2016) define the monsoon as a: “Dominant seasonal mode of climate variability in the tropics and are critically important conveyors of atmospheric moisture and energy at a global scale”. The North American Monsoon (NAM) system dominates the actual climate over the Mesoamerican region. Some locations in the Mesoamerican region receive around of 70% of their annual precipitation associated to NAM during July, August and September (e.g. Douglas et al 1993).

The monsoon circulation is associated with distinct tropical circulation systems. The land-ocean contrast results due to the lower surface heat capacity of the continent compared to the ocean, generating the flow of moist air from the ocean to the land during summer. Raising continental air branches release latent heat and rainfall in the continental region (Mohtadi et al., 2016). Surges of easterly waves from the Gulf of Mexico propagating moisture across the Mesoamerican area can play and important role in the monsoon precipitation. Actually, the Gulf of Mexico and Caribbean, the Intra-Americas Sea (IAS) are considered to be the predominant moisture sources for the monsoon precipitation, in the north-central Mesoamerica and into the SW USA (Metcalfe et al., 2015) probably due to small body of water that the Gulf of California represents. Nevertheless, Interrelationships between SSTs of the Gulf of California and rainfalls in the SW USA and north Mesoamerican sectors were found (Mitchell et al. 2002, Barron et al., 2012). In agreement, Higgins et al. (1997) argue that the monsoon has a strong influence in the SW USA sector. These may suggest that advected moisture from the Gulf of California mainly dominates the rainfall regimen in the Northern Mesoamerican sector and its pacific side. Tropical storms can also influence the amount of precipitation in the monsoon season. However, these storms are sporadic and do not affect the whole Mesoamerican region. Thus there is not a strong dominance of these elements, and it is possible that there is no overall dominant mechanism. Cavazos and Turrent (2009) argue that the intensity of a monsoon season is directly related to the precipitation, so more intense monsoons have greater moisture flux convergence than weaker ones.

Oscillation in global atmospheric-oceanic forces can cause fluctuations in the intensity of monsoon rains across Mesoamerica. The Hadley cell regulates the spatial distribution of tropical rain and meridional heat transport in the atmosphere. The intertropical converge zone (ITCZ) located in the ascending branch of the Hadley cell (Donohoe et al., 2013) is defined as a low-pressure system, where strong solar heating causes air to expand upward and diverge toward the poles which results in a narrow band of high precipitation. The ITCZ migrates towards the north or south pole, following the sun in the annual seasonal cycle (e.g., McGee et al.,2014). In the central Atlantic and Pacific oceans, the ITCZ migrates 9° N in boreal summer and 2° N in boreal winter (Schneider et al., 2014).

Thus, the ITCZ moves towards the warmest hemisphere during the boreal summer season, in the case of the Mesoamerican region, via the Hadley circulation (McGee et al.,2014), producing an extended rainy season, and severe drought season during the boreal winter season (Fig. 2.5).

Other important atmospheric factors that alter the monsoon circulation are the subtropical high-pressure cells, trade winds and the low-level jets. The subtropical high-pressure cells are formed by atmospheric subsidence of cold-dry wind, forming a high pressure or anticyclonic area (e.g., Dyer et al.,1979). The position and intensity of these cells are also related to the annual rainy seasonal cycle. For example, during the boreal summer, the northward migration of the subtropical high pressure generates a continuous trade wind flow over the Mesoamerica area, carrying moisture from the Gulf of Mexico and Caribbean (Metcalfe et al., 2015) (Fig 2.2B). The variability of the Caribbean Low-Level Jet (CLLJ) has been linked with the latitudinal position of ITCZ and variability in precipitation. When the CLLJ is stronger there is a lower latitudinal center of mass resulting in less precipitation in the Pacific Slope and southern Mesoamerica (Hidalgo et al., 2015). In other instances, the precipitation on the Pacific side is also strongly related with the ITCZ position, and with additional factors such as the warm pool of the Tropical Pacific and the Low-level jet of the Gulf of California (Mitchel et al.,2002; Metcalfe et al., 2015).

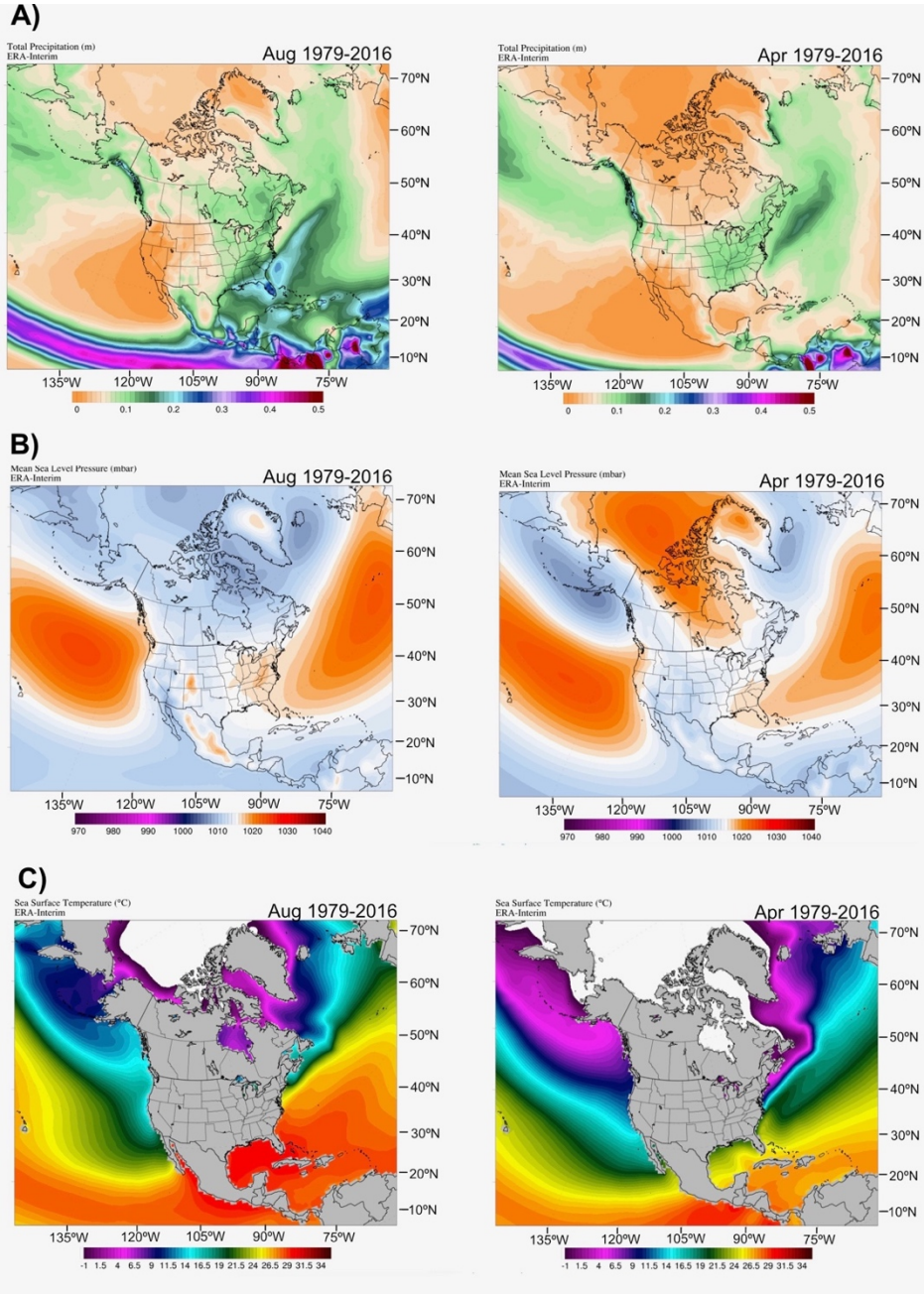

Figure 2.5- A) Total precipitation levels in the Mesoamerican region between 1979-2016 during August-April B) Sea levels pressure levels in the Mesoamerican region between 1979-2016 during August-April C) Sea surface temperature levels in the Mesoamerican region between 1979-2016 during August-April (Images from EarthNow Team. National Oceanic and Atmospheric Administration https://sphere.ssec.wisc.edu/).

The monsoon system can be modified by diverse decadal or annual, atmospheric/oceanic forces. During El Niño southern oscillation years (ENSO) decrease in summer monsoon occurs. Gochis et al. (2007) describe two mechanisms: the first is the reduction of the land-thermal contrast resulting in a reduction of onshore moisture convergence. The second mechanism suggests that an anomalous descent over Mexico and Central

America reduces the convection. Magaña et al. (2003) highlighted that during ENSO summers and positive phase of PDO, the monsoon strength is reduced due to the following factors (Magaña et al., 2003):

A) Southwards shift of the ITCZ around 2° – 3° in the eastern Pacific
B) Reduction of the thermal gradient between ocean/continent
D) Enhancements of atmospheric subsidence

In contrast, in La Niña summers and negative PDO phase monsoon precipitation increase due to the follow mechanisms (Magaña et al., 2003):

A) Northward displacement of the ITCZ by about 10ºN
B) Weakening of trade winds
C) Weakening of atmospheric subsidence
D) High number of tropical storms in the Atlantic

Recent moisture budget models reveal that anomalous descent strongly contributes to negative precipitation during the spring until the peak of the event. These conditions generate atypical advection due to anomalous winds and the amount of moisture coming into the continent (Bhattacharya and Chiang, 2014)

Atlantic SSTs anomalies play an important role in monsoon modulation. During the positive (warm) phase of Atlantic Multidecadal Oscillation (AMO) the SSTs of the tropical Atlantic increase, shifting the position ITCZ to the north, thus increasing precipitation and tropical cyclones (e.g. Ting et al., 2011). The North Atlantic Oscillation (NAO) is a dominant force over the North Atlantic region. Its positive phase is marked by the increase of sea level pressure between the Icelandic low and North Atlantic Subtropical High (e.g., Giannini et al., 2001). The NAO oscillations can reduce or increment the rainfall in the Mesoamerican region. During the positive phase of NAO trades winds increase and SSTs cool, reducing the moisture available for convection. In consequence, precipitation over Mesoamerica decreases (Battacharya et al., 2017). The monsoon precipitation can chance in response to forcing in SW USA and Mesoamerica regions. Positive Atlantic SSTs, la Niña or negative PDO resulting in wet Mesoamerica and dry SW USA. Contrary to this, negative Atlantic SSTs anomalies, El Niño or positive PDO generate dry conditions in Mesomaerica and wet conditions in SW USA (Stahle et al., 2012).

Millennial-scale monsoon fluctuation in the Atlantic can be related to the Atlantic Meridional overturning circulation (AMOC). A more vigorous and stable AMOC is associated with high precipitation in Mesoamerica, due to shifting in the mean position of the ITCZ towards the warming hemisphere, in this case, the northern hemisphere. In turn,

recent simulations describe that AMOC shutdown is not always related to vigorous drought conditions. This infers that other factors play a fundamental role during drought periods (Battacharya et al., 2017). Global climatic impact of the weakening of AMOC has been described. During the early deglaciation period, pulses of meltwater reduced AMOC strength and suppressed the rain in both hemispheres (Bond et al., 2001). Aerosols may also affect the monsoon system, via perturbing the land-sea thermal contrast by the absorption or scattering of solar radiation (Mohtadi et al., 2016). Soil moisture can play a role in the monsoon regime. Small (2001) argues that wet soil enhances July precipitation within the monsoon area.

The incursion of cold fronts, called “Nortes,” strongly affected the weather in the Mesoamerica. These systems enhanced temperature fluctuation in the NE Mesoamerican region and produce precipitation over the Caribbean and Central Mesoamerica, wherever they occur and especially when they are frequent (Henry, 1979). The occurrence of cold fronts increases from September to October, reaching a maximum in winter. The frequency and degree of penetration in the tropics areas are related to the position, amplitude, and strength of mid-latitude circulation. After the incursion of cold fronts, the return of warm moist air in the tropics occurs (Henry, 1979).

2.4-High resolution paleoclimatic studies in the Central and Northern Mesoamerican region

The relationship between climate and cultural change in the Mesoamerican region is complex. Recently, high-resolution paleoclimate and paleoenvironmental records have been used to explain the possible link between climate oscillations and the social development of ancient societies in Mesoamerica. Diverse natural archives such as lake sediments, stalagmites and tree rings have been employed for this purpose. In the next lines, a brief review of recent literature focusing on high-resolution paleoclimatic and paleoenvironmental records is given.

Persistent wetter conditions mark the begin of the Holocene period in the Mesoamerican region (Metcalfe et al., 2015). The multiproxy study (magnetic susceptibility, pollen and geochemistry) of Rincon de Parangueo and San Nicolas craters, conducted by Park et al, (2010), describes paleoclimatic oscillations over the last 11 600 yr BP in the NMF. A comparative analysis between the two records indicates faster oscillations of wetter and drier conditions around 11600-9000 yr BP. In contrast, the isotopic speleothem record of Cueva del Diablo, which is one of the few high resolutions records that cover the entire Holocene in Mesoamerica, just reveals two significant hydrological disruptions, the 10.3 and 8.3 ka events. Both episodes reflect a decrease in the intensity of the NAM, as a consequence of cooling in the North Atlantic due to meltwater pulses of last remaining of the Laurentide Ice sheet (Bernal et la., 2011).

Among lake records in central Mesoamerica just reveal one short period of dryer conditions (Metcalfe et al., 2015).

Around 5 500 to 5 600 yr BP reduction in precipitation occurred during the end of Early Holocene peak isolation period (EHPI) described as the peak of the NAM tightly related to the decrease of solar insolation by the precision cycle (Wanner et al.,2008). In this context, the high-resolution XRF Ti of Juanacatlan basin recorded the end of wetter conditions around 5 100 yr BP (Davies et al., 2018). The paleolimnological record of Rincon de Parangueo, described by Park (2005) is also in agreement with this interpretation, revealing the start dry conditions between 6300-4000 yr BP. The records from Rincon de Parangueo and San Nicolas crater lakes reflect the establishment of dry conditions during the Mid-Holocene (5700-3800 yr BP) as well. The lake record of La Piscina de Yuriria compares well with the works previously described. Reduced effective moisture leading the enhanced evaporative enrichment under drier conditions is described for this record (Holmes et al., 2016).

Around 4000 yr BP a complex paleoclimatic pattern is interpreted such as High hydrological variability or drought conditions (Metcalfe et al.,2015). The rise of ENSO activity and the southward migration of ITCZ are the most prominent mechanism involved in this climate variability. A dry event around 4000 cal yr BP is described in the Zirahuen lake and linked with the rise of ENSO activity (Lozano-Garcia et al., 2013). Cueva del Diablo record compares well with this interpretation. This record describes that the Pacific moisture and ENSO force became more dominant since the 4300 yr BP establishing the current climatic conditions (Bernal et al., 2011). The Juanacatlan record shows, the start predominant Pacific forces, such as ENSO or ENSO-type variability like Pacific Decadal Oscillation, started between 4000 to 3000 yr BP (Jones et al., 2015).

The increase of human impact across Mesoamerica around 2000 cal yr BP difficult the correct paleoclimate interpretation of the records. Nevertheless, severe drought conditions are interpreted during the Epiclassic period (600-900 CE), affecting the social dynamics of diverse Mesoamerican civilizations. Diverse high-resolution records corroborate this hypothesis. The Juxtlahuaca isotopic record is interpreted as a hydroclimate reconstruction for the western Mesoamerica sector over the last 2250 years. Drought conditions during the Epiclassic were related with the enhanced of ENSO and North Atlantic Oscillation forces. Nevertheless, pluvial periods were interpreted to coincide with the strongest La Niña conditions. The oscillations in the Mesoamerica monsoon are also linked with population migrations, due to the impact of freshwater supplies affecting agricultural productivity (Lachniet et al., 2017) (Fig. 2.6D). A prolonged dry period between 500 CE to 1150 CE was interpreted using the

isotopic, geochemistry and pollen records of Aljojuca maar lake, located in the Serdan Basin. The colder SST of Tropical Atlantic and decreasing strength of Atlantic Meridional Circulation (AMOC) were suggested as the principal drivers in this reduce of precipitation. In addition, these drought conditions are linked with the abandonment of the Pre-Hispanic city Cantona and massive migrations for diverse Mesoamerican areas (Bhattacharya et al., 2015) (Fig. 2.6C).

The isotopic record of Rincon de Parangueo has been linked with severe drought conditions for the period 600-700 CE as well. This drought period is associated with the collapse of the Teotihuacan culture. Contrasting the idea about the Epiclassic drought, the pollen record of San Nicolas maar lake indicates that there is not strong evidence about of a significant climatic change between 1000-1500 CE, suggesting that the expansion/retraction of the NMF is not related with climatic factors (Brown, 1984). Finally, the monsoon variability reconstruction, using the dendrochronological Amealco, (Queretaro) record, highlight that multidecadal SST oscillation of tropical Atlantic and El Niño force played an essential role in the Mesoamerica droughts, especially during the Terminal Classic drought (Stahle et al., 2012).

The Little Ice Age reveals dry conditions in the Mesoamerican region (Metcalfe et al., 2015). The Juanacaltan record provides support to this idea. A dry phase of Juanacatlan record interpreted between 1400 to 1600 CE correlates with positive phases of PDO and ENSO (Jones et al., 2015). The decrease in solar activity over the last 1000 yrs is associated with reduced runoff in the area.

Finally, the varve analysis of the younger lacustrine sequences of La Alberca (1852-1973 CE) and Rincon de Parangueo (1839-1943 CE) reveals short-term climatic fluctuations in Valle the Santiago region (Kienel et al., 2009). These sequences were anchored by the Colima,and Paricutin tephras, deposited in 1913 and 1943/1944, respectively, and ^{210}Pb chronology. Varve structures are formed by the alternation of dark and white laminations in both lakes. These structures were formed due to seasonal variability. The dark laminations represent the period of constant rainfall during summer increasing the organic and clastic input and white laminations the period of high evaporation rates during summer, inducing the precipitation of calcium carbonates. Accordingly, with this varve study, drought periods with a duration of 3-7 years were found at: early 1859s, 1865, 1880, 1895, 1905, 1915 and 1920s. A transition from calcite to aragonite precipitation is interpreted by the intensification of groundwater exploitation after 1940 (Kienel et al., 2009).

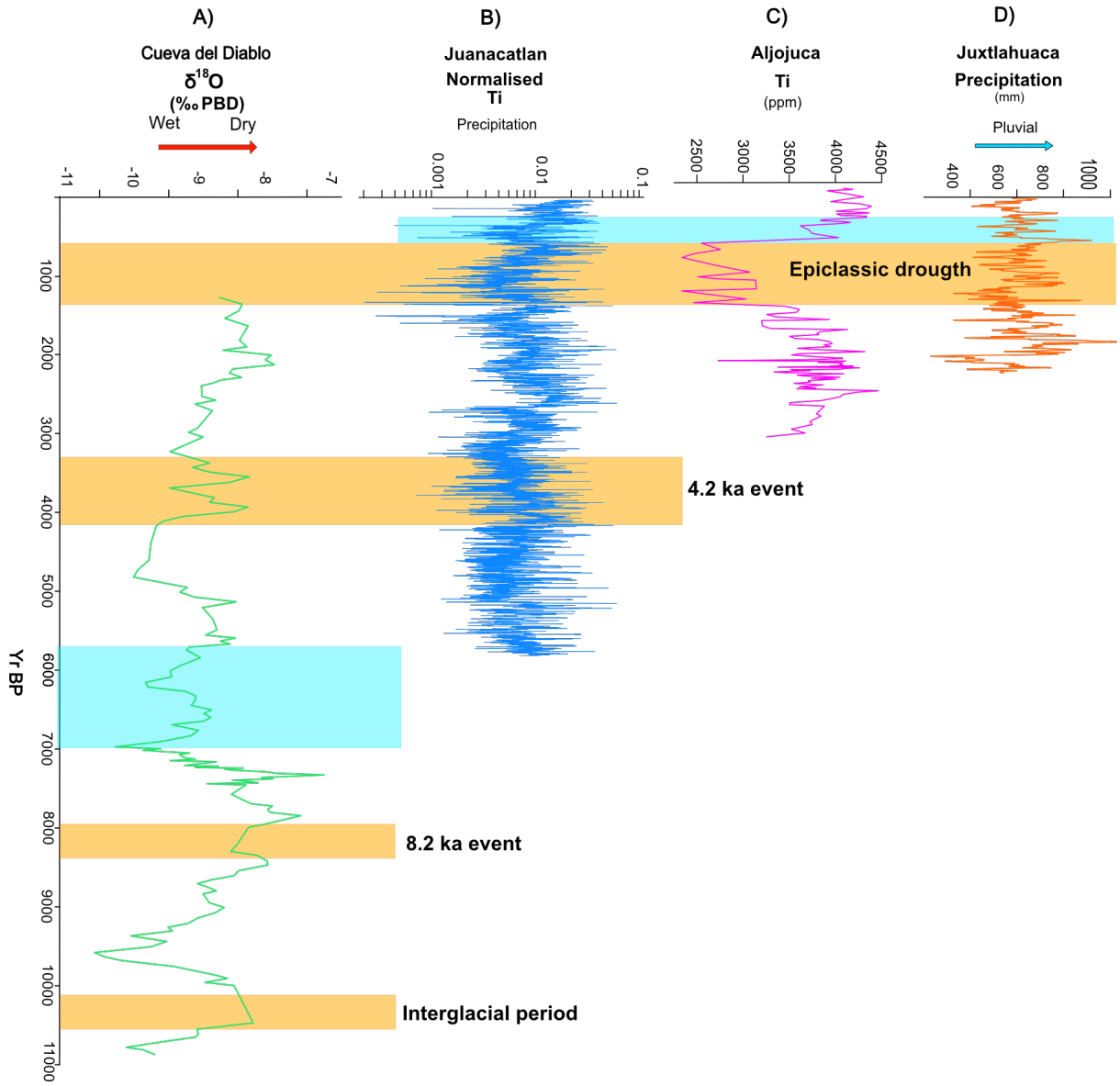

Figure 2.6-High resolution paleoclimatic records of Cueva del Diablo, Juanacatlan, Aljojuca and Juxtlahuca. The orange shadow areas represent relevant climatic dry events and blue bars wetter periods during the Holocene.

2.5-Archeology of the Northern Mesoamerican Frontier

Mesoamerica is divided into eight principal sectors, defined by its linguistic, historical and geographic characteristics: Northern Mesoamerican Frontier, Basin of Mesoamerica, Gulf, Guerrero, Oaxaca, Central America, South Coast and Maya sector (Zamora, 2004) (Fig. 2.7 A). In this work, I focus my paleoclimatic-paleoenvironmental study on the NMF. The modern geographic distribution of NMF is described by Kirchhoff (1960) as follows: "The NMF runs from the Río Fuerte in Sinaloa, east across the Sierra Madre Occidental and then turns southeast passing to the east of the eastern foothills of the Sierra Madre Occidental to the Tunal Grande of San Luis Potosi where it curves northeast to the headwaters of the Rio Soto de la Marina which it follows to the sea". This zone is divided into three principal sectors: Oriental, Center and Occident (Zamora, 2004) (Fig. 2.7 A). The center sector is one of the most important regions in the NMF and is formed by the actual states of Querétaro, Guanajuato, San Luis Potosí, and by the Lerma river and its affluents Laja, San Juan, Turbio, Guanajuato and Angulo.

The actual annual precipitation in this area lies between 400 to 900 mm, arid conditions increase towards the northern regions, and is located in the limit of tropical rain belt. These climatic features suggest that rainfall is marginal to allow temporal farming, which was the main agricultural technique employed by pre-Hispanics population. Additionally, Armillas (1969, 1991) noted that these climatic conditions in NMF represented the limit between the civilized farmers societies settlements in the south and roaming hunters-gatherers in the north.

Using archeological evidence Armillas (1969, 1991) interpreted that after 600 CE the agricultural frontier moved northwards to the Lerma river until the year 1000 CE, describing this period as the maximum northern extension of the NMF. Afterward, severe drought conditions around 1100 CE provoked a general exodus of ancient farmers, reducing the permanent settlements, thus resulting in the retraction of the NMF south of the Lerma River Valley. The consequence of this retraction resulted in political and social degradation in the NMF.

Recent studies revealed at least four additional expansions of NMF (Dueñas, 2017) (Fig. 2.8):
- In the Late Pre-Classic period around 150 BCE-200 CE the first expansion of Mesoamerican societies towards the north of Lerma river occurred
- The second expansion was during the Classic period between 200 to 600 CE
- The Epiclassic (600-900 CE) represents the biggest expansion of the NMF population towards the north

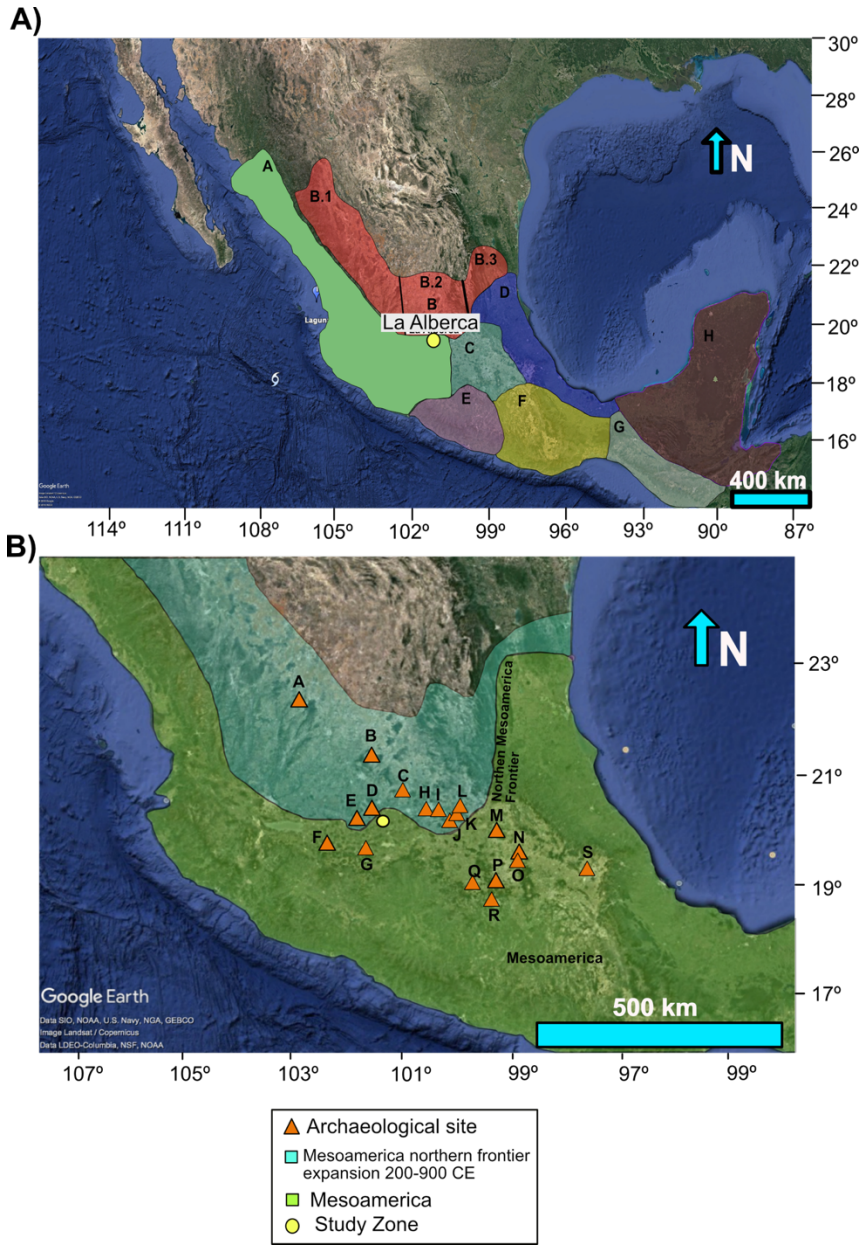

Figure 2.7- A) Geographic distribution of Mesoamerica regions. (A) Occident;(B) Northern Mesoamerican Frontier (NMF), (C) Basin of Mesoamerica, (D) Gulf, (E) Guerrero, (F)Oaxaca, (G) South Coast (H)Maya. Principal sectors of Northern Mesoamerican Frontier. (B.1) Occident, (B.2) Center and (B.3) Oriental (Zamora, 2017). **B)** Map of distribution of principal archeological sites of Northern Mesoamerican Frontier. ;(A) La Quemada, (B) El Coporo, (C) Cañada de la Virgen, (D) Peralta, (E) Cerro Barajas, (F) El Opeño, (G) Tarascan empire, (H) El Cerrito, (I) El Colorado, (J) El Rosario, (K) La Trinidad, (L) Santa Rosa Xalay, (M) Tula, (N) Teotihuacan, (O) Tenochtitlan, (P) Cuicuilco, (Q) Teotenango, (R) Xochicalco, (S) Cantona.The shadow light-dark green areas represent oscillations of Northern Mesoamerican Frontier. The study zone is represented by yellow circle.

-A general retraction of NMF occurred between 900-1500 CE

Even though Armillas (1969) indeed only mentioned that severe drought conditions around 1100-1500 CE produced by the Little Ice Age event resulted in the oscillation of NMF, the author suggests in general terms that climatic changes were the principal mechanism involved in the NMF population migrations. Other authors do not be in agreement with Armilla´s hypothesis and rather propose environmental degradation by the intensification in agricultural practices, deforestation and exhaustion of mines as the principal mechanism involved in the NMF oscillations (Brown, 1984; Elliot et al., 2010; 2012).

Socially the NMF is described by the pluricultural character of its population, a dynamic region with a continuous social change, habited by stratified societies and hunter-gatherers. Its history is divided into five principal phases (Fig 2.8):

- Opeño-Capacha-Tlatilco 1800-1200 BCE
- Tradición Chupicuaro 350 BCE-350 CE
- El Desarrollo Regional 350- 700 CE
- Tradición Tula 900-1150 CE
- Tradición Tarasca 1350 CE

El Opeño and Capacha represents the earliest archeological sites of the NMF, with an estimated age between 1000-2000 BCE. Both sites are located in the western flank of NMF (Fig. 2.7B). El Opeño and Capacha were shaft Tomb complexes. The typical characteristics of these burials were the content of ceramic offerings, hollow figurines and guardian figurines (Fig. 2.9 A, C). Similar ceramic offerings and figurines were founded in Tlatilco archeological complex, in the center region of Mesoamerica (Cardenas,1999). This indicates a possible connection between the Central Mesoamerica and NMF cultures.

Chupícuaro was one of the most influential pre-Hispanic cultures in the region NMF. Its occupation period along the Rio Lerma, southeast of Guanajuato and Cuitzeo Basin, was dated between 650 BCE-250 CE (Gorenstein, 1985). This culture is defined by the production of high-quality polychrome ceramics and figurines with unique forms (Fig. 2.9 B). While most of the Chupicuaro artifacts were found near the Lerma river basin, there is evidence of its ceramics and vessels in Central Mesoamerica (Mexico City) and La Quemada (Zacatecas) archeological site. Chehuayo and El Cenicero, both located in the Cuizeo Basin could be considered to be the principal sites of this culture. The origin of this culture still an enigma, some authors refer that colonization of the Lerma region was

conducted by groups of Central Mesoamerica (Porter, 1956) and some others claim for groups of the Occident (Braniff, 1998; Florance, 2000).

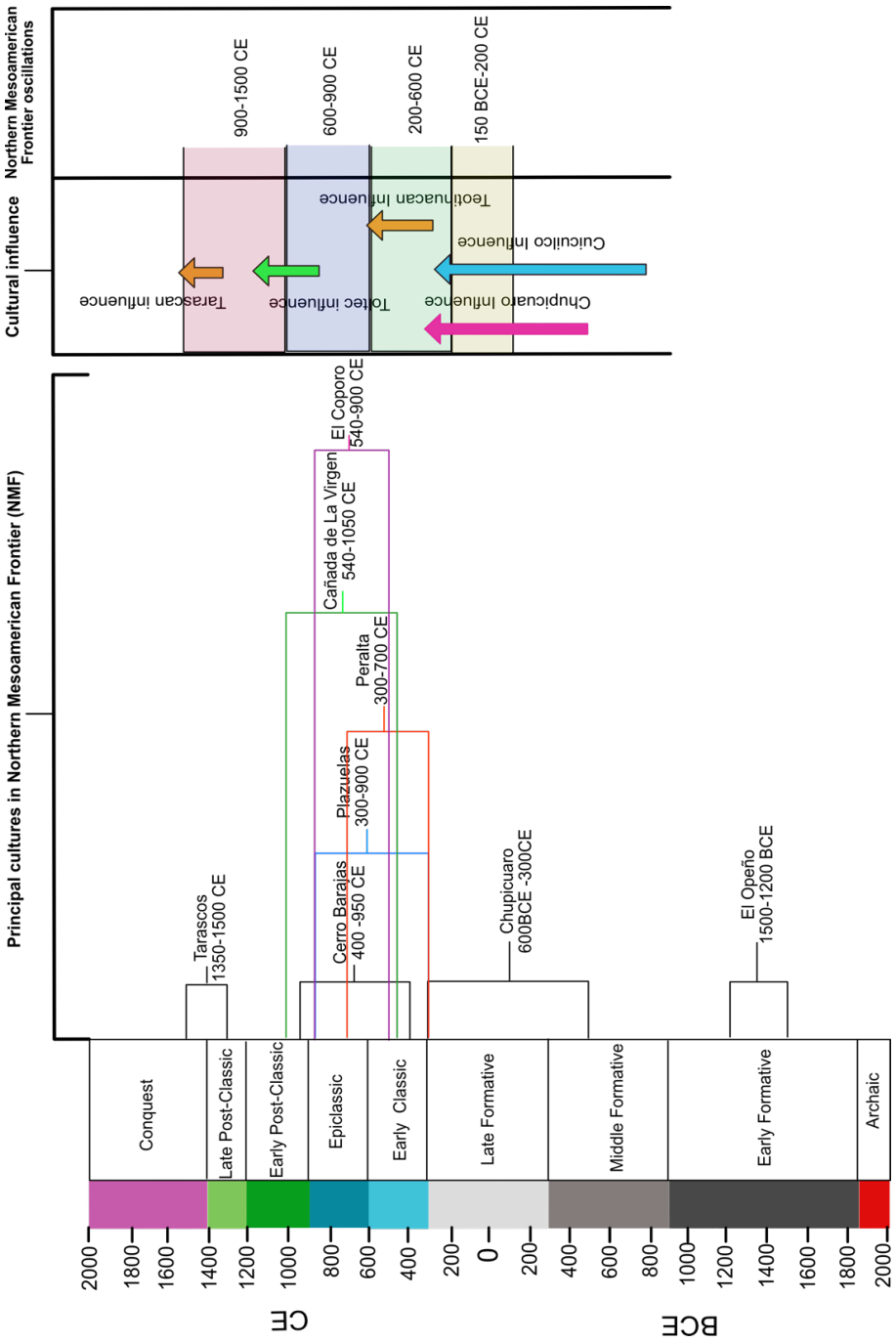

Figure 2.8- From left to the right, graphic representation of occupation periods to diverse Mesoamerican cultures in the Northern Mesoamerican Frontier, periods of influence of principal Mesoamerican cultures in the region and principal oscillations of the frontier (Gorenstein, 1985; Braniff, 1998; Florance, 2000).

The study of Chupicuaro culture has been divided into three main phases: Early Chupicuaro (600-400 BCE), Late Chupicuaro (400 BCE-100 CE) and Mixtlan phase (0-250 CE). Early Chupicaro was characterized by the presence of rudimentary villages near to Lerma river and low social development. During the Late Chupicuaro phase, the increase of habitants in the Lerma Basin was accompanied by the establishment of a hierarchical state and the constant northwards migrations following the Lerma, Turbio and Laja rivers (Florance, 2000). In addition, the typical construction of circular buildings called Guachimontones and the constructions of sunken patios started. The Mixtlan phase, in general, is represented by the evolution in the architecture style of the sunken patios and different constructions. The expansion to the north continues evidenced by the archeological site Morales with a chronology between 300 BCE to 100 CE. Most of the Chupicuaro settlements based its economy in agricultural activities (Florance, 2000).

Hunters-gatherers occupied the area and the emergence of stratified societies was delayed compared with other Mesoamerican regions (Viramontes, 2008). During the late Pre-Classic period (100 BCE-250 CE), the Chupicuaro culture, considered to be the most influential culture of the region (Gorenstein, 1985), started to migrate from the Acambaro Valley towards the northern region of NMF following the Lerma, Turbio and Laja rivers´ traces (Viramontes , 2008). Until these days, the reasons behind the population migrations in the NMF are poorly understood. O´Hara et al. (1994) proposed that long term agriculture in the NMF was not viable due to the climate variability, concluding that flexibility in the cultivation methods in the driest places and out-migration were typical practices of the ancient cultures of this region.

Moreover, the role of the first ancient agriculturists in the modification of the landscape in the Valle the Santiago area is not well understood. The start of incipient agricultural activities is indicated by the pollen records of San Nicolas and Parangueo lakes around 3700 BCE (Park et al., 2010). Based in the pollen record from La Alberca lake, Conserva (2003) describes a general occupation period of the Chupicuaro culture between 400 BCE-150 CE. The scarcity of high-resolution paleoclimate and paleoenvironmental records hinders the correct comprehension of the relation between climate change and population dynamics in NMF and in the Valle de Santiago region.

Around 300-700 CE, the cultures in the NMF evolved into more complex societies. This stage is known as the Bajio Tradition. Towns and cities with monumental and ceremonial architecture start to dominate the region (Braniff, 2000). This phase is also represented by the large number of archeological sites such as: Cerro Barajas, Plazuelas, Peralta, Cañada de La Virgen and El Coporo. This period also describes the rise of habitants, constant migrations, the establishment of commercial network and abandonment and formation of different pre-Hispanic towns. The growing number of habitants in the NMF

provoked the colonization of new regions and intensification of agricultural activities (Zamora, 2017). A Teotihuacan influence, during this period is described by the presence Thin Orange ceramics in El Coporo, Guanajuato and other archeological sites near to Querétaro.

Around 900 CE in the Epiclassic period agriculturists of the NMF, start to abandon the area and returned to hunting and gathering lifestyle, and new colonization of hunters and gatherers occurred (Braniff, 2000). Sites located in the NMF were never occupied again. This episode marks the transition between the Epiclassic to Post-Classic period (Braniff, 2000). Another interesting feature about the Post-Classical period is the possible Toltec intrusion in the NMF evidenced by new architectural patterns and ceramics artifacts. Additionally, a Toltec complex was recognized in El Cerrito close to Querétaro city (Braniff, 2000).

Between 1350 and 1500 CE the rise of the Tarascan culture took place. This culture represented a demographical, political and economic core in the western part of NMF. Due to the proximity, contemporaneity and dominance Tarascans were always involved in a military hostilities with the Aztecs (Pollard, 2000). In the 17th century, Spanish started the conquest of NMF. However, the unfavorable environmental conditions for life and the strong resistance offered by the population of the north called Chichimecas difficulted the conquest. This opposition ending with defeated of Chichimecas in the Mixton War (Warren, 1971).

A)

B)

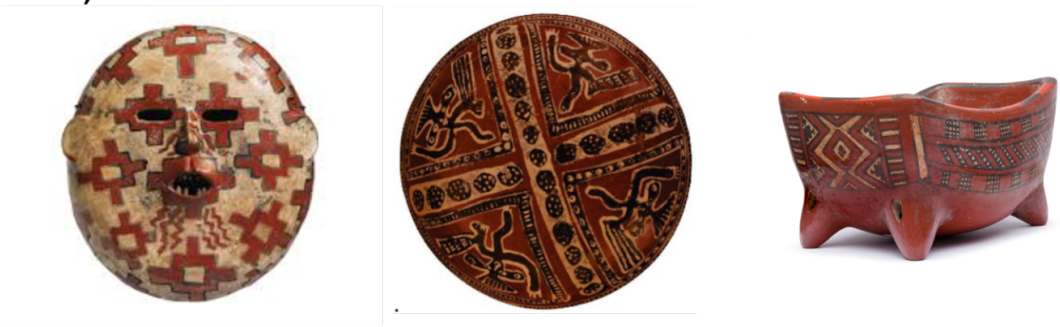

C)

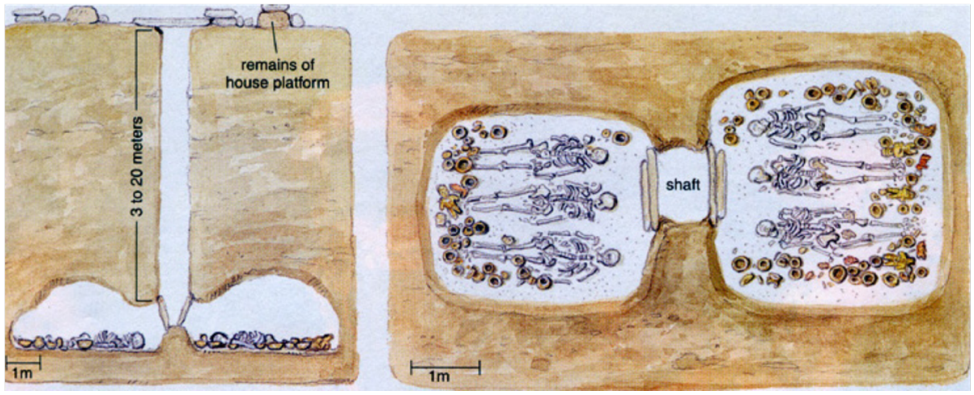

Figure 2.9- A) Chupicuaro figurines of maternity cult; B) Typical polychromatic ceramics of Chupicuaro tradition; C) Schematic representation of shaft tombs of Capacha and El Opeño traditions (Modified image from Willians, 1979).

2.6-The possible effect of 4.2 ka event in the paleoclimate conditions and Mesoamerican societies.

Little is known about the paleoclimatic effects of the 4.2 ka global event in Mesoamerica, and its possible social consequences. In the southern Mesoamerican region, sparse evidence described the presence of a dry climatic event with correspondence of timing with 4.2 ka event. The chemical, pollen, phytolith and charcoal data from mangrove core in Pacific coastal Guatemala reveals a major forest disturbance or a drying period during the 3000 to 2000 BCE. Kennett et al., 2010 based in the pollen, phytoliths and charcoal evidence of two cores from Acapethua and Chantuto mounds interpreted high fire activity between 2350 and 2250 BCE and between 3850 and 3650 BCE. The occurrence of natural lightning strikes more regularly caused forest fires in an increasingly dry environment is hypothesized. Among of paleoclimatic records in the Mesoamerican area reveals a complex paleoclimatic pattern, the rise of ENSO activity or the start of predominant Pacific forces (Bernal et al., 2011; Jones et al., 2015). In contrast the Zirahuen pollen record reveals the presence of a single dry event around 4 500 to 4 200 yr BP ka associated with a global rapid climate change (Lozano- García et al., 2013).

The 4.2 ka climatic event corresponds to the final part of the Archaic and the onset of Formative periods of the archeological chronology in the region. The Archaic is constrained between 9000-4000 yr BP; but precise definition of this period is not a simple matter. Some generals characteristics such as the transition from primitive Paleo-Indian hunters to little developed semi to sedentary societies, the initial domestication of maize, the intensification of agricultural activities between 7000 to 5500 yr BP, the rise of small villages, and minor social changes (Piperno et al., 2007; Kennet, 2012) have been used for defining this period. Despite the debate about where, when, and whom started domestication of maize still continues until today, this is considered the most important economic and social activity on the Archaic. There are multiple archaeological sites where the impact of early agricultural activities in Archaic communities, have been recognized. Two of the most studied Archaic sites are the Tehuacan Valley and the Balsas Basin. Maize recovered in Tehuacan Valley was dated by AMS C-14 around 5700 yr BP (Long et al., 1989). In the Balsas Basin (Guerrero) AMS C-14 data reveal the presence of maize remains around 8700 yr BP (Rosenswig, 2015). The Archaic pre-dates ceramic use in Mesoamerica, but other artifacts that reveal Archaic activity, like modified river cobbles, are also present in this latter location (Piperno et al., 2009).

The Formative Period is marked by the appearance of ceramic vessels, intensification of food production, (mainly maize), social stratification and the beginning of monumental art (Rosenswig, 2015). The Olmecs in San Lorenzo, Veracruz, were the first culture that adopted a stratified society and political organization dating around 2300 yr BP (Clark,

2007). They are considered to be the most advanced civilization in the Middle Formative, evidenced by several constructions such as monumental pyramids, elite residences, public buildings, ball-courts and drainage systems (Grove, 1997). In coastal Chiapas, the first small villages and ceramic artifacts extended back to 2900 yr BP. Archeological studies in Ulua, Honduras, suggest the beginning of complex societies at 2850 yr BP, displayed by the construction of pyramids in Los Naranjos and Yurumela (Joyce and Henderson, 2007). In the Oaxaca Valley, San Jose Mogote was the largest Mesoamerican city in the area reaching its maximum social and architectural development ca. 3000 yr BP (Flannery and Marcus 1981). In the Valley of Mexico, three city-states emerged between 3300 and 3150 yr BP: Tlapacoya, Tlaticl and Coapexco.

These data suggest that the most significant transformation in Mesoamerica, the evolution into more complex societies that characterized the Middle Formative period in Mesoamerica occurred around 3000 yr BP; this is about 3 kyr after the domestication of maize and 1200 years after the 4.2 ka event. Did the 4.2 ka event occurs and affect the development of Mesoamerican cultures? Concerning this enigmatic issue, Rosenswig (2015) set forward two interesting ideas. First, the major archeological transition between the Archaic and Formative occurred during the 4.2 ka event. Second, the author argued, the paleoclimate conditions were not the sole cause affecting the development of Archaic societies. Rosenswig (2015) says, “Correlation between changing subsistence practices, demographic patterns, and social institution on the one hand and climatic pattern on the other can not be ignored.”

Chapter 3

Methodology

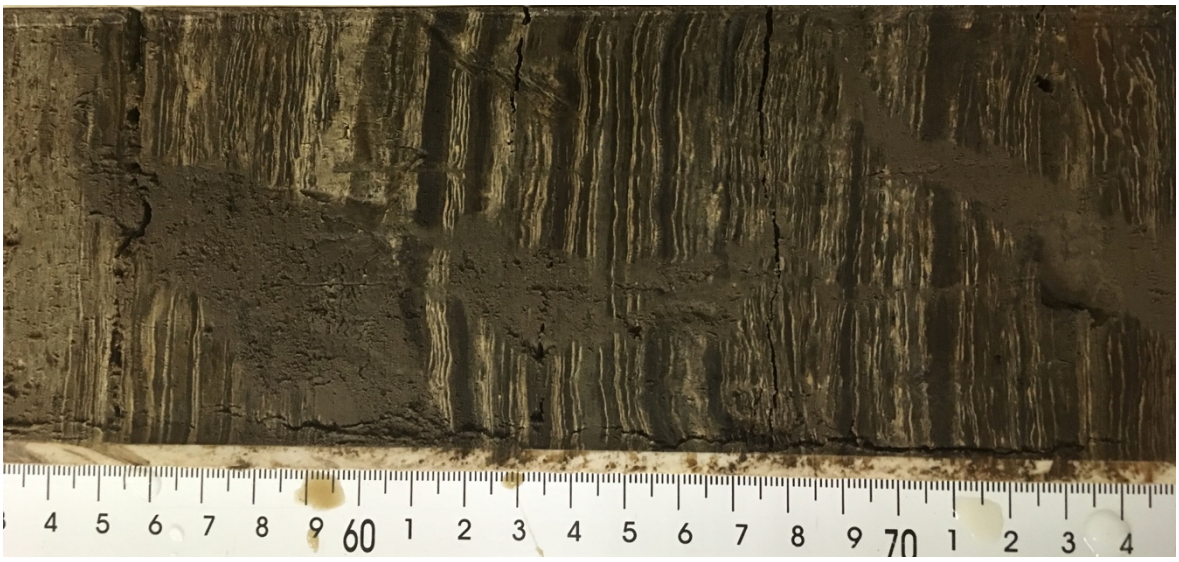

Laminated lake sediment from La Alberca maar lake by Kurt Wogau.

3.1-Introduction

One of the major goals of this work is to understand the paleoclimate variability of the last 6700 yr BP in Mesoamerica, especially in the Northern Frontier, and the possible role of the climatic oscillations for the rise and fall of Mesoamerican societies. To achieve these goals, I investigated laminated lake sediments as a high-resolution archive by means of different physical, geochemical, and sedimentological proxies. The applied multi-proxy approach allows a better understanding of the complex climate variability and its possible relation with the cultural evolution in the NMF.

3.2-Fieldwork, sampling and lithostratigraphic descriptions

Maar lake La Alberca was sampled close to its central part, where two parallel cores were recovered, with total combined lengths of 8.69 m and 6.39 m, named Alberca Azul (AZ) and Alberca Rojo (AR), respectively (Fig. 3.1). The coring device employed was developed in the Paleomagnetism laboratory of Geoscience Center of National University of Mexico (CGEO). This system uses 76 mm PVC tubes, an internal piston for sediment recovery and a hydraulic percussion system for penetration of the total length of the core sections (3-6 m). The cores were transported and stored in the cold room of Centro de Geociencias, UNAM, Campus Juriquilla, at 4º C before the analysis.

Figure 3.1- Location of drilling sites of cores Alberca Rojo and Alberca Azul.

Cores were cut into halves and photographed. One half was used for non-destructive core scanning (XRF) and then archived in a cold room. The second half was sub-sampled for different analyses. For measurement of magnetic parameters, oriented small plastic samples with a volume of 8 cm^3 were taken at every ~ 2.3 cm. These samples were measured in the Laboratory for Paleo and Rock Magnetism of Section 5.2 of the Helmholtz Centre Potsdam (GFZ) German Research Centre for Geosciences. Macro fossil plant remains were selected for radiocarbon dating. For the lithostratigraphic characterization, texture and macroscopic components were described using a binocular microscope Leica GZ6E. I used high-resolution magnetic susceptibility curves, and lithostratigraphic indicators, such as tephra layers to correlate both cores.

High-resolution images, magnetic susceptibility data, and stratigraphic markers were used for correlating the AZ and AR cores (See results chapter). I selected AZ as a master core, which was the longer and better-preserved record. In addition, bulk sedimentary $\delta^{18}O$, $\delta^{13}C$ records and pollen data were compiled from a third core called Hoya Alberca (Appendix 7,8) drilled during 2001 in the same location by a joint team of the Centro de Geociencias Campus Juriquilla, UNAM and UC Berkley. In order to use the data from earlier Hoya Alberca core, I performed a correlation with our master record (AZ) using magnetic susceptibility curves, isotopic data, XRF Ca/Ti ratio and an independent age model.

3.3-Laboratory methods

3.3.1-Radiocarbon dating

For the age model construction, I used nine radiocarbon dates from AZ and three radiocarbon samples from AR cores. Based on the lithostratigraphic correlation between both cores, I found the equivalent depth from samples of AR in the master core AZ (Appendix 8). The materials employed for ^{14}C analyses were: two samples of organic gyttja and ten samples of macrofossil plant. Samples were processed on Beta Analytic, Inc. (USA) laboratory using the mass spectrometry method. Before producing tie points of the age-depth model, ten layers interpreted as turbidites were removed from the stratigraphic section (see chapter 5.1 and Appendix 10). For the calibration of the ages and construction of the age model, I used the Clam software (Blaauw, 2010). This software has been written in the open-source statistical environment R (R Development Core Team, 2010). For the calibration of the age and the related 2σ values, I used the Intcal 13.14 curve (Reimer et al., 2013). The Clam software produces an age model over every calibrated sample distribution. This sampling process was repeated 1000 times, generating a diverse calendar age for every point. The calculation of the “best” age is based on the weighted mean of all the sample calendar years (Blaauw, 2010).

3.3.2-XRF

High resolution XRF core scanning (ITRAX XRF Core Scanner, COX; e.g., Croudace et al., 2006) was performed at the Leibniz Institute for Baltic Sea Research Warnemünde (IOW), to determine the major element distribution in ONE split halves of the cores. To avoid evaporation, the core halves were covered with an ultrathin plastic foil before being measured with a Cr-tube operated at 30 kV and 30 mA. Step sizes were chosen according to lithological features ranging from 200-500 µm with an exposure time of 15 seconds per step. Here I mainly report on the elements Al, Si, K, Ca, Ti, Mn, Fe, Sr, Zr, and Ba.

3.3.3-XRD

X-ray diffraction was performed to determine the primary mineralogical components on the sediments. A total of fourteen bulk sediments samples were selected for XRD analyses along the core using a Miniflex Rigaku equipment with copper radiation Kα 1.5406Å, between 5 and 80 degrees 2θ, with a step of 0.02 degrees and 0.06 s for point.

3.3.4-Pollen identification

Pollen identification was carried out in the University of California at Berkeley using the Museum of Paleontology (UCMP) pollen reference collection. The analysis comprised of counting a minimum of 400 pollen grains and fern spores on 44 samples, using standards procedures for the extraction (Faegri and Iversen, 1989). A Zeiss microscope with a 40x Planapochromat objective and a total magnification of 400x was used for the counting. (e.g., Conserva, 2003). For this study, I used only *Amaranthaceae* and *Zea mays* results, for describing possible anthropogenic land use in the surrounding areas of the lake.

3.3.5-Rock magnetism measurements

To determine the magnetic mineralogy of the lake sediments, rock magnetic measurements sensitive to concentration, type of minerals and grain size were performed. High-resolution magnetic susceptibility was measured with a Bartington MS2E sensor, every two millimeters. This parameter mainly responds to the concentration of ferrimagnetic minerals, but also to their grain size and the presence of dia- and paramagnetic minerals (Liu et al., 2012). Volume-specific magnetic susceptibility (k, in dimensionless SI units) of the 8 cm^3 samples was measured with a Kappabridge magnetic susceptibility system, using a field of 200 A/m with a frequency of 976 Hz.

Saturation of isothermal remanent magnetization (SIRM), was imparted with a 2G Enterprises pulse magnetizer model 660, applying fields of 1.5 T and a backfield with opposite direction -200 mT. The resulting IRMs were used to calculate the S-ratio according to Bloemendal (1992) definition. This ratio has a value close to one if ferrimagnetic minerals are dominating and values significantly lower than one with an increasing contribution of high coercivity minerals like hematite. Nevertheless, this ratio can also be sensitive of a concentration of magnetic minerals, if ferrimagnetic fraction domains (e.g., Heslop, 2009). Additionally, on selected samples, unmixing of coercivity distributions derived from IRM curves, were carried out using the web application MAX UnMix. This program was designed in statistical software R and built using shiny for R studio (Maxbauer et al., 2016).

Anhysteretic remanent magnetization (ARM) was produced using a peak alternating field of 100 mT field, and a superimposed bias field of 50 micro Tesla with a 2-G Enterprises demagnetizer. This parameter is a sensitive proxy to identify magnetite of single domain and pseudo single domain grain sizes (King et al., 1982). The demagnetization experiment was performed with a step sequence of 0,10, 20,30,40,50,65,80 mT. Medium destruction field was calculated to determine the relative variability, between the soft and hard magnetic fraction. The susceptibility of ARM (kARM) was calculated, dividing the ARM intensity by the direct bias field.

The interparametric ratios kARM/klf and ARM/SIRM were used to determine relative grain size variations. Both ratios increase with the presence of fine magnetic particles, however, for the correct interpretation of the ratios, ferrimagnetic mineralogy has to be uniform.

Thermomagnetic curves were acquired in an argon atmosphere using the high temperatures accessories of the Kappabridge susceptibility system. This system measures the variations of magnetic susceptibility with temperature, reaching 700ºC. Hysteresis curves and first-order reversal curves (FORC) were produced in a Micromag 2900 AGM system. The hysteresis curves were produced applying a field between 1.5 mT and inverse field of -1.5 mT. FORC curves were performed on irregularly spaced field grids, following the Zhao et al. (2015) protocol.

3.3.6-SEM observations

Seven samples characterized by the different behavior of magnetic properties were selected for scanning electron microscope (SEM) analyses. To do this, magnetic mineral extraction was performed, using the protocol described in Nowaczyk (2011). The equipment employed for the SEM analyses was the Carl Zeiss SMT model Ultra 55 Plus, which has a spatial resolution of 1 nm at 15 keV. High-resolution images were obtained

using a secondary, backscattered electrons, and for analyzing the relative chemical composition of the minerals, energy dispersive spectroscopy (EDS) was employed at the energy level of 20 keV was employed. Four sediment samples were also studied with the SEM technique, in order to characterize the principal mineralogical and organic fraction of the laminated sections of the core.

3.3.7-Organic carbon content

Organic carbon can be present in soils and sediments and is formed by cells of microorganism, plants and animal residues. For this analysis, cores were sub-sampled at regular intervals of 2 cm. Samples were subsequently oven drying at 40ºC, homogenized and ground using agate mortar. Using the CM 5014 coulometer (UIC Coulometrics Illinois, USA) organic carbon was determined. Bulk samples of 20 mg were heated until to 900 ºC. The organic carbon proportion was estimated by the subtraction of inorganic carbon.

3.3.8-Microfacies analysis

Microfacies studies can provide valuable information about lamination micro-fabrics, sedimentological structures and the main mineralogical components (Brauer and Casanova, 2001). For this purpose, I selected varved sediment intervals of core AZ between 100 to 289 cm. According to the age model, this section represents the transition between Late Preclassic to Classic archeological period. A total of twenty-three overlapping thin sections of embedded epoxy-resin-impregnated sediments blocks (10x2x0.5cm) were prepared following standard procedures (Brauer and Casanova, 2001). For microfacies characterization and varve counting, an Olympus BX-53 microscope was used. Detailed thickness measurements of every seasonal sublayer, that form different varve types were performed using the 50x magnification objective. Varves were counted three times in order to estimate the standard counting error. The average age of massive layers was inferred using the sedimentation rates from neighboring varves.

3.4-Statistics

Principal component analysis (PCA) is a standard statistical method in geosciences. This technique provides a roadmap for how to reduce a large set of data to a lower and representative dimension (Shlens, 2014). PCA uses the covariance or correlation matrix to represent variables in the coordinate plane. Fundamentals goal concerning PCA are:

- Find relationships between variables
- Simplification or reduction of data matrix
- Variables selection

- Outlier detection

The PCA analysis was conducted on the XRF data set for identifying patterns, that represent diverse sedimentological and geochemistry processes in the lake. The most significant elements and components of different clusters were then selected and plotted through time. This analysis was performed using the statistical R environment with the Vegan packages.

Time series aims to evaluate underlying periodicity in the data. It thus helps to understand better physical-climatic processes, which generate the variability captured in a time series. In this work, Ti series in stages where anthropogenic activity was not present (see discussion section) were selected for time series analysis. For this propose, the Acycle software which integrates the analysis of paleoclimate time series using the Matlab programming language was employed (Li et al., 2019) using the following procedure: (1) The extraction of the long-term secular trend was conducted with a high-pass LOESS filter. (2) A continues wavelet transformation was performed using a Morlet wavelet type. The 95% confidence contour level was calculated used the chi-square distribution (3) Simple periodogram analyses were also used for the detection of underlying principal periodicities in the Ti series. Significative frequencies were then selected using Red noise analysis with a 99% percentage of confidence. (4) Based on the inferred prominent wavelengths and peridiograms cyclicites, Gaussian Bandpass was applied.

Chapter 4

Results

Polychromatic Chupicuaro figurines. Imaged by Tinajero Morelos

4.1-Results

Cores AZ and AR displayed a high correlation, described by the susceptibility curves and similar stratigraphic facies distribution (Fig. 4.1A). For this study, I selected AZ as a master core which is the longer and better-preserved sedimentary sequence. Moreover, the correlation between Hoya Alberca register and the study core using independent ages models is also high (Fig. 4.1B), allowing us to use the pollen and isotopic data from Hoya Alberca and core AR for % C for this study.

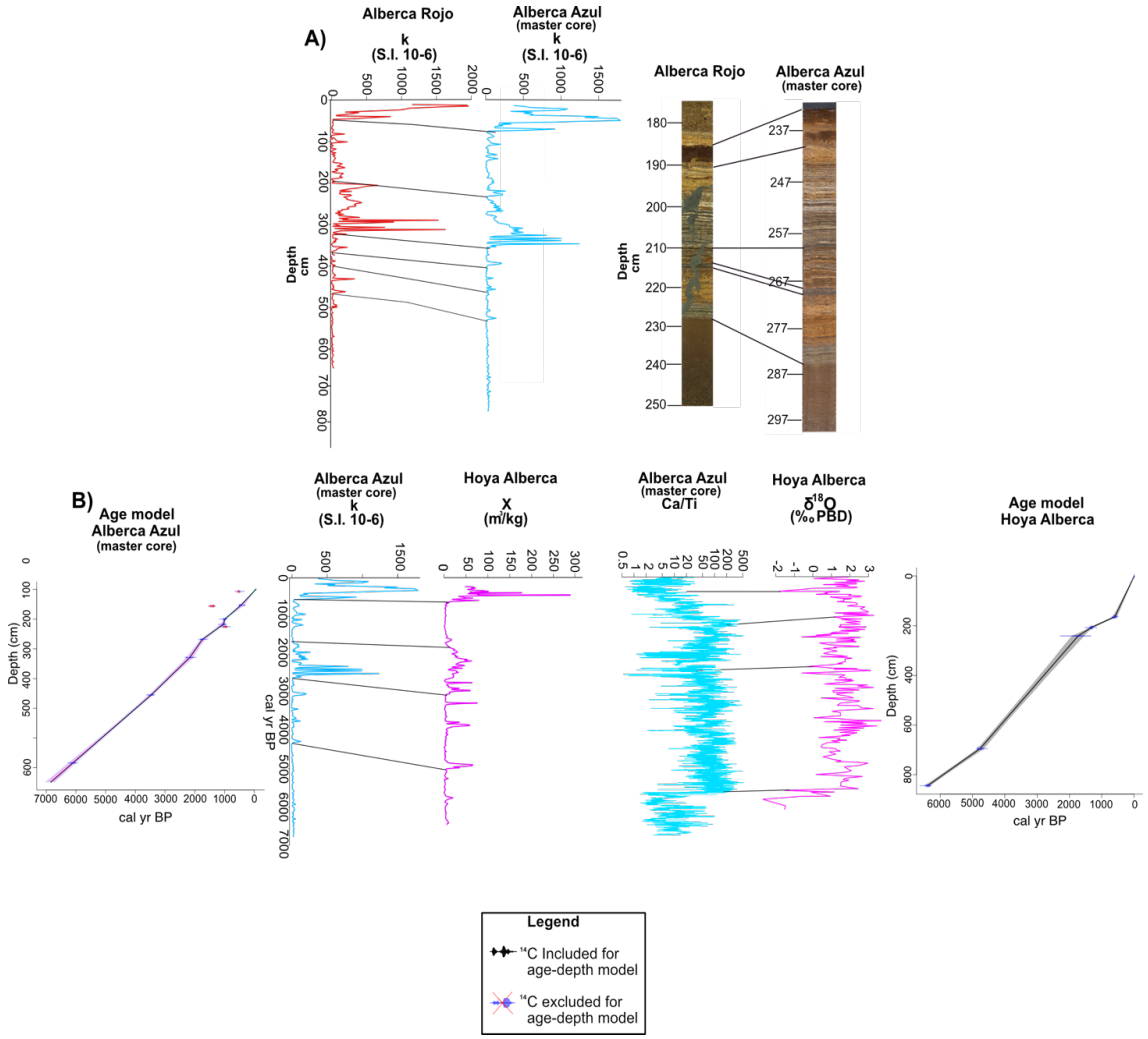

Figure 4.1- A) Correlation between Alberca Azul (master core) and Alberca Rojo cores using high resolution magnetic susceptibility curves and stratigraphic characteristics. B) Correlation between Alberca Azul (master core) and Hoya Alberca core, using high resolution magnetic susceptibility curves, Ca/Ti ratio from Alberca Azul and $\delta^{18}O$ from Hoya Alberca. The correlation was performed using independent ages model for both cores.

4.2-Lithostratigraphic

The stratigraphic section of “La Alberca” consists of five different lithostratigraphic facies (Fig. 4.2).

Facies A. These facies are mainly composed of silty-clay, with a high content of organic matter, like plants remains, and sporadic blurry white laminae.

Facies B. Consists of laminated white and dark shale. The white laminae are formed by well-preserved aragonite crystals, with a maximum size of 10 μm and the sporadic presence of calcite crystals. The dark laminae are composed of quartz, plagioclase, pyroxene, pyrite crystals, rounded volcanic lithics, rounded carbonate crystals, glass shards and remnants of macro-fossil plants. Different species of large littoral diatoms include *Nitzschia palea, Rhoiscophenia abbreviata, Nitzschia ovalis, Luticula frecuentissima, Luticula mutica, Gomphonema, Achcanthes minutissima, Nitzschia incospicua, Nitzschia palea and Navicula cryptotenella*. Between dark and white laminae, both erosive and flat contacts were observed. The third type of lamination observed in the record is entirely composed by *Nitzschia palea* and *Cymbella muerelli* species with dimensions less than 20 μm. More details are described in section 4.6.

Facies C. A poorly or non-laminated massive sandy-silt layer composed of all the components described for Facies B.

Facies D. Sandy layers, consisting of quartz, plagioclase, pyroxene, carbonate crystals, volcanic lithics and organic matter. The proportion of organic matter is higher than in facies C. This unit shows normal gradation, clasts of facies B floating in the matrix and occurrence of erosive contacts at the base.

Facies E. This unit consists of tephra layers mainly build up by plagioclase crystals of, angular shapes and with a maximum size of 200 μm. Glass shards and lithics are observed in less proportion (Fig. 4.2).

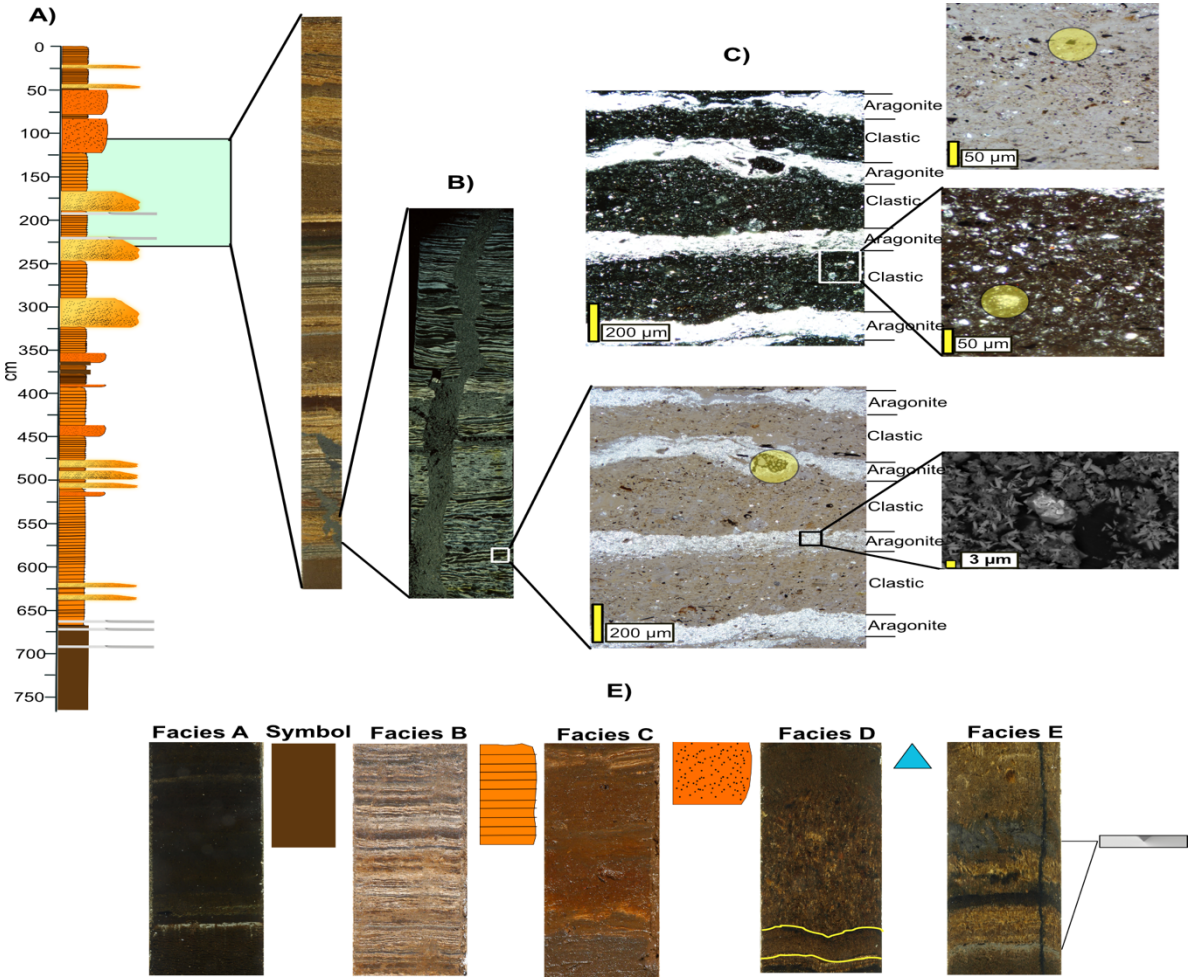

Figure 4.2-A) Stratigraphic column from AZ core, symbology and high-resolution images of the five lithostratigraphic units. The light green shadow area, displays the interval where thin sections were produced; B) Thin section photos of laminated sediments; C) Microscopic photo showing the two different type of laminations; D) From top to bottom: microscopic images of detrital lamination, displaying different characteristics like rounded carbonate crystals highlighted in a yellow shadow and organic matter. SEM image of aragonite crystals. E) Symbology of sedimentary facies. Massive organic strata (Facies A), laminated section (Facies B), massive strata (Facies C), turbidites (Facies D) and tephras (Facies E

4.3- Sediment chemistry

XRD results revealed the dominance of two principal groups of minerals: feldspars and calcium carbonates. The feldspars group formed by anorthite, anorthoclase and albite are widely distributed along the core. The carbonate group is composed of aragonite, monohydrocalcite, dolomite, and ankerite (Appendix 9).

I divided the core into six stages, using the variability in geochemical signature of Ti, Fe, magnetic parameters and facies distribution (Fig. 4.3). XRF logging results, in general, display a similar variation of Ti and Fe and this also holds for Ca/Ti and Sr. Ti and Fe are generally used to document the variations of terrigenous sediment delivery (e.g., Arz et al., 2003) and in the case of Fe as a redox-sensitive element (e.g., Sluijs et al., 2009). Fe may be found with O as Fe oxide minerals like hematite and magnetite around the catchment of the lake. Ti mainly comes from heavy minerals such as rutile (TiO_2), brookite (TiO_2), ilmenite ($FeTiO_3$), and titanomagnetite ($Fe^{2+}(Fe^{3+}Ti)2O_4$). Ti is not prone to a diagenetic or biological process. Ti and Fe often correlate well with magnetite susceptibility. High Fe in intervals with low *k* reveals Fe oxide dissolution and the correlation between Fe, Ti with *k* indicates that digenetic processes are minimal (Davies et al, 2015).

High values of Ti-Fe are observed in stage VI with the entirely presence of facies type A. The stage V is defined by uniform amplitude variations of Ti-Fe, magnetic parameters and facies type B. High amplitude variations of Ti-Fe, magnetic parameters and the alternations between facies type A, B, C and D describe the stage IV. The stage III comprises an increase in Ti-Fe, magnetic parameters and facies type B, C and D. High amplitude variations of Ti-Fe, magnetic parameters are again observed during the stage II with the presence of facies B and C. The stage I describes high intensities in Ti-Fe, magnetic parameters and facies type B and C.

The origin of Ca in lake sediments is commonly related with biogenic, detrital and endogenic sources. The consumption of CO_2 by algal blooms increase the pH and decreasing the solubility of the carbonates provoking its precipitation. High evaporation conditions in the lakes, increases the salinity modifying the pH as well (Drager et al., 2017). The precipitation evaporative minerals are reached as soon of a specific mineral solubility is reached (Zolitschka et al., 2015). Detrital carbonate input is produced by the erosion of rocks with a high content of carbonates around the catchment area such as volcanic rocks and limestones.

I used the Ca/Ti ratio to estimate the abundance of calcium carbonate minerals and to suppress the possible effect of detrital input from volcanic rocks with a high content of Ca located around the catchment area. In the record, a generally uniform increase of carbonates in the sediments is observed above stage V, but in stages III to I Ca/TI and Sr curves reveal a more variable in amplitude. The increase in carbonate concentration is related to the presence of facies type. The XRF Ti parameter reflects a high visual correlation with all mineral magnetic concentration parameters (e.g., *k* and SIRM), sensitive with detrital input, and clearly opposite trend respect the Ca/Ti ratio (Fig. 4.3, 4.4).

XRF results depend on the element concentration but also reacts with matrix effects, physical properties and the sample geometry. The high correlation of Ti-Fe XRF results and magnetic parameters dependent of ferrimagnetic concentration, both independent methods, suggest the low effects of these processes in the XRF data, allowing the use of individual elements in the results section (Fig. 4.3, 4.4).

Post depositional degradation of organic matter plays an important role in the diagenetic chemical changes in lake sediments. Microbial respiration of organic matter leads to oxidative degradation of reactive organic compounds in the organic matter. When the oxygen is depleted the next efficient oxide is used in the next order: nitrates, manganese oxides, iron oxides, sulphate and organic matter (Roberts, 2015). To determine the impact of redox diagenesis on the lake sediments the ratio Mn/Fe was used. Mn may be sensitive to redox conditions in the lake according to the progressive consumption of oxidants explained in the previous lines. An increase of this ratio is observed between stage VI-V, and stages IV and II display high amplitude variations.

The PCA results display two significant components (PCA1 and PCA2), which in combination explained the 99.95 % of the variance in the set of XRF data. The geochemical elements Ti, Fe, Si, Zr, Al, Ba, K, Rb, all sensitive to detrital input contribute heavily to PCA1 (Fig. 4.4). For this reason, in the discussion section, this component is employed as a lithogenic proxy. The PCA 2 is strongly shaped by geochemical elements related to the presence of carbonates such as Ca and Sr. Mn appears as an isolated element with a low correlation or anticorrelation with respect to the other cluster. This behavior may be related to the redox-sensitive of this element. The screeplot explains that the PCA1 retains the maximum number of variations, which is related to detrital input (Fig. 4.4).

4.4-Organic C

Percent of organic carbon of the sequence ranges from 4 % to 11.7 %. In general, the parameter describes roughly an opposite down-core trend with respect to magnetic

parameters. One prominent peak is displayed in stage VI. High variability of this parameter is captured in stages IV-II. The rest of the stages remained relatively stable with values around 6%, but slightly higher values are observed in stage V.

4.5-Stable isotopes $\delta^{18}O$ and $\delta^{13}C$

In general, both isotopic records ($\delta^{18}O$ and $\delta^{13}C$), displays similar trends. $\delta^{18}O$ and $\delta^{13}C$ values fluctuate between 2 to -3 ‰ and 0 to 8 ‰ respectively. Both isotopic records show high amplitude variations between 975 cm to 650 cm and minor variations until 350 cm. Two major amplitude variations are observed between 150 and 0 cm. In addition, the Ca/Ti ratio displays comparable variations with both isotopic records (Fig. 4.3).

4.6-Pollen

Amaranthaceae and *Zea-Mays* pollen records provide essential information about human disturbance related to agricultural activities. There are two major increases of the percent of both species. The first one occurred between 475 cm to 375 cm and the second one is observed between 100 cm to 0 cm (Fig. 4.3).

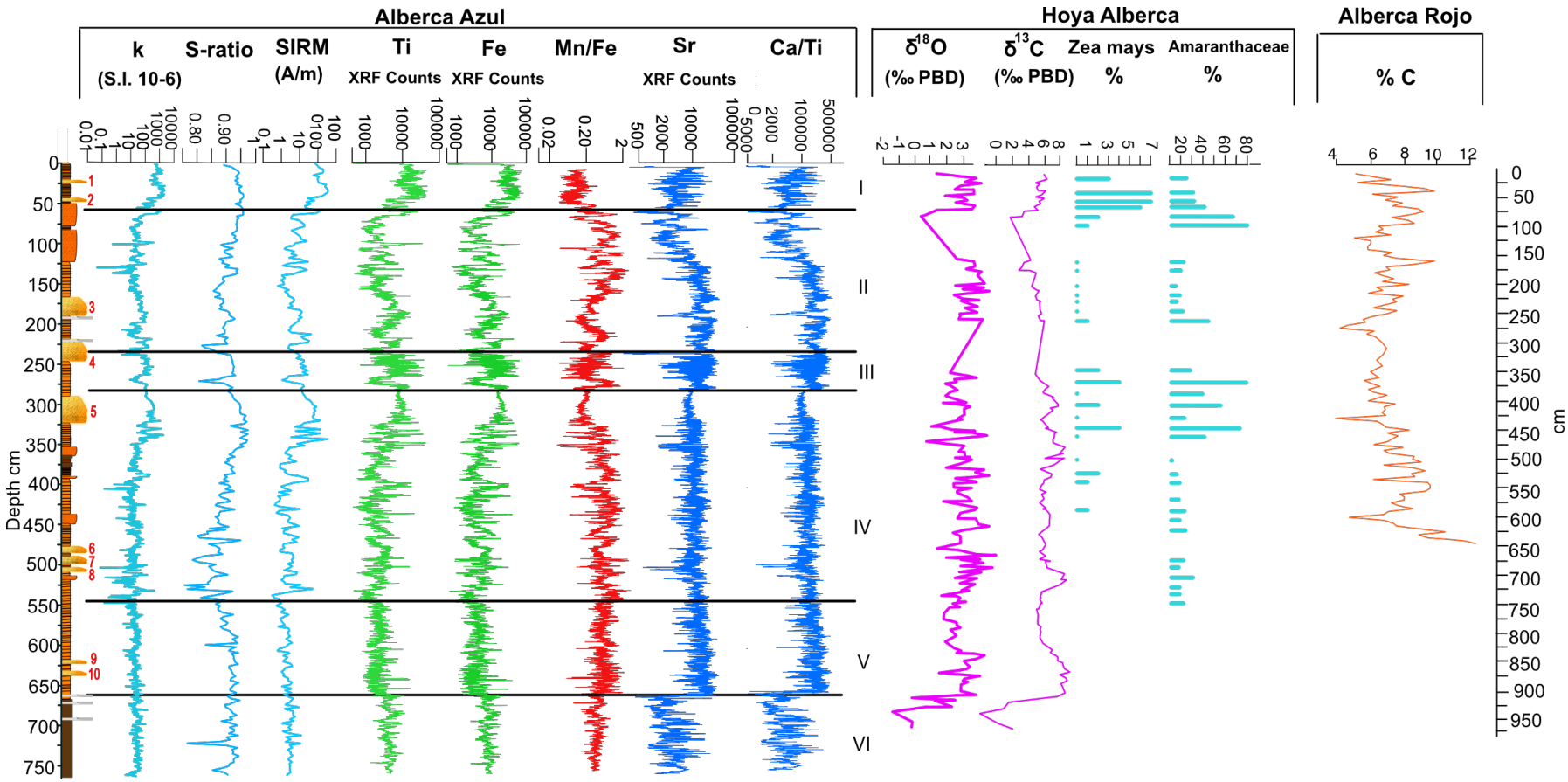

Figure 4.3- Alberca Azul Stratigraphic column and downcore, magnetic properties and X-ray fluorescence. From Hoya Alberca core, isotopes and pollen data. Magnetic susceptibility (*k)*, S-ratio, Fe and Ti are parameters sensitive to detrital input, Sr and Ca/Ti indicate the concentrations of carbonates. The Mn/Fe displays the redox conditions of the lake. Hoya Alberca record of $\delta^{18}O$ and $\delta^{13}{}^{3}C$ are representative of E/P ratios, and *Amaranthaceae*, *Zea mays* pollen are indicators of anthropogenic landscape disturbance. Using the variability on detrital, magnetics parameters and facies distribution, the master core is dived in six main stages. Turbidites facies are indicated by red numbers.

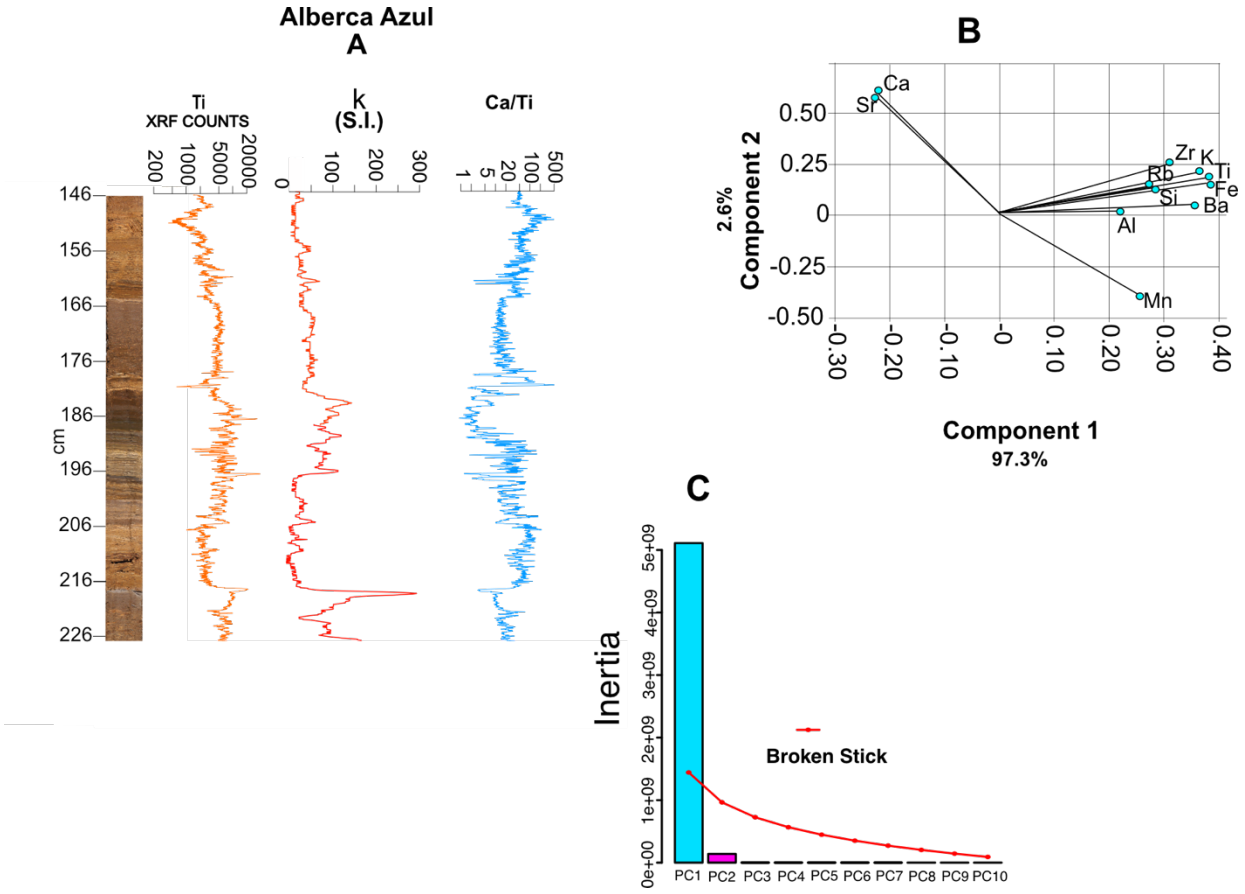

Figure 4.4-A) High resolution X-ray fluorescence data of Ti and Ca/Ti between 146-226 cm. B) PCA reveals three groups of elements: Ca, Sr, sensitive to carbonate presence Zr, Ti, Fe, Ba, Si, Al; indicative of detrital fraction; Mn, sensitive to redox conditions C) Broken stick of PCA.

4.7-Microfacies results

4.7.1- Sediment profile

I focus a detailed analysis on stage III (~175.5-236 cm) of the La Alberca lake sedimentary sequence. This stage is mainly described by the presence of alternations of dark-light laminations intercalated with massive layers. According to the stratigraphic characteristics and the degree of laminae preservation, six principal sub-stages were distinguished (Fig. 4.5).Sub-stages III.a, III.c, and III.f are characterized by the presence of well-preserved laminate sections, the sub-stage III.b is formed by alternations between well-preserved laminations and thick massive layers. The sections III.b and III.d are well described by low preservation in the laminae sequence.

4.7.2- Sedimentary textures of laminations

In the study sequence, three main layer types are observed and accordingly to their principal texture characteristics were classified as detrital organic layers (DOL), aragonite layers (AL) and organic layers (OL). Microscopic inspection reveals two typical successions of such layers: DOL-AL (Type 1) and DOL-OL-AL (Type 2) (Fig. 4.6 A, B). Type 1 seems to predominate in substages III.a, III.b, III.d and III.e. The type 2 predominates in substages III.c and III.f.

4.7.3- Laminate characteristics

This red-brown layer is mainly comprised of clastic detritus, organic detritus, and plant fragments supported in an organic mud. The thickness of this layer oscillates between 1.40 to 0.20 mm with flat and erosive contacts. The largest thickness is observed in stages III.c and III.f. (Fig. 4.5). The clastic detritus fraction consists of feldspars (anorthite, anorthoclase, albite), quartz, pyrite crystals with angular shapes, rounded carbonate crystals and rounded andesitic lithic fragments bigger than 3 mm. The organic mud is composed by highly preserved and broken valves of planktonic diatoms such as *Nitzschia palea, Nitzschia ovali, Nitzschia incospicua, Nitzschia palea*, *Navicula cryptotenella* and *Cymbella muerelli*. Ostracode shells occur rarely (Fig. 4.6 A.1).

The aragonite layers have a maximum thickness of 1.26 mm and a minimum thickness of 0.10 mm. The maximum thickness variability is described in sub-stage III.c (Fig. 4.5). This layer is dominated by the presence of aragonite crystals with rice shapes form, not longer than 0.01 mm. The dominance of aragonite is corroborated by SEM images and XRD analysis (Fig. 4.6 A.1) calcite is rare in this layer and no gradation in crystals sizes is observed.

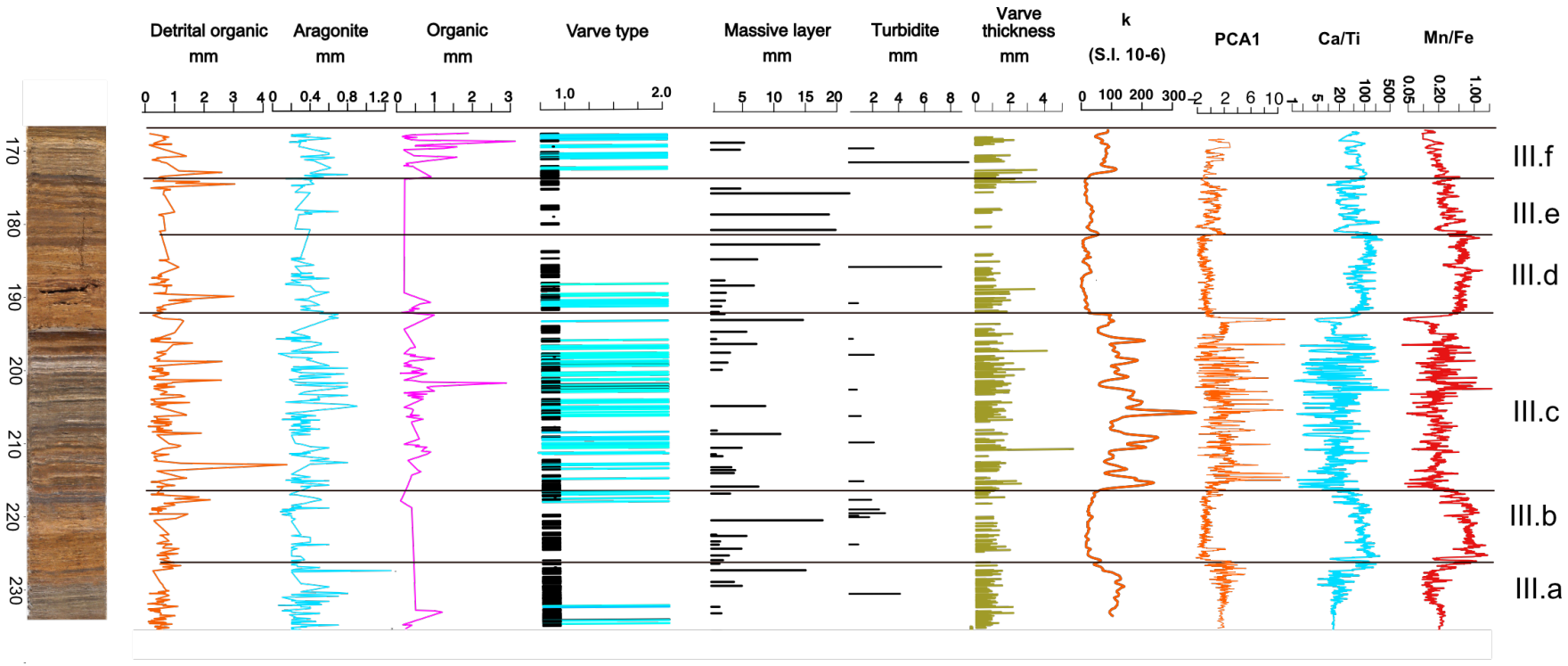

Figure 4.5-Stratigraphic column of La Alberca lake between 170 to 230 cm. Thickness of detrital-organic, aragonite, organic, turbidite and massive layers. Measured thickness of Type 1 and Type 2 varves and its pre magnetic susceptibility, XRF data such as PCA1, Ca/Ti and Mn/Fe ratios**.**

The thickness of these layers is between 0.14 mm and 1.60 mm. It is entirely formed by well-preserved diatoms valves and is only observed in sub-stage III.a and III.f (Fig. 4.5). *Nitzschia palea* species dominates the assemblage, however, some other of its variants (*Nitzschia ovali, Nitzschia incospicua*) and *Cymbella muerelli* species are present as well (Fig. 4.6 B.1).

Massive red-brown or white layers at naked eye seems to be homogeneous, nevertheless, microscopic observations reveal that they are mainly composed by reworked carbonate crystals, clastic detritus such as feldspars crystals, fragments of diatoms valves and in low proportion reworked plant debris (Fig. 4.7 A). The maximum thickness (20 mm) of this layer is present in stages III.b and III.f (Fig. 4.5). Turbidite layers are graded, ranging from fine sand to clay size at the top, and with an erosive contact at the base (Fig. 4.7 B). The layers are dominated by the presence of angular classic detritus and a high content of organic debris, such as plants remains. These layers are observed in all the section, increasing its thickness in sub-stages III.d and III.f (Fig. 4.5).

4.7.4- XRF element scanning

The PCA 1 reflects detrital delivery during periods with high runoff , variation in carbonate precipitation is described with the Ca/Ti ratio, and oscillation between anoxic/oxic conditions in the hypolimnion of the lake is given by Mn/Fe ratio. Ti reveals a high detrital input in stages III.a, III.c and an increasing trend between III.e and III.a sub-stages (Fig. 4.5). The high concentration of carbonates correlates well with the increase on anoxic conditions suggested by the Mn/Fe ratio, especially on the sub-stages III.b and III.d characterized by low laminae preservation. High amplitude variations in the three parameters occur on the sub-stage III.e..

4.7.5- Magnetic susceptibility

The magnetic susceptibility curve reveals a high concentration of ferrimagnetic minerals on the sub-stages III.a and III.f. The high(low) presence these minerals correlate well with the increase(decrease) of the thickness of DOL and Ti, suggesting a relation between detrital input and the magnetic susceptibility (Fig. 4.5).

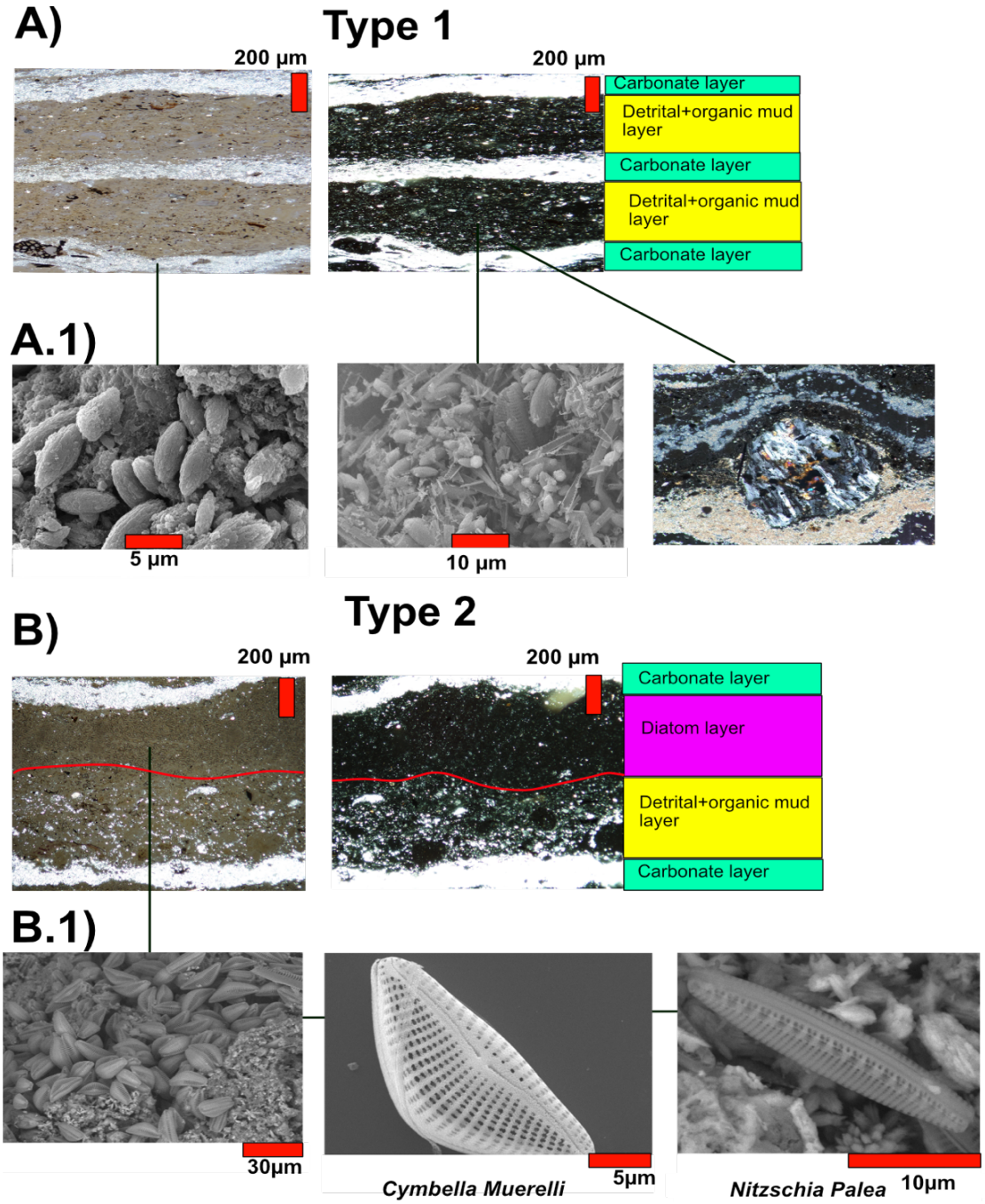

Figure 4.6- (A, B) Thin section photos, SEM images and layer arrangement of varve type 1 and varve type 2. (A.1) From left to right: SEM images of aragonite crystals, organic mud and detrital lithic. (B.1) From left to right: SEM picture of diatom bloom and the principal diatom species (*Cymbella murelli and Nitzschia palea*).

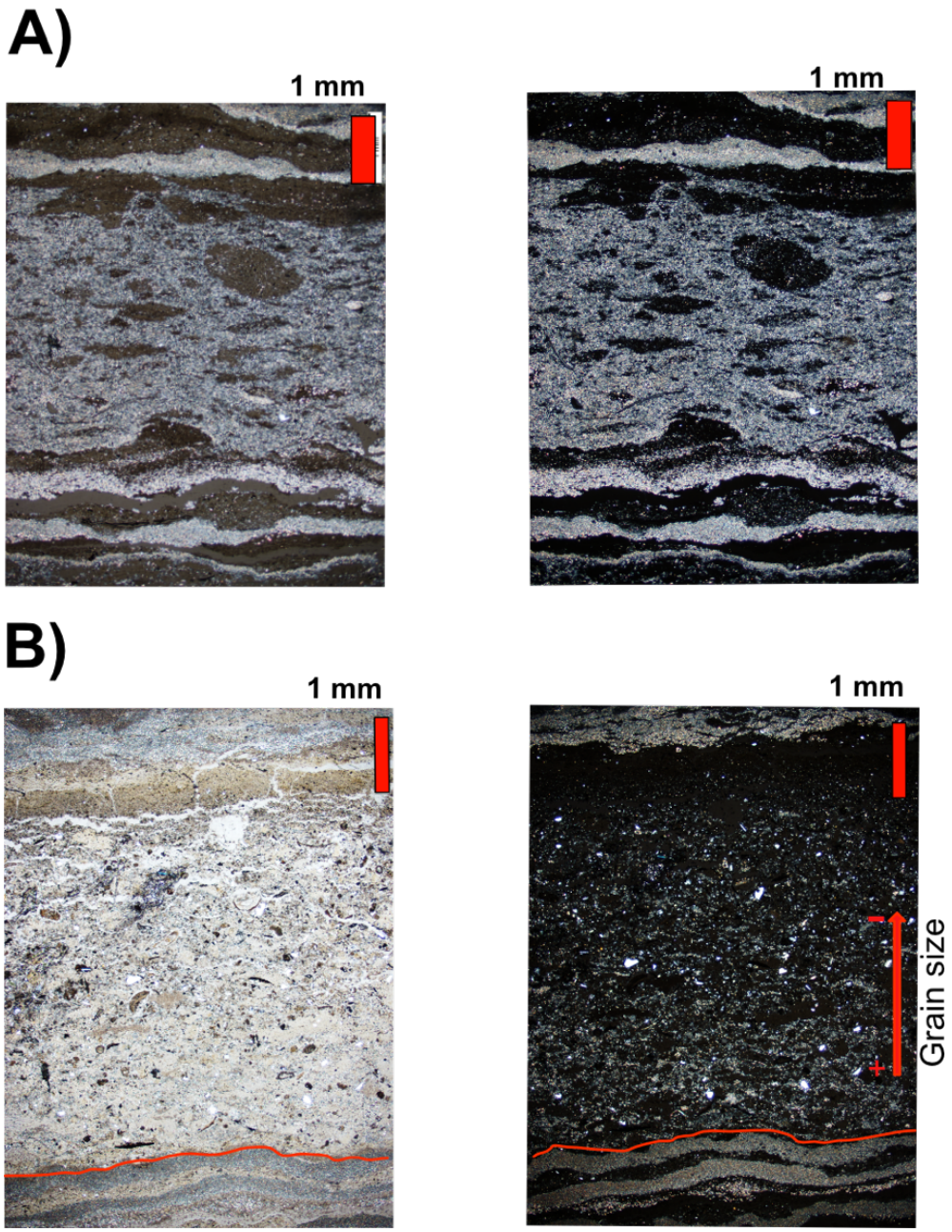

Figure 4.7-A) Thin section photos of massive layers with parallel and crossed Nichols. These layers comprise a mix of detrital, calcium carbonate and organic components. B) Thin section photos of turbidites layers with parallel and crossed nichols. These layers display normal gradation, erosive contacts and high content of organic material.

4.8-Magnetic mineralogy

4.8.1- Concentration dependent magnetic parameters

In general terms, all magnetic concentration-related parameters, such as *k*, SIRM, and ARM, follow similar down-core variations (Fig. 4.8). The correlation between magnetic susceptibility and parameters related to magnetic remanence (e.g., SIRM-ARM), indicates that magnetic susceptibility is sensitive to change in the proportion of ferrimagnetic minerals.

Variations of bulk magnetic-concentration parameters *k*, SIRM, and ARM together with Ti XRF counts, and facies distribution define six main stages; three peak stages (III, IV and VI) and three background stages (I, II and V) (Fig. 4.8). Peaks IV and VI are dominated by high magnetic susceptibility values and strong magnetization, indicating a high abundance of ferromagnetic minerals. The peak III is described by an increasing trend of concentration of ferrimagnetic minerals reaching its maxima around 350 cm. Low magnetic susceptibility and magnetization levels in stages VI, V and IV can be related to the abundance of dia-paramagnetic and low content of ferrimagnetic minerals. In addition, a notable difference in amplitude of the oscillation of these parameters are observed. Stages I and II show small amplitude variations, contrasting with stages III and IV where the largest amplitude variations on the magnetic parameters occur throughout the core.

4.8.2-Grain size dependent magnetic particles ratios

Grain size indicators such as kARM ARM/SIRM and kARM/k_{LF} display comparable amplitude variations, but kARM/k_{LF} appears to be the most sensitive parameter. Higher values of Karm suggest the dominance of stable single domain (SD) particles in the zones I, III and at the end of stage IV. The inter-parametric ratios ARM/SIRM, kARM/k_{LF} follow broadly the same distribution, but with some particularities. The lowest values of kARM/k_{LF} occur during stage III, also suggesting that the increase in concentration parameters is a response to increase multi-domain (MD) particles. Similarly, the upward increase in concentration parameters in stage IV is accompanied by an upward decrease in kARM/k_{LF}, suggesting an increase in magnetic particle grain size. Relatively higher content of SD magnetic minerals is observed in stage IV. Stages VI, IV and II are characterized by high amplitude variations in all the inter-parametric ratios (Fig. 4.8).

4.8.3-Type of magnetic minerals

The S-ratio shows systematic variations in all the zones, indicating that magnetic mineralogy is not homogenous. Besides, the good agreement with magnetic parameters dependent on concentration, like *k* and SIRM, suggests that these parameters are representative of the concentration of the ferrimagnetic minerals (Fig. 4.8). The MDF and ARM show a clearly opposite trend with respect the S-ratio. This supports the inference that low coercivity particles, display S-ratio values close to one. Both parameters, MDF and S ratio, indicate that low coercivity ferrimagnetic minerals dominate the stages III, the upper section of stage IV and I. A drastic increase in the anti-ferromagnetic fraction is observed at the base of stage IV. Stage II displays high amplitude oscillations, between anti-ferromagnetic and ferrimagnetic fractions (Fig. 4.8).

4.8.4-Hysteresis curves

Hysteresis curves for selected samples show simple shapes with either paramagnetic or diamagnetic contributions. Curves suggest for the most part a single magnetic phase since there is no evidence of wasp-waisted contours. Nevertheless, there is a systematic behavior between the background stages (VI, V, and II) and peak stages (IV, III, and I) (Fig. 4.9). For the background stages (e.g., stage II and the first section of stage IV), the samples do not reach saturation of the magnetization, due to the strong contribution from diamagnetic minerals. On the other hand, peak stages (e.g., stages I and II) exhibit narrow curves with low coercivity values (Fig. 4.9) and small contributions from paramagnetic minerals.

4.8.5-FORC Diagrams

FORC diagrams are useful to describe the distribution of the coercivity and interaction fields of magnetic minerals (Liu et la., 2012). In this study, FORC diagrams for representative samples of stages VI and IV show coercivity peaking at ~ 40 mT and open contours that diverge away from the origin in the Hu axis ~ 40 mT (Fig. 4.9). This pattern is related to the presence of PSD magnetic minerals (e.g., Muxworthy and Roberts 2007).

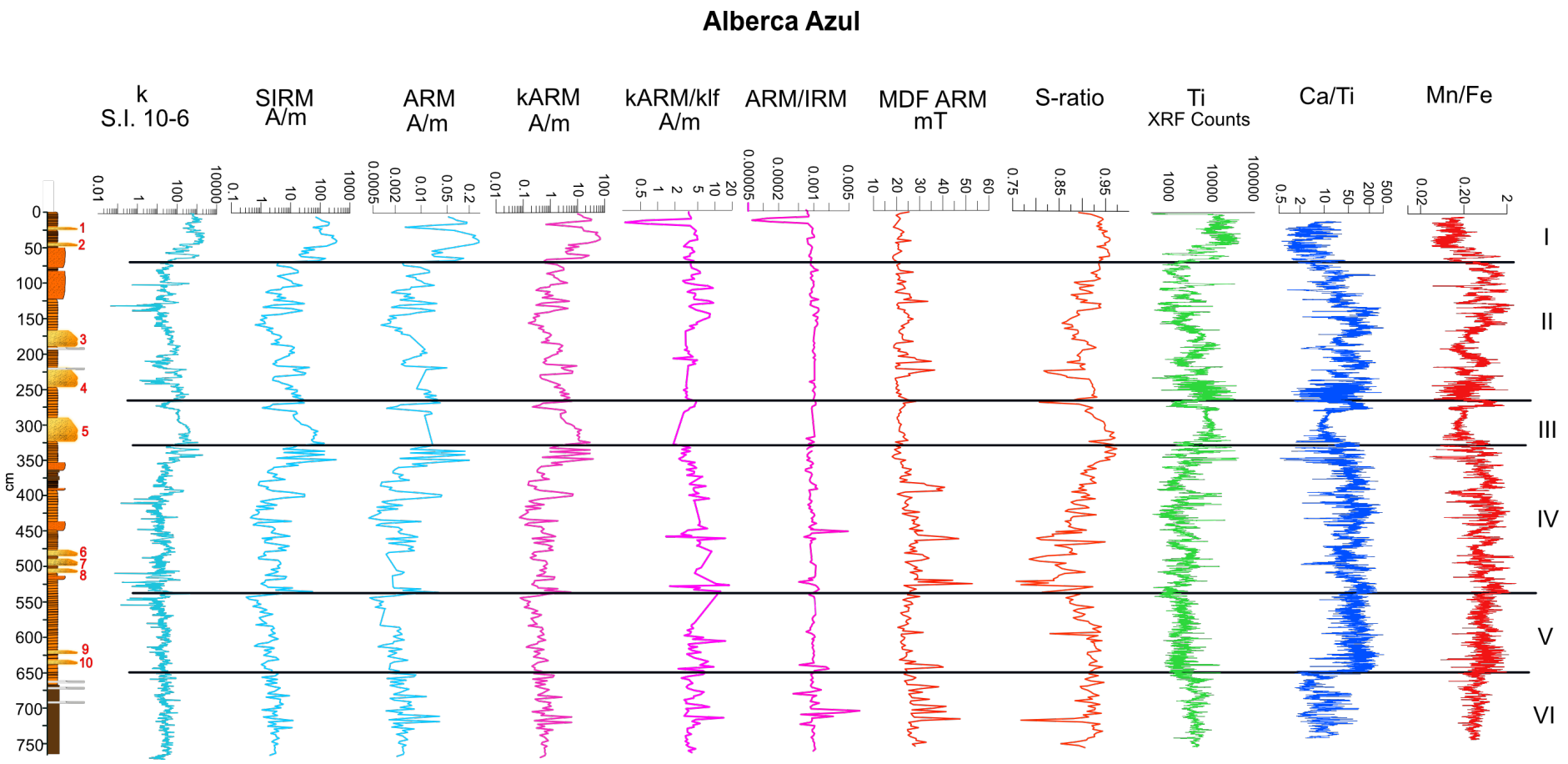

Figure 4.8- Down core variations of magnetic properties and stratigraphic column of "La Alberca" maar lake. Red numbers on the stratigraphic column represent turbidites. Magnetic parameters with blue lines(k, SIRM, and ARM) are sensitive to the concentration of ferromagnetic fraction, parameters with purple lines (kARM ,ARM/SIRM and kARM/klf) are sensitive to grain size of ferrimagnetic minerals and parameters with red lines (MDF, ARM and S-ratio) are sensitive to the presence of ferrimagnetic minerals. Solid black lines indicate the division of the six main stages.

4.8.6-Thermomagnetic curves

Temperature-dependent magnetic susceptibility (*k*-T) curves of magnetic extracts, performed on argon atmosphere, show similar behavior for stage I and the final part of stage IV. An inflection or hump of the *k* is observed between 50-100 ºC, probably produced by the dehydration of clay-minerals or crystalline iron (oxyhydr)oxides, such as goethite (De Boer and Dekkers, 1998). The rest of the *k* decays around 560-580 ºC, which likely reflects the presence of low Ti- magnetite as the main magnetic mineral (Özdemir and Dunlop, 1997) (Fig. 4.10). Most of the samples do not display a reversible trend during the heating/cooling process and have a lower susceptibility than of the unheated sample, which indicates the transformation of original magnetic mineralogy to a lower susceptibility phase (such as oxidation to form hematite). Other samples have higher susceptibility after heating, indicating creation of a magnetic phase during the experiment (such as alteration of metastable Fe bearing minerals to form magnetite).

4.8.7-IRM coercivity spectrum analysis

Statistical analysis of coercivity spectra in representative samples of stages I and III, identified two types of components. A low coercivity component is present in both stages, with a mean coercivity B1/2 of ~15– 20 mT and a wide dispersion DP of 0.36. Low coercivity values suggest the presence of ferrimagnetic minerals such as (titano)magnetite. In a few sites, a high coercive force contributes to the IRM in small proportion (~10%) to the IRM; it could be related to hematite or goethite, but the mean coercivity suggests that hematite is more likely (Heslop et al., 2002) (Fig. 4.10).

.

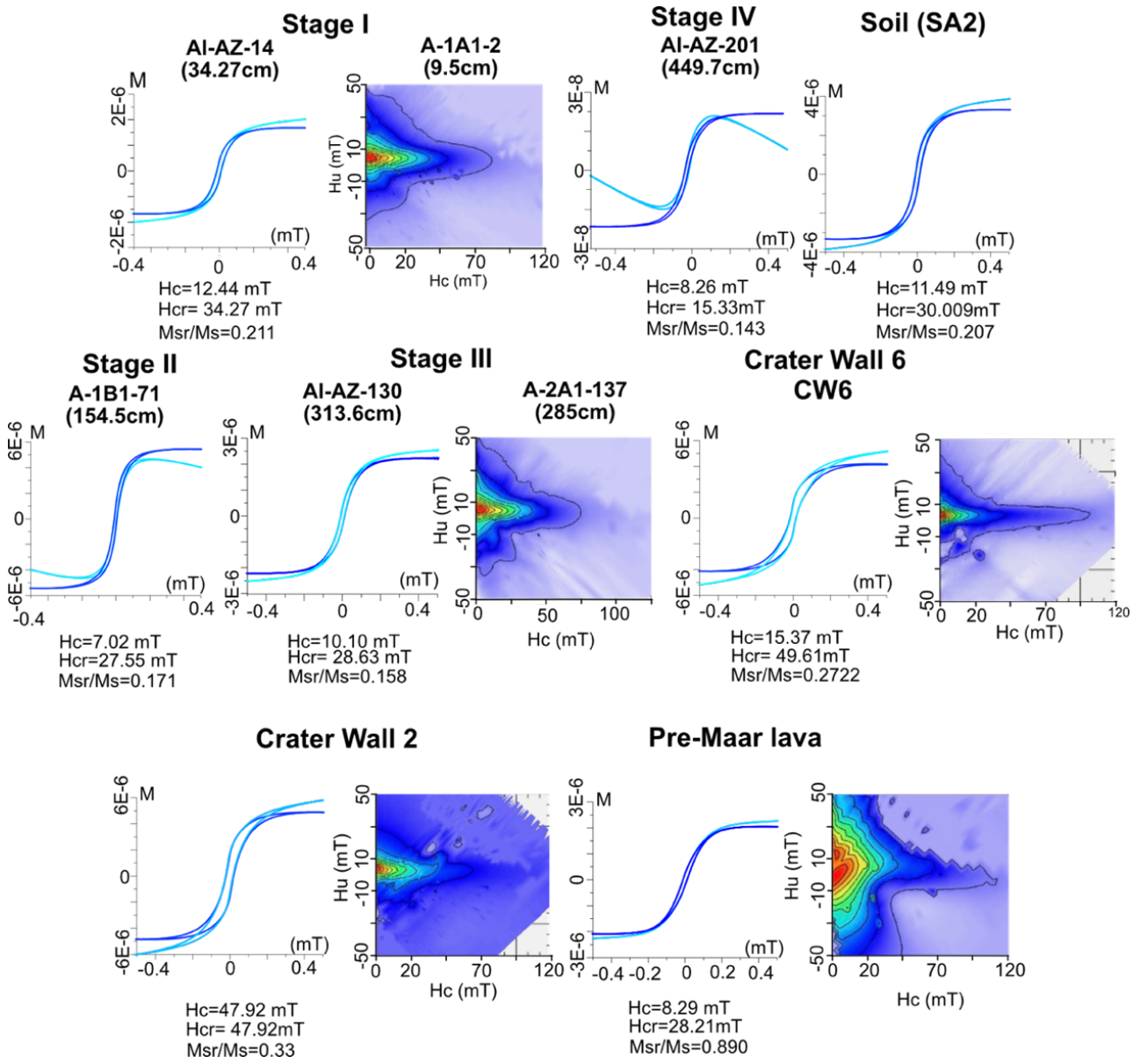

Figure 4.9- FORC diagrams and hysteresis loops for representative samples of the “La Alberca” lacustrine sequence, soil located around the lake, crater walls and pre-maar lava. Dark blue solid line represents the hysteresis loop curve after the subtraction of dia-and paramagnetic contribution.

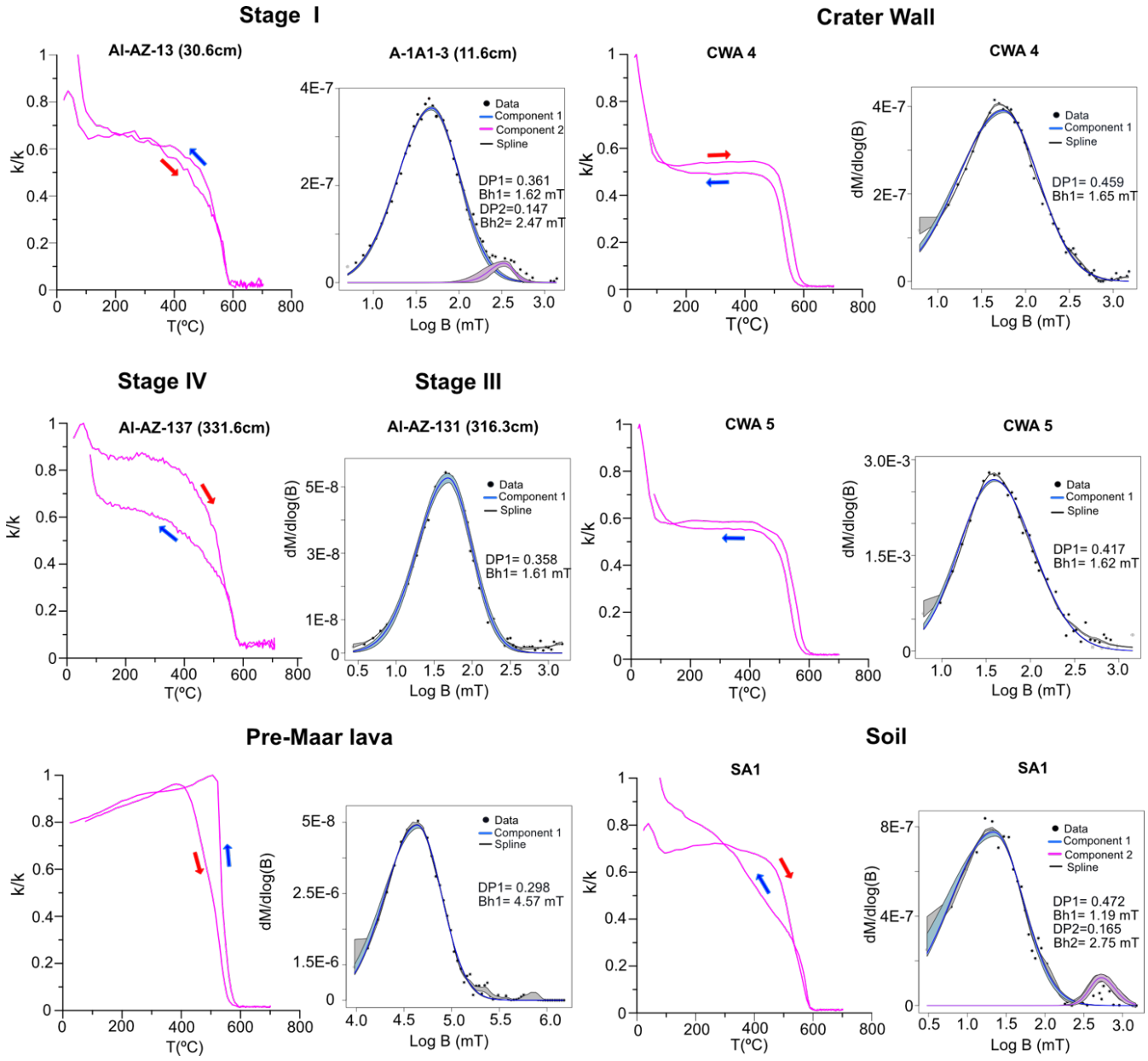

Figure 4.10- Normalized temperature-dependent magnetic susceptibility and spectral analysis of isothermal remanent magnetization acquisition curves of selected samples. Red arrows on normalized temperature-dependent curves indicate heating process and blue arrows indicate the cooling process. Black dots on coercivity spectrum represents the coercivity distribution, blue and purple lines, indicates the number of magnetic components and shaded area represents error envelopes of 95% confidence interval. Coercivity (Bh) and dispersion parameter of every (DP) component is also displayed.

4.9-SEM description

Complementary description of magnetic mineralogy using SEM images and EDS analysis on magnetic extracts from all six stages reveals that the main iron oxides found in all the stages are: (titano-) magnetite (Fig. 4.11A,B, 4.13A, 4.12E), (titano-) maghemites (Fig. 4.11D,4.13B), hematites and skeletal ilmenites (Fig. 4.12A ,D). Iron-carbonates like siderite and iron sulfurs such as cubic and framboidal aggregates of pyrite were also observed (Fig. 5.5B, 5.6D).

Stages III, I and the final part of stage IV (peaks) are dominated by high concentrations of (titano-) magnetites and (titano-) maghemites particles (Fig. 4.11A, B, C, D, 4.13, A,B). The form of the crystals varies from idiomorphic cubic-octahedral to broken crystals with irregular shape and their size varies between 3 to 30 μm (Fig. 4.11 A, B, C, Fig. 4.12 E). Some crystals show abundant shrinkage cracks on its surfaces which is a clear indication of maghemitization (e.g., Nowaczyk, 2011) (Fig. 4.11D, Fig. 4.13B).

In comparison, the magnetic mineralogy in stages VI, V and II (backgrounds) in different; (titano-)magnetite and (titano-)maghemites particles are less abundant; also, they present irregular shapes, shrinkage-cracks, and abundant crystals with a skeletal ilmenite lamella (Fig. 4.11D, Fig. 4.12A,D, Fig. 4.13B). Iron sulfide (pyrite) is also present in the background stages, with crystals that have either a cubic shape or the typical framboidal aggregate structure (Fig. 4.12B,4.13D). The size of the crystals varies between 1 to 10 μm. Additionally, iron carbonates like siderite with irregular shapes, and sizes around 20 μm are observed in these stages (Fig. 4.13C).

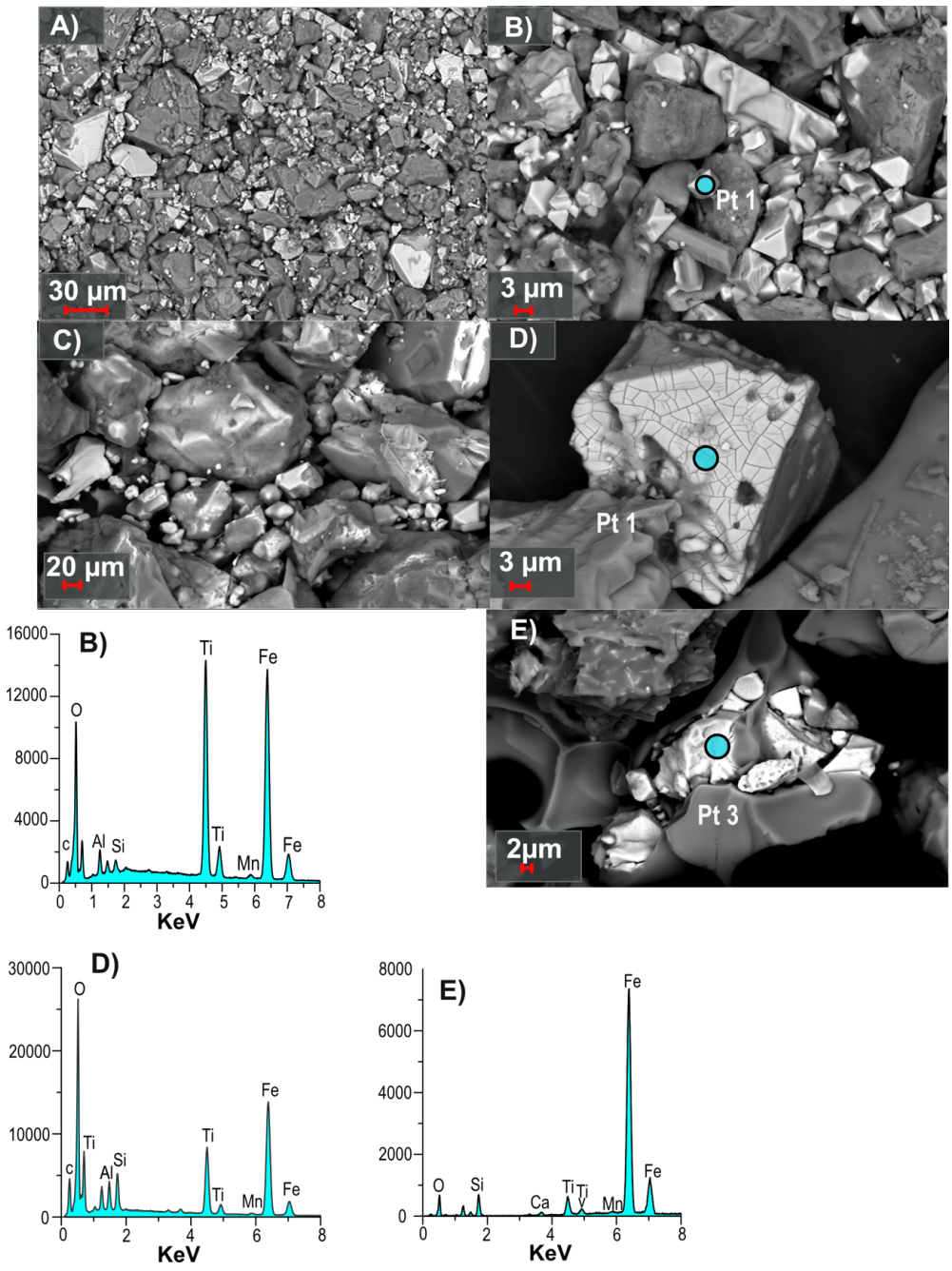

Figure 4.11- Representative SEM images of stages VI, IV and III. High concentration with diverse grain size and shapes of (titano-) magnetites (A), close view of (titano-) magnetites with octahedral shapes (B) (C), (titano-) magnetites with shrinkage-cracks indicative of mahemitazation process and small crystals of (titano-) magnetites inside of a volcanic glass shard (E). Blue circles indicate locations of X-ray spot element analysis.

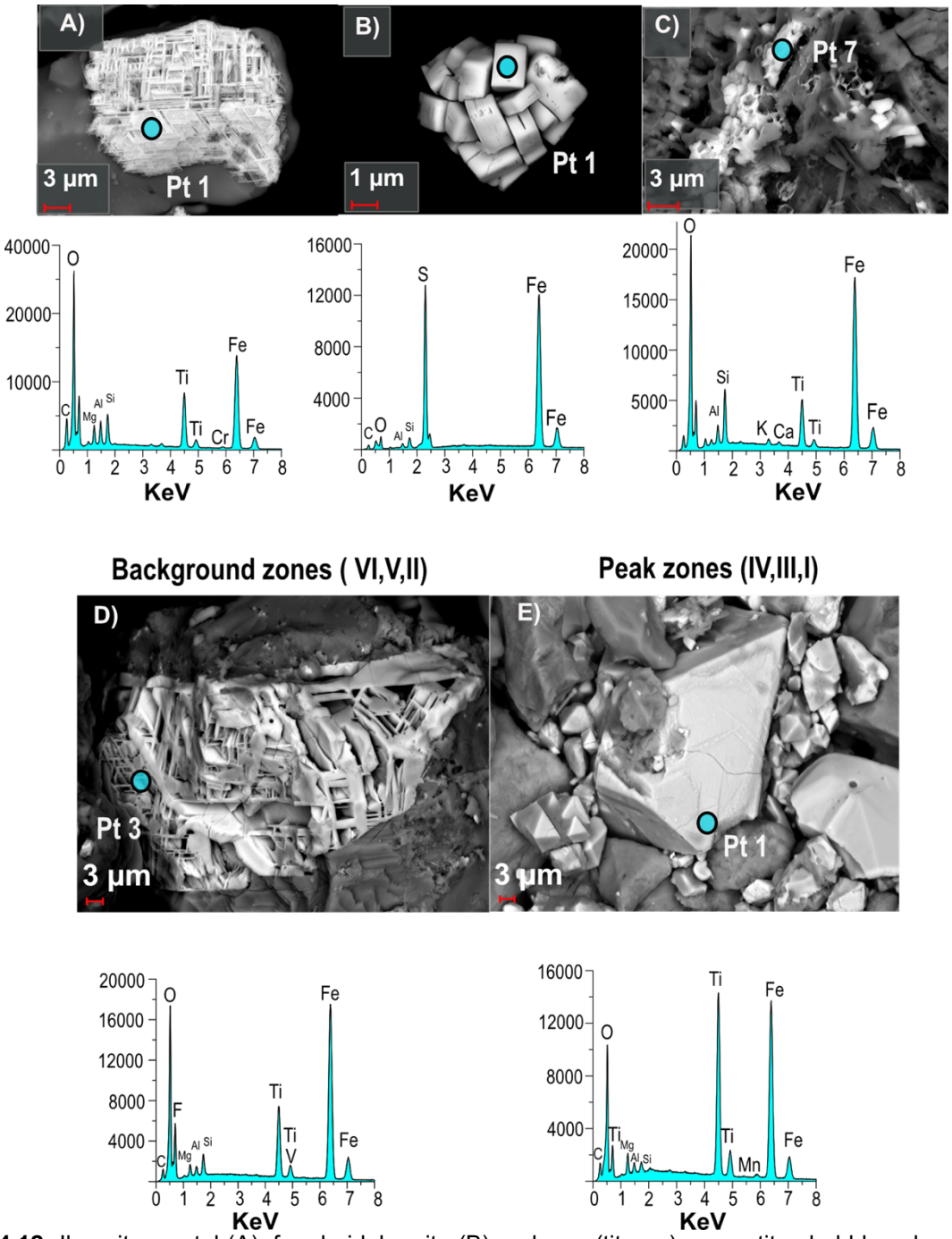

Figure 4.12- Ilmenite crystal (A), framboidal pyrite (B) and rare (titano-) magnetites bubbles observed on background stages (V,II,I).Comparison between typical magnetic crystals found it in background stages (V,II,I) and peaks stages (VI,IV,III) (D, E). Background zones are dominated by the presence of ilmenite crystals or (titano-) magnetites affected by dissolution and peak stages (VI, IV, III) by mostly well-preserved (titano-) magnetites with octahedral shapes. Blue circles indicate X-ray spot element analysis.

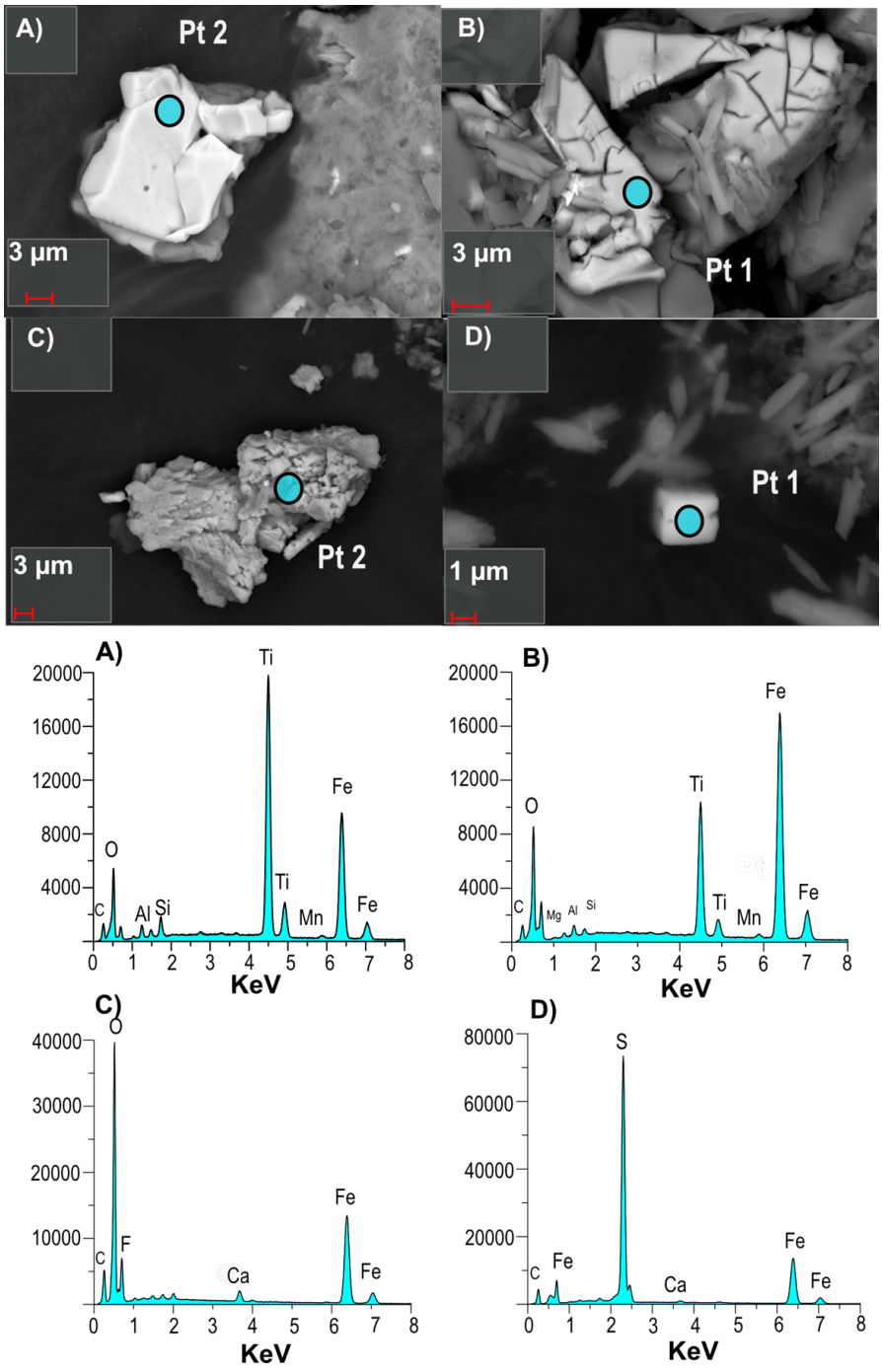

Figure 4.13- Some other typical crystals found it on background stages (V, II, I). Irregular shaped borders (A) and etching features (B) indicate the dissolution process (B) of (titano-)magnetites crystals. Iron carbonates like siderite (C) and cubic pyrite (D) are also common.

4.10-Magnetic properties of catchment area samples

Samples from soils located around the lake area but within the crater, volcaniclastic material of the crater walls and pre-maar lava exposed in the crater were collected for the study of their magnetic properties and determine the possible sources and genesis of magnetic crystals in the lake sediments.

Principal rock magnetic features of soil samples are: Curie temperatures ~580 ºC; the presence of two components to the IRM derived from coercivity spectrum analysis, with B1/2 of ~11 mT, DP of 0.47 and B1/2 of ~27 mT DP of 0.16 respectively (Fig. 4.10). Hysteresis loops have a narrow shape with low coercivity values of about ~1.19-276 mT (Fig. 4.10). SEM images describe a high concentration of (titano-) magnetites with idiomorphic cubic-octahedral shapes, broken shapes and incipient presence of exsolution lamellas (Fig. 4.14 A, B, E).

Samples of volcaniclastic material from the crater wall, exhibit Curie temperatures of 580 ºC and the coercivity spectral analysis displays the presence of only low coercivities components with B1/2 of ~16.5 mT- 16.2 mT and wide range of coercivities (DP between ~0.45) (Fig. 4.10). Hysteresis curves have wasp-waisted contours with coercivities between 15 and 47 mT. FORC diagrams have a coercivity peaking at ~70 mT and closed contours in the Hu axis ~20 mT (Fig. 4.9). SEM analysis reveals the presence of titano-magnetite with idiomorphic cubic-octahedral shapes or broken shapes with sizes between ~1-100 μm (Fig. 4.14). Moreover, overgrows of hematite were observed on the titanomagnetite surfaces. These characteristics suggests that titano-magnetite and autogenic hematite are present in the crater wall samples (Fig. 4.14 C, D).

Pre-maar lava samples have Curie temperatures around 560-580 ºC, one predominant moderate coercivity component with B1/2 of 45 mT and DP around 0.3 (Fig. 4.10). Hysteresis curves are narrow, with coercivities around 8.29 mT, and FORC diagrams are characterized by moderately high coercivity peaking around 80 mT and open contours shape along the Hu axis up to about 50 mT (Fig. 4.9).

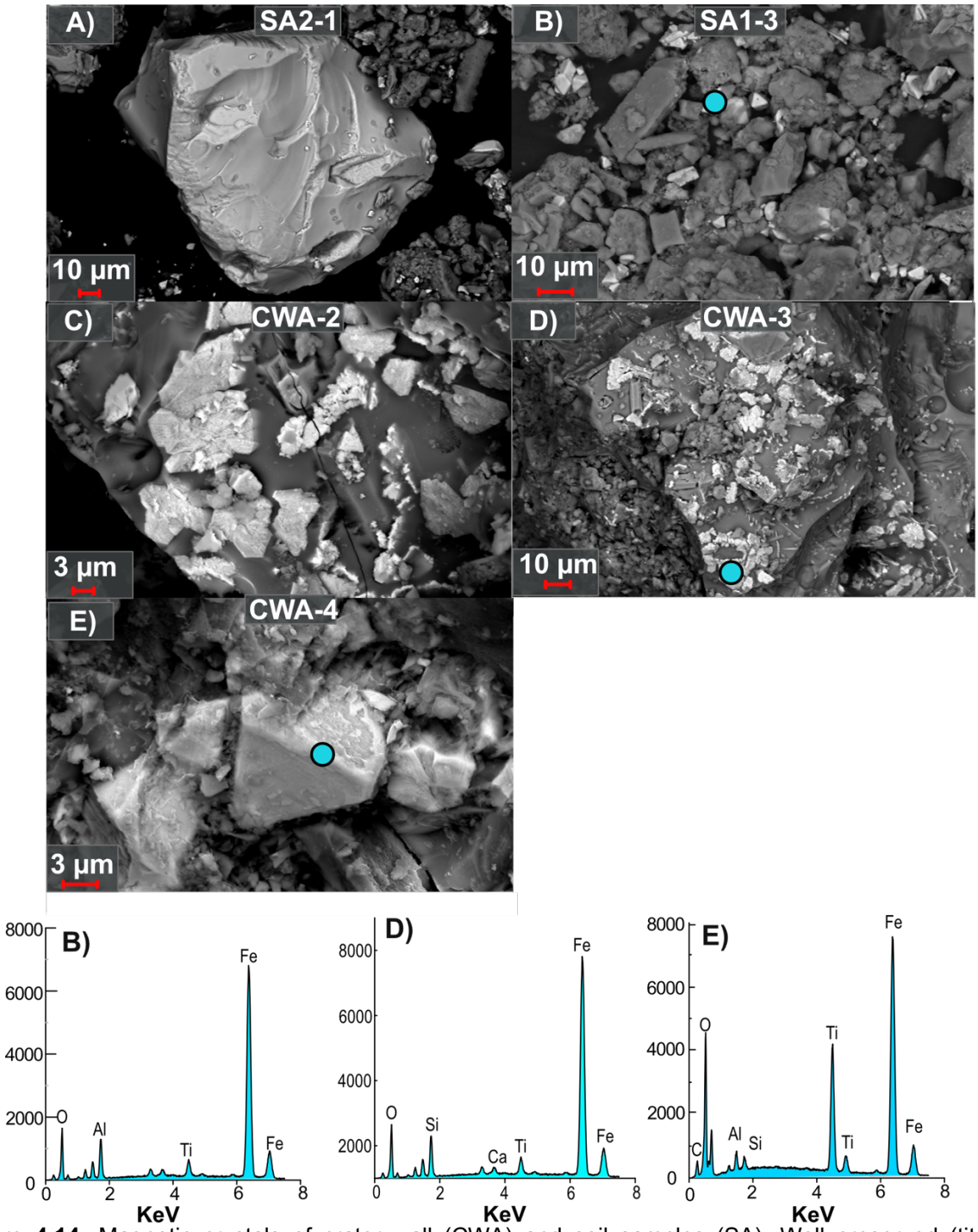

Figure 4.14- Magnetic crystals of crater wall (CWA) and soil samples (SA). Well preserved (titano-) magnetite crystal in soil sample and high concentration of (titano-) magnetite crystals with diverse shapes and sizes (B). Intergrows of hematite on (titano-) magnetite surfaces (C, D) observed on crater wall samples. Octahedral (titano-) magnetite crystal (E).

4.11-^{14}C ages

First of all, I excluded ten type facies D deposits, which I interpreted to be formed by rapid sedimentary processes that do not represent significant time in the chronology but have a considerable thickness (see Discussion) (Appendix 10). The results of the AMS ages are displayed in Table 4.1. In general, most of the ages increase with depth, however, four of the twelve ^{14}C ages did not continuously increase with depth. The ages at 7 cm and 56 cm had older age than the expected. Those samples were identified as an aquatic plant (Michael Slowinski, personal communication), which are susceptible to hard water effects (Philippsen, 2013). Therefore, I decided to remove these data from the age model. The sample at 125.5 cm was also removed because it presented an inverted age compared with the close samples. On the other hand, the AMS ages at 261.5 cm and 646 cm, were collected from bulk of organic matter. These samples appear to be old ages with respect to the others. I attributed this to the presence of old reworked carbon matter, thus both ages were removed from the age model and extrapolation was performed to know the maximum age of the core (Fig. 4.15). In conclusion, the maximum age of the age model is 6748 cal yr BP and the calculated local sedimentation rate varied from 0.08 to 0.35 cm/yr.

For varve counting, (see chapter 4 results and discussion section) two radiocarbon dating constrain the study section (~175.5-238 cm) dating at 1810 ± 30 (168 cm) and 2150 ± 30 (229 cm). According to the weighted mean average of the calculated ages for the study section the error is ±205 years. This section covers a calendar time interval between 204 CE-309 BCE, which corresponds to the final part of the Pre-Classical archeological period. Triple varve counts of the study section display a standard error of 12.01 %. The age model reveal that the sedimentation rate observed in this section is 0.14 cm/yr, which is the highest in all the sedimentary sequence (Fig. 4.16).

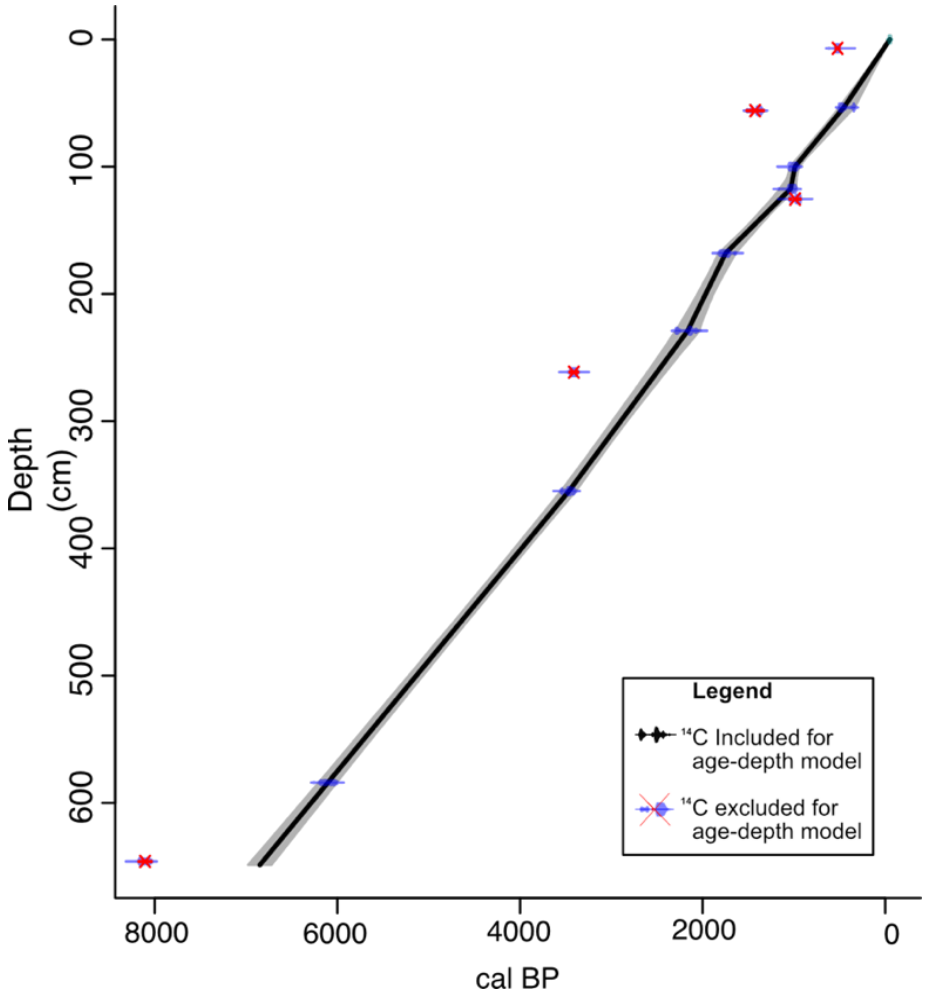

Figure 4.15-Age-depth model of "La Alberca" maar lake. Light blue and purple shading represent the accumulated error of the data; black marks represent the included data in the model; data with the red mark are excluded from the model.

Table 4.1- AMS ^{14}C data acquired from terrestrial plant, fragments of wood and organic sediment, calibrated with Clam software (Blaauw, 2010) using the IntCall 13.14 calibration curve (Remier et al. 2013). AMS ^{14}C analyses were carried out by Beta Analytics.

Lab Code	Depth (cm)	Material	AMS ^{14}C	Error	2 σ cal. Age regne BP	BCE/CE	Included in the age model
2aup-1	7	Plant fragment	490	30	501-544	1449-1406 CE	
2aup-2	53.5	Plant fragment	400	30	429-513	1521-1437 CE	+
2aup-3	56	Plant fragment	1510	30	1329-1421	621-529 CE	
2alo	100	Plant fragment	1100	30	952-1062	998-888 CE	+
2alo-1	117.5	Wood fragment	1126	25	962-1081	990-871 CE	+
2alo-2	125.5	Wood fragment	1059	25	927-1001	1025-951 CE	
A-1b2-1	168	Plant fragment	1810	30	1693-1822	259-130 CE	+
A-1b2-7	229	Plant fragment	2150	30	2040-2183	88-231 BCE	+
2b1	261.5	Organic sediment	3190	30	3362-3458	1410-1506 BCE	
A-2b2-3	355	Wood fragment	3240	30	3390-3515	1440-1565 BCE	+
A-2b3lo	584	Wood fragment	5330	30	5999-6202	4047-4250 BCE	+
A-2b3lo-1	646	Organic sediment	7310	30	8180-8030*	6230-6080 BCE	

Chapter 5

Discussion

5.1-High resolution paleoclimate and paleoenvironmental reconstruction in the Northern Mesoamerican Frontier for Prehistory to Historical times

Polychromatic Chupicuaro figurines. Imaged by Tinajero Morelos

5.1.1-Introduction

This sub-chapter presents the full record discussion**.** This discussion is divided into two parts. The first one (named here “Prehistory”) is referring to the paleoclimate and paleoenvironmental variations during the prehistorical period between 6700 to 2500 yr BP. This period includes social-environmental events such as the first appearance of maize in the NMF. The second part from about 2500 yr BP to present is called “Historical times” where I describe short-term paleoclimate and paleoenvironmental events, that occurred since the development of the Chupicuaro society in the late Pre-Classic until the colonial period. To explain the relevant climatic and social events regarding time, the notation BCE/CE is used. A more detail discussion of stages IV and III can be found in sub-chapter 5.2 and 5.3 respectively.

In order to describe the variations of the monsoon system in the NMF region and paleoenvironmental changes, I selected proxies sensitive to detrital input, evaporation states, redox and drought conditions in the lake. The PCA1 proxy (sensitive to detrital input variability) has higher values in facies types C and D with a low portion of carbonates, and also reacts in the presence of dark laminae in facies B. Magnetic parameters correlate with PCA1 distribution with slight differences. These differences obey to the sensitivity of magnetic parameters being affected by redox conditions (e.g., Roberts, 2015). This interpretation is supported by the consistent opposite trend observed down core of Mn/Fe ratio compared to magnetic parameters (Fig. 5.1). Thus, I interpret that the magnetic parameters (k and S-ratio) reflect variations in the delivered detrital input to the lake. The Ca/Ti ratio is related to the high content of carbonates in facies type C and the carbonate laminae in facies B. I inferred that the variations in the Ca/Ti ratio react with authigenic precipitation of carbonates due to evaporative concentration.

The mechanisms that form Facies B (composed by dark and white laminae) are: Microscopic observations evidenced that the dark laminae are the result of mechanical processes; they consist of rounded crystals, reworked organic matter and large diatoms from littoral zones. The deposition of these laminae are due to a detrital input process. In the XRD analysis (fourteen samples) (Appendix 9) along the core and microscopic observations reveal that aragonite is the predominant carbonate in white laminae. Aragonite laminae are related to closed basin conditions (Glenn and Kelts, 1991) and occur in the dry season when the dissolved carbonates start to concentrate and precipitate in the epilimnion of the lake. I hypothesize that the dark laminae are formed under summer rainfall conditions and white laminae during the dry season. This way, a couplet of laminations may have formed under annual seasonality variations.

Variability in $\delta^{18}O$ can reflect diverse processes like changes between calcite and aragonite content or kinetic fraction due to evaporation. According to the thin section observations, changes from calcite to aragonite are rare. Moreover, a shift between both minerals formed under the same conditions would represent an enrichment of $\delta^{18}O$ of only 0.6 to 0.9 ‰ (Grossman and Ku, 1986). These changes are too small to describe the $\delta^{18}O$ oscillations in the record. Furthermore, the comparable variability between $\delta^{18}O$, $\delta^{13}C$ and endogenic carbonates shown by the Ca/Ti ratio curve (Fig. 4.2) suggests a closed basin system where kinetic fractionation due to evaporation is the most likely process for $\delta^{18}O$ enrichment (Li et al., 1997; Leng et al., 2004). I conclude that high (low)values of $\delta^{18}O$ display an increase(decrease) in the evaporation to precipitation ratio.

According to the results, I divided the core into six different stages: Stage VI (~ 6700-5600 yr BP), stage V(~ 5600-4400 yr BP), stage IV (~ 4400-2200 yr BP), stage III (~ 250 BCE-225 CE), stage II (225-1500 CE) and stage I (1500-0). The interpretations of the "Prehistory" stages (VI to IV) are compared with local and regional paleoclimate records from Rincon de Parangueo lake, Cueva del Diablo cave, Juanacatlan basin, Cariaco basin, El Junco lake and the Northern Hemisphere summer insolation curve (Berger and Loutre, 1991; Conroy et al.,2008 ; Park et al., 2010, Metcalfe et al., 2010, Bernal et al., 2011; Davies et al., 2018). For the "Historical times" stages (III to I), I compare my interpretations with the paleo rainfall reconstruction of Juxtlahuaca cave, El Junco lake record, Cariaco Basin record, the SST variability from the tropical Atlantic and North Atlantic Oscillation index (Haug et al., 2001; Conroy et la., 2008; Trouet et al., 2009 ;Wurtzel et al., 2013; Lachniet et al., 2017).

5.1.2-Paleoclimate and paleoenvironmental reconstruction for the Prehistory period.

Stage VI (~ 6700-5600 yr BP)

During this period, only facies type A were deposited (Fig. 5.1). The predominance of high detrital input over blurry carbonate laminations is probably the result of high detrital input and well-mixed lake conditions, carrying a high proportion of organic material such as macro and micro plant remains from the surrounding area and the littoral zone to the center of the lake. The well-mixed state of the lake decreased the preservation of laminated sequences. This is supported by a generally high lithic element concentration (Fig. 5.1) indicating increased of detrital input (PCA1). Additionally, the depletion of $\delta^{18}O$ values and the low carbonate content indicated by Ca/Ti ratio (Fig. 5.1), point to high lake levels and dominantly humid conditions. Magnetic susceptibility k is small. I argue that the high concentration of organic matter produced post depositional diagenetic effects and deteriorated the preservation of the magnetic fraction.

Humid conditions at lake La Alberca are consistent with local records from San Nicolas and Rincon de Parangueo lakes, where high *Alnus* pollen percentages and good pollen preservation, as well as a decrease of evaporation indicators like Na_2O and SO_2 were observed (Park et al., 2010) (Fig. 4.6). The comparison to the Cariaco Basin record of to the ITCZ position (Haug et al., 2001) suggests that this humid period is related to the northernmost position of the ITCZ during boreal summer (Wahl et al.,2016). This period also corresponds to the peak of the NAM (Harrison et al., 2003; Barron et al., 2012; Metcalfe et al., 2015) and represents the late part of the Early Holocene peak insolation period (EHPI), when the Northern Hemisphere received approximately 8 % more of solar radiation than today due to the earth precession minimum (Roberts, 2013).

Finally, the first ocurrece of *Amaranthaceae* pollen ~6000 yr BP is interpreted as the incipient start of agriculture in the zone (Fig. 4.6). The archeological evidence reveals that the principal anthropogenic activity in this period was located in “El Opeño” archeological site in the southern part of the Lerma Basin (Braniff, 2000) (Fig. 4.1A).

Stage V (~ 5600-4400 yr BP)

In this stage facies type B dominates, characterized by the presence of aragonite laminae, which suggest the establishment of generally dry conditions (A more detailed discussion about laminae formation can be found in sub-chapter 5.3). The increase in carbonate deposition indicates a decrease of lake level, producing saturation of carbonates in the hypolimnion and the subsequent precipitation of aragonite. Detrital input dropped as the result of declining rainfall as suggested by enrichment of $\delta^{18}O$ (Fig. 5.1). High carbonate concentration produced a chemical-density stratification decreasing the oxygen availability in the hypolimnion and constraining bioturbation (Zolitschka et al., 2015). The increase of the Ca/Ti and Mn/Fe ratios and the good preservation of laminae confirm this process (Fig. 5.1) and represent the start of anoxic conditions around ~ 5600 yr BP.

Local and regional records from San Nicolas and Rincon de Parangueo also suggest this dry period, with the increase of evaporation indicators such as Na_2O, SO_2 and Cl (Park et al., 2010) (Fig. 5.1). The $\delta^{18}O$ speleothem record from Cueva del Diablo provides information about summer rainfall variability in southern-central Mesoamerica and also confirms this dry period with the rise of $\delta^{18}O$ values (Bernal et al., 2011). The Cariaco basin record suggests a southward migration of the ITCZ, during the Mid-Holocene, which likely weakened the NAM strength and produced dry conditions in La Alberca region since about 5600 yr. These changes are attributable to the progressive decrease of summer insolation (Fig. 5.1) (Hodell et al., 1991; Haug et al., 2001; Poore et al., 2003; Peterson and Haug, 2006)

Stage IV (~ 4400-2200 yr BP)

This stage is characterized by the decrease in varve preservation, and the increasing presence of facies types C and D, a high amplitude variation of detrital input displayed by PCA1, *k*, and high amplitude variations in the E/P ratio revealed by the $\delta^{18}O$. Facies C representS periods of high detrital input to the central part of the lake during short humid periods, increasing mixing in the lake, and oxic conditions, thus preventing the formation and preservation of laminations. This interpretation is also supported by the rise of high amplitude variations in the Mn/Fe and a trend to better preservation of the ferrimagnetic fraction as displayed by S-ratio (Fig. 5.1). These conditions are interpreted as the start of high hydrological variability (Fig. 5.1). The onset of variable climate conditions is observed in the Juanacatlan record between 4200 to 4000 yr BP as well. This record responds to NAM variability and lies in the western region of NMF (Davies et al., 2018).

The presence of facies D IS associated with turbidity currents triggered by strong rainfall events, also pointing to the occurrence of heavy storms. This hypothesis is supported by the direct observation of a normal gradation, and clasts of facies type B floating in the matrix and erosive base of such layers. I propose that the possible rise of the large century-scale variations in the ITCZ position, described between ~3 800 to 2800 yr BP in the Carico Basin record (Haugh et al., 2001), motivated the beginning of variable hydrological conditions in the NMF (Fig. 5.1).

Global paleoclimatic records and archeological data describe the onset of major climatic changes, the start of a weak summer monsoon and cultural changes around ~4000 yr BP (e.g., Walker et al., 2012; Dixit et al.,2018). The sand percent and lake level record from “El Junco” lake (Galapagos Islands) responded to changes in precipitation related to Pacific Walker Circulation and ENSO events (Conroy et al., 2008). This record reveals an onset of ENSO activity around 4000 yr BP, which correlates with the start of detrital input variability in “La Alberca” region (Fig. 5.1). One possibility to explain the hydrological variability observed on stage IV, is due to the increased of ENSO activity, via increasing the fluctuations of ITCZ position resulting in an alteration of summer monsoon strength in the NMF. A complete discussion of this stage is presented in sub-chapter 5.2.

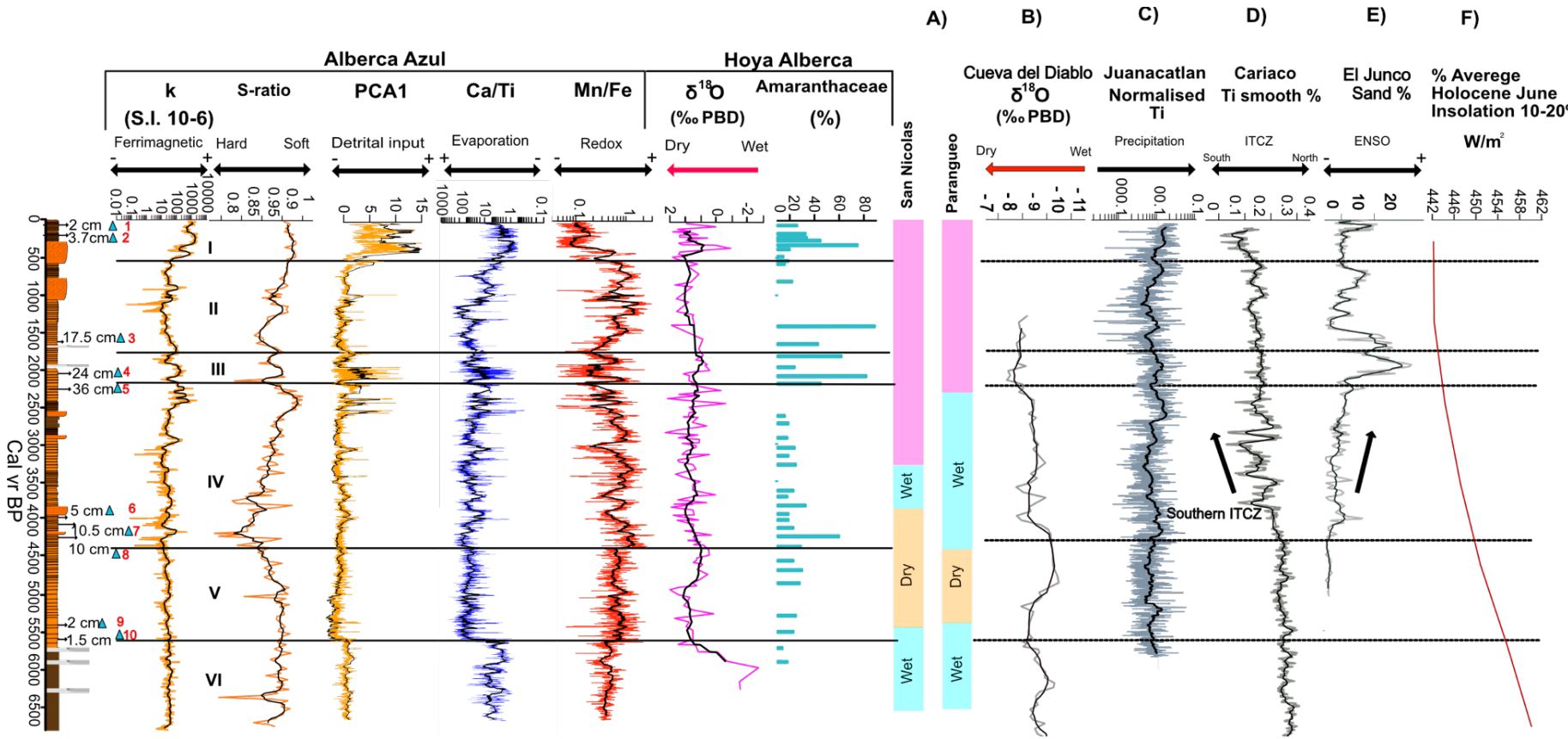

Figure 5.1- Comparison between selected magnetics (k, S-ratio), chemistry (PCA1, Ca/Ti, Mn/Fe), oxygen isotopes and pollen records from "La Alberca" with local and regional records. A) Paleoclimate and paleoenvironmental Interpretation of local records of San Nicolas and Parangueo, based on pollen counts and geochemistry of the sediments. Blue columns are interpreted as wet periods, brown columns as represents dry periods, and the purple columns indicates anthropogenic disruptions (Park et al., 2010); B) $\delta^{18}O$ record of speleothem "Cueva del Diablo" located in the western part of Mesoamerica, influenced by moisture form North Atlantic basin until 4300 yr BP (Bernal et al., 2011); C) Ti record from Juanacatlan Basin sensitive to NAM variations (Metcalfe et al., 2010); D) Ti record of "Cariaco Basin". This record is influenced by the position of ITCZ (Haug et al., 2001). E) Percent of sand of "El Junco" sensitive record of ENSO frequency (Conroy et al.,2008); F) June summer insulation curve for 30ºN (Berger and Loutre, 1991).

5.1.3-Paleoclimate and paleoenvironmental reconstruction in Historical times

Stage III (~ 250 BCE-225 CE)

Mesoamerica is known as one of the most important regions in the world where the domestication of plants started (Pope et al.,2001). Agriculture was vital for Mesoamerican cultures, to support dense human populations, the development of more complex societies, commerce between city-states, and the payment of tribute. Mesoamerican cultures developed diverse agriculture technologies like sophisticated irrigation systems, terracing, and floating gardens called “chinampas” all used according to the type of landscape and ecology (Whitmore and Turner, 1992). This increase in anthropogenic impact during the last two millennia complicates the paleoclimatic interpretation of lacustrine records in the Mesoamerica region (Metcalfe et al., 2015).

In stage III the high percentage of *Amaranthaceae* pollen is in agreement with the increase of terrigenous flux into the lake described by *k* and PCA1 parameters (Fig. 5.2), besides, according to the age model the sedimentation rate increased from 0.09 to 0.14 cm/yr. I interpreted that an intensification of agricultural activities in the area hindered any paleoclimatic interpretation in the record during this stage. This interpretation is in agreement with other studies in the region (O´Hara et al., 1994; Conserva et al., 2003; Park et al., 2010). Chupicuaro is considered to be the mother culture in the NMF area between 500 BCE until 200 CE, although more recent archeological evidence extends this period between further to 250-300 CE (Darras and Faugère, 2007). This culture produced high quality ceramic artifacts and maintained trade routes to the central part of Mesoamerica (Braniff, 1988). I suggest that the Chupicuaro culture could be involved in the landscape modification due to the correlation between its occupation period and the anthropogenic activity interpreted in the record (Fig. 5.2).

In addition, this stage is characterized by the presence of a well laminated section. Preservation and formation of varves in lakes can also be influenced by anthropogenic impact (e.g., Kienel et al., 2013; Dräger et al., 2017). Further microfacies analysis are needed to determine the possible impact of human activities in the formation and preservation of laminated sediments in the NMF. A more detailed discussion of this stage can be found in sub-chapter 5.3.

Stage II (~ 225 CE- 1500 CE)

Terrigenous indicators and Amaranthaceae pollen percent, display a reduction in the anthropogenic activities in the area, around ~340 CE. One possible explanation for this trend is the loss of influence of the Chupicuaro culture ~250-300 CE by decreasing agricultural activities (Darras and Faugère, 2007). The subsequent increase *Amaranthaceae* pollen could be related to the renewed agricultural expansion in the NMF (Fig. 5.2). After this, the record has a remarkable correlation with the paleo-rainfall isotopic reconstruction of the Juxtlahuaca cave (Lachniet et al., 2017), suggesting that the sedimentation process is again dominated by climatic forces, rather than anthropogenic activity (Fig. 5.2).

Between 600 CE to 880 CE, there is a slight increase in the carbonate content (Ca/Ti), followed by a clear decrease between 880 CE to 1500 CE (Fig. 5.2). This decrease can be explained by reduced drought conditions, particularly during pluvial periods around 900-1020 and 1400-1500 CE. Moreover, massive facies type C with low content of carbonates start to dominate this stage. These facies may have formed when lake levels were high, preventing the abundant precipitation of the carbonates.

During the Classical Mesoamerican period (250-600 CE) big urban centers like Teotihuacan and Monte Alban consolidated (Saint-Charles, 2007). Afterward, the fall of Teotihuacan generated a social, economic and political reorganization in central Mesoamerica and the NMF (Fenoglio et al., 2008). Conversely, the Epiclassic period (600/700-900/1000 CE) is characterized by the boom of cities with defensive characteristics like fortified walls, controlled access and mobility inside of the cities (Saint-Charles, 2007). Santa Rosa Xajay, La Trinidad, El Pedregoso and Cuicillo Colorado are Mesoamerican urban centers located in the NMF with such characteristics (Fig. 4.1B). Other similar places are also observed in central Mesoamerica like Xochicalco, Teotenango, and Cantona (Saint-Charles et al., 2010). Archeological studies suggest that the implementation of defensive characteristics in important urban centers of the Epiclassic was motivated by high social instability, which was accompanied by massive migrations and constant wars (Armillas, 1969). The principal driver for the social instability in the Epiclassic period is poorly understood. However, climatic change and environmental degradation have been proposed as a possible driver for the collapse of ancient civilizations (Butzer, 2012). Akkadian, Maya, and Tiwanaku civilizations are some of the most famous examples (deMenocal, 2001). Armillas (1969) argues that the expansion and subsequent collapse of sedentary agricultural societies in the Epiclassic period in the NMF was controlled by climatic oscillations such as an increase of aridity, affecting the agriculture that was mostly depended on annual summer rainfall. In contrast, some studies do not support the idea of environmental-climatic stress driving the social

collapse, claiming that the Classic and Postclassic periods were climatically stable (Brown, 1992; Frederick 1995; Trombold and Israde, 2005; Elliott et al., 2010;2012).

My findings suggest that an increase of precipitation occurred between ~600-700 CE, revealed by the gradual rise in PCA1 parameter and the decreasing calcium carbonate content as shown by Ca/Ti counts. After this period and until ~700-880 CE, a drastic decrease in rainfall is reflected by an increase of carbonate concentration (Ca/Ti) reduction of detrital input into the lake as displayed by PCA1 concentration and poor preservation of laminations (facies type B), just interrupted by a short wet period ~ 790 CE. This interpretation has a remarkable correlation with the rainfall decrease observed in the Juxtlahuaca record (Fig. 8A), and mainly correlates with a reduction of SSTs of the tropical Atlantic (Wurtzel et al., 2013) and a southward displacement of the ITCZ. This period is defined as the Epiclassic Drought, linked with the collapse of the Maya civilization in southern Mesoamerica (Hodell et al., 1995,2005; Curtis et al., 1996), the collapse of Cantona in the eastern part of Mesoamerica (Bhattacharya et al., 2015), and the dispersion of population in central Mesoamerica (Sanders et al., 1979). Consequently, the data set support Armillas´s theory about a persistent drought during the late Epiclassic period, however, the record suggests two short dry periods between ~ 700-790 CE and ~810-880 CE. These successive dry periods, probably resulted in a scarcity of resources which triggered social changes and massive migrations (Evans, 2008), a decline of sedentary settlements, a subsequent change in architectural style an increasing fortification of urban centers in order to repel constant outside attacks.

Between 900-1050 CE, PCA1 increases and calcium carbonate content decreases as indicated by the Ca/Ti proxy, which is interpreted as a period of dominantly humid conditions, in agreement with a northward migration of the ITCZ and a rise of SSTs in the tropical Atlantic basin, increasing NAM strength. This period is known as a Post-Classic pluvial, also observed in the rainfall reconstruction of Juxtlahuaca (Lachniet et al. 2017) (Fig. 5.1A). This period coincides with an increase in population in central Mesoamerica and the rise of the Toltec culture. In the NMF, a Toltec intrusion occurred, interpreted by their occupation of “El Cerrito” archeological site (Braniff, 2000). The pluvial period was followed by a dry interval between 1350-1280 CE, characterized by decreasing SSTs temperatures and the southward migration of the ITCZ, reducing the humid transport to the continent. During this period, the Toltec culture in central Mesoamerica collapsed (Fig. 5.2).

The progressive increase of detrital input suggested by the PCA1, and the decrease of calcium carbonates concentration (Ca/Ti proxy) are interpreted to be related to a pluvial period between 1400-1500 CE, which correlates with an increase in temperature of SSTs of the tropical Atlantic and northward migration of the ITCZ. The record thus suggests

that the development of the Tarascan Empire, which became a political and economic power in the region (Pollard, 2000), was accompanied by favorable humid conditions. In the Juxtlahuca record, the same trend towards wetter conditions was observed during the “Aztec Pluvial” period, when the Aztec empire expanded. Both cultures were the dominating powers in central Mesoamerica and NMF, and in consequence offensive or defensive military actions were common (Pollard, 2000). Besides, in agreement with our interpretation, Villanueva et al. (2012), using a network of cypress chronologies for paleo-lake levels reconstruction of Chapala lake with inter annual to multi annual resolution, reveal wet conditions between 1493-1498.

Stage I (~ 1500 CE- 2000 CE)

Some studies have suggested that the agriculture practiced by the Spanish conquerors generated more soil clearance than the traditional Mesoamerican techniques, because of the introduction of exotic biota, grazing animals, demographic population explosion, and management practices (Super, 1988; Whitmore and Turner, 1992). In contrast, O´Hara et al. (1993) describe three significant episodes of erosion before the arrival of the Spanish (1650-1150 BCE; 550BCE-750CE; 1100 CE-0), during the Preclassic, Classic, and Postclassic, claiming that the introduction of plough agriculture in Colonial times in fact decreased the erosion rate of agricultural systems.

The high correlation between PCA1 and *Amaranthaceae* data suggests that the detrital input coming into the lake during stage I is mainly controlled by anthropogenic activities, perturbating any paleoclimatic signal in the stage. The data indicate that with the start of the colonial times the increase of erosion responded to the foundation of Valle the Santiago city in 1607, and to the establishment of agricultural activities around the lake, by means of increased soil clearance.

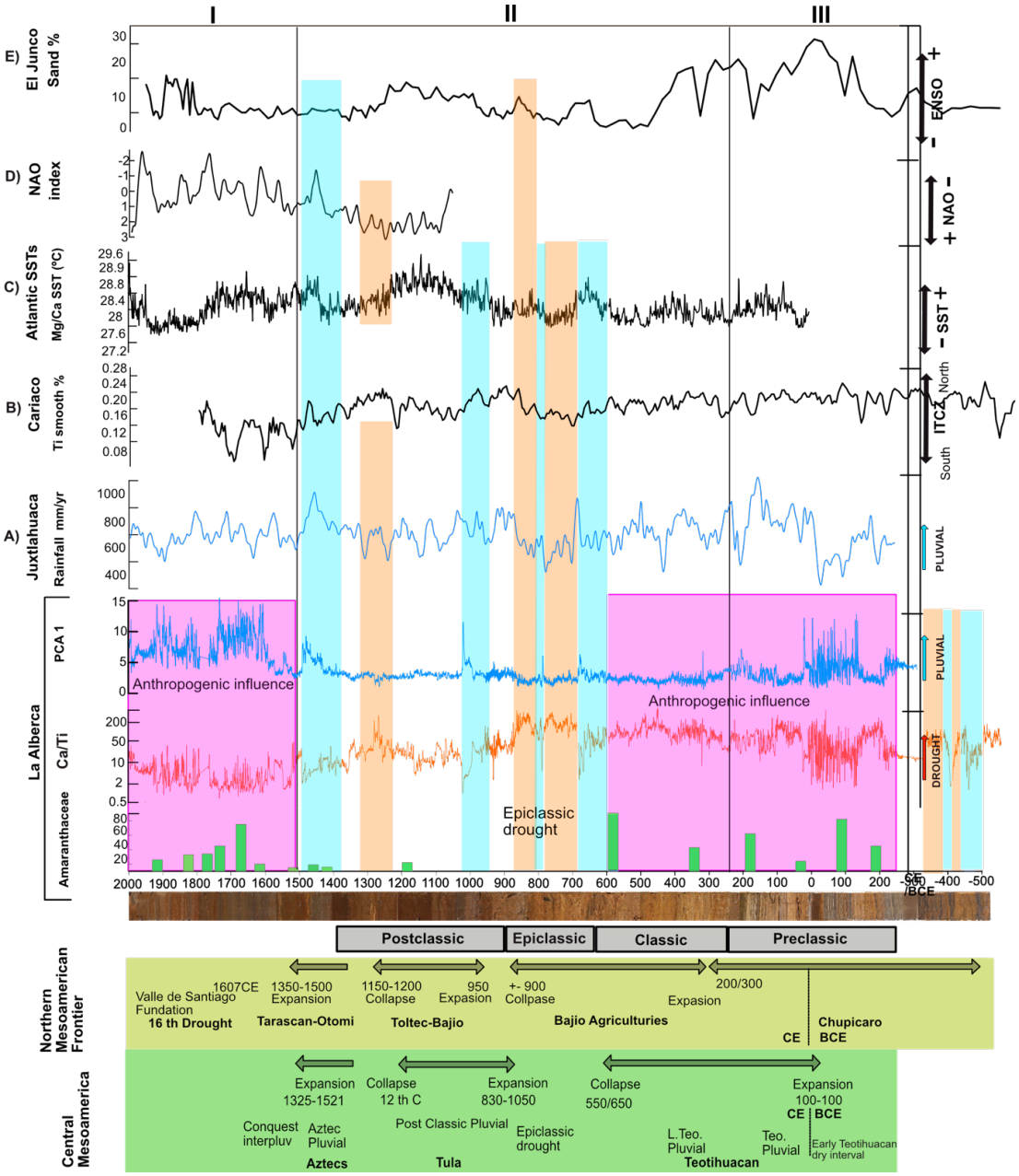

Figure 5.2- Comparison between La Alberca maar lake record, local-regional paleoclimatic records and archeological data. A) Mesoamerican monsoon rainfall reconstruction over the last 500 BCE obtained from Juxtlahuaca record (Lachniet et al., 2017); B) Ti record of "Cariaco Basin" sensitive to ITCZ variability (Haug et al., 2001); C) SST reconstruction of tropical Atlantic (Wurtzel et al., 2013); D) North Atlantic oscillation index (Trouet et al., 2009); E) Percent of sand of "El Junco" sensitive record of ENSO frequency (Conroy et al.,2008). At the bottom of the image, principal historical events from Central Mesoamerica and Northern Mesoamerican Frontier (Sanders et al., 1979; Darras and Faugère, 2007). Blue bars represent pluvial period, orange bars mark drought interval and purple bar displays anthropogenic activity. Remarkable correlation between the study record and Juxtlahuaca paleo rainfall reconstruction is observed between 400 to 1500 CE.

5.1.4-Climate forcing of La Alberca paleolimnological changes

The record of La Alberca displays correlations with climatic proxies from the tropical Atlantic and eastern Pacific, revealing that both basins influenced in the climate variability on the NMF during the last 6700 yr cal. BP. However, the correlation between the study register with diverse records sensitive to ITZC position, SST variability or ENSO activity in some specific sections seem to be lost (Fig. 5.1 and Fig. 5.). Differences in sensitivity of climatic proxies from record to record or diversity of climate from region to region exclude that every climatic event could be captured or be present in all the records (Mayewiski et al., 2004). Additionally, I propose that anthropogenic disturbance such as agricultural activities, modified the original paleoclimatic signal of the lake in some specific sections (Fig 5.1). Despite these difficulties, La Alberca record captures diverse regional climatic events, such as the end of Holocene Thermal Maximum, the onset of more variable climate conditions around 4 200 yrs BP, the Epiclassic drought ~ 700-790 CE and ~810-880 CE and the Aztec pluvial between 1400-1500.

The spectral analyses describe the presence of the 200-year cycle between 6300 to 5500 cal yr BP and the intermittent presence of the 60-year cycle (Fig. 5.3 and 5.4) in stage VI and stage V as well. The 200 yr cycle is similar to the described 206-year solar period in cosmogenic records (e.g., Steinhilber et al., 2009). In the Mesoamerican region, the Juanacatlan record and the Chichancanab records describe the occurrence of this solar cycle during the Holocene as well (Metcalfe et al., 2008; Hodell et al., 2001). Endless debate about the possible underlying physical climate mechanism associated with solar activity continues until today. Changes in the ultraviolet part of the solar spectrum, which affects ozone production, the effect of cosmic ray intensity on cloud formation, change of strength or position of Hadley circulation or tropical convective activity have been suggested for explain this complex relation (Usoskin et al., 2016). The 60-year cycle could be potential associated with PDO and AMO mechanism shaped by 60-70 year multidecadal variability (Minobe, 1999; Gray et al., 2004).

Bernal et al. (2011) argue that the speleothem record of the El Diablo cave is influenced by moisture that comes from the North Atlantic. The isotopic record correlates well with the Cueva del Diablo paleoclimatic record $\delta^{18}O$ record, which suggests that the variation in SSTs in the North Atlantic basin played an important role in summer precipitation in the NMF. In addition, this raises the possibility that the 60-year cycle identified from the time series analysis could be associated with the AMO.

The abrupt termination of massive deposit and the start laminated section around 5 500 yr cal BP describes the presence of a rapid climate change occurring within decades to centuries. This paleoclimatic transition marks the end of the EHPI and the establishment

of a weak monsoon. A rapid climate change occurs when “the climate system is forced to cross some threshold, triggering a transition to a new state at a rate determined by the climate system itself and faster than the cause’’ (Alley et al.,2008). In a global view, this prominent reduction of the monsoon strength around ~5600 yr cal. BP broadly coincides with glacier advances in the Alps, Alaska, New Zealand and Patagonia and with the fourth Bond cycle around 5530 cal yr BP (Bond et al., 2001). In the Mesoamerica region, this climatic transition is described as well in the paleoclimatic record of Lago Paixban (Wahl et al., 2016). The mechanism behind this climatic change refers to the orbitally induced change in the insolation enhanced by a non-linear reaction of the climate system (Wanner et al., 2008).

The comparison between the study record and the Cariaco basin record suggests that the variability in hydrological conditions interpreted between ~4400-2200 yr cal. BP obeys to the latitudinal fluctuation in the ITCZ position. These variations of the ITCZ could be explained by the onset of ENSO forcing around ~4400 yr cal. BP revealed by the El Junco record. Modern instrument data shows that during ENSO years, ITCZ shifts towards southern positions, decreasing the monsoon strength in Mesoamerica (Magaña et al., 2003). ENSO forced is related to change in the monsoon strength and seems to have of global character, as it has been described in a number of proxy records, for example, from India (Berkelhammer et al., 2012), the Gulf of Oman (Staubwasser et al., 2003) and the Middle East (Arz et al., 2006). The RedFit spectral suggests the dominance of high frequency cycles of 3,4,5,6,7, yrs (Fig. 5.4). These results support the idea that the rise of variable hydrological conditions due to increase of ENSO activity. Besides, the 125 and 200 yr cycles still present during stage IV, suggesting that modulation of climate variability still linked with solar activity (Fig. 5.3).

The lack of correlation between the study record and the rainfall reconstruction of the Juxtlahuaca speleothem from 600 BCE to 200 CE is attributed to intensive anthropogenic landscape disturbances around the lake, thus hindering any paleoclimatic signal during this period. From 600 to 1550 CE I compared the results with major climatic factors potentially controlling the lake environment like shifts of the ITCZ, SST of the tropical Atlantic, North Atlantic Oscillation index and ENSO activity (Haug et al., 2001; Conroy et la., 2008; Trouet et al., 2009; Wurtzel et al., 2013; Lachniet et al., 2017). Blue (orange) bars show the correlation between pluvial (drought) periods and the possible climatic forcing involved (Fig. 5.2). The data suggest a southward displacement of the ITCZ forced by an increase of ENSO activity is evident during the dry period between ~810-890 CE. However, drought (pluvial) periods seems to be linked with the decrease (increase) of the SSTs of the Atlantic.

I propose that the SSTs of the tropical Atlantic played an important role in pecipitation variability in the NMF, via displacement of the ITCZ. Drought periods observed in the

record around 700-880 and 1230-1310 CE correspond to low SSTs resulting in a displacement of the ITCZ toward the warmer hemisphere, in this case the southern hemisphere (Haug et al., 2001; Xie and Carton, 2004; Winter et al., 2011; Chiang and Friedman, 2012; Bhattacharya et al., 2017) with a subsequent reduction of precipitation in the NMF. Pluvial periods interpreted at 900-1050,1400-1500 correlate with high SSTs, producing northward shift of the ITCZ and a precipitation increase over the NMF. This mechanism was also observed during the 8.2 ka event and the Younger Dryas (e.g., Peterson et al., 2000; Overpeck and Cole, 2006; Bernal, 2011; Arbuszewski et al., 2013).

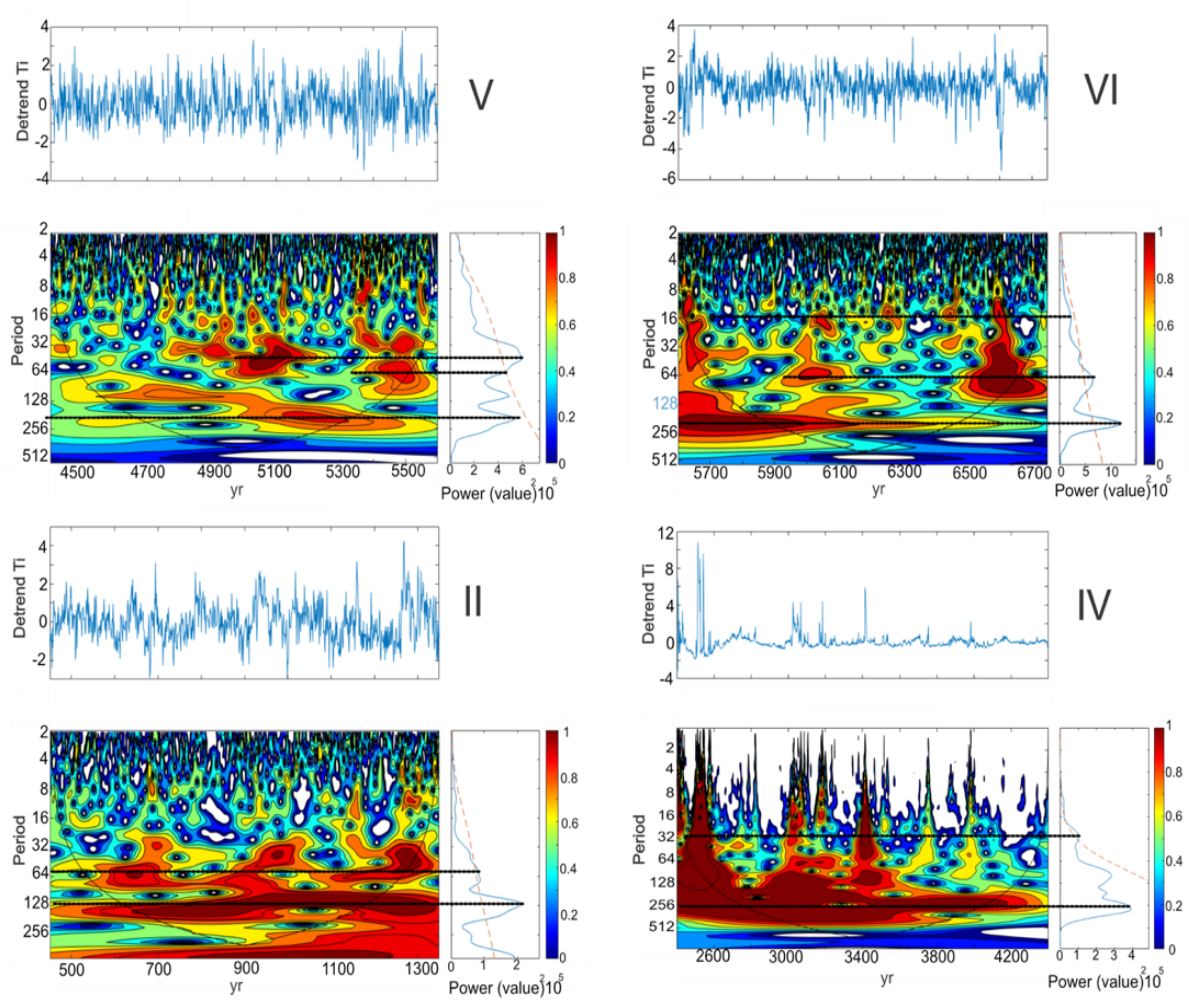

Figure 5.3- Wavelets analysis and its respective detrended Ti values of stages VI, V, IV and II.

SSTs anomalies of the tropical Atlantic have been linked to a different atmospheric/oceanic mechanism such as the strengthening or weakening of Atlantic Meridional Overturning Circulation (AMOC) (e.g. Wurtzel, 2013). Some studies suggest that AMOC variations affect the ITCZ position (e.g. Chiang et al., 2008). Recent models

of the AMOC index over the Mesoamerican region, however, reveals extended drought periods when AMOC decreased, but a reduction of AMOC strength did not always correspond with drying periods, suggesting that other factors can play an important role in the NAM modulation (Bhattacharya et al. 2017).

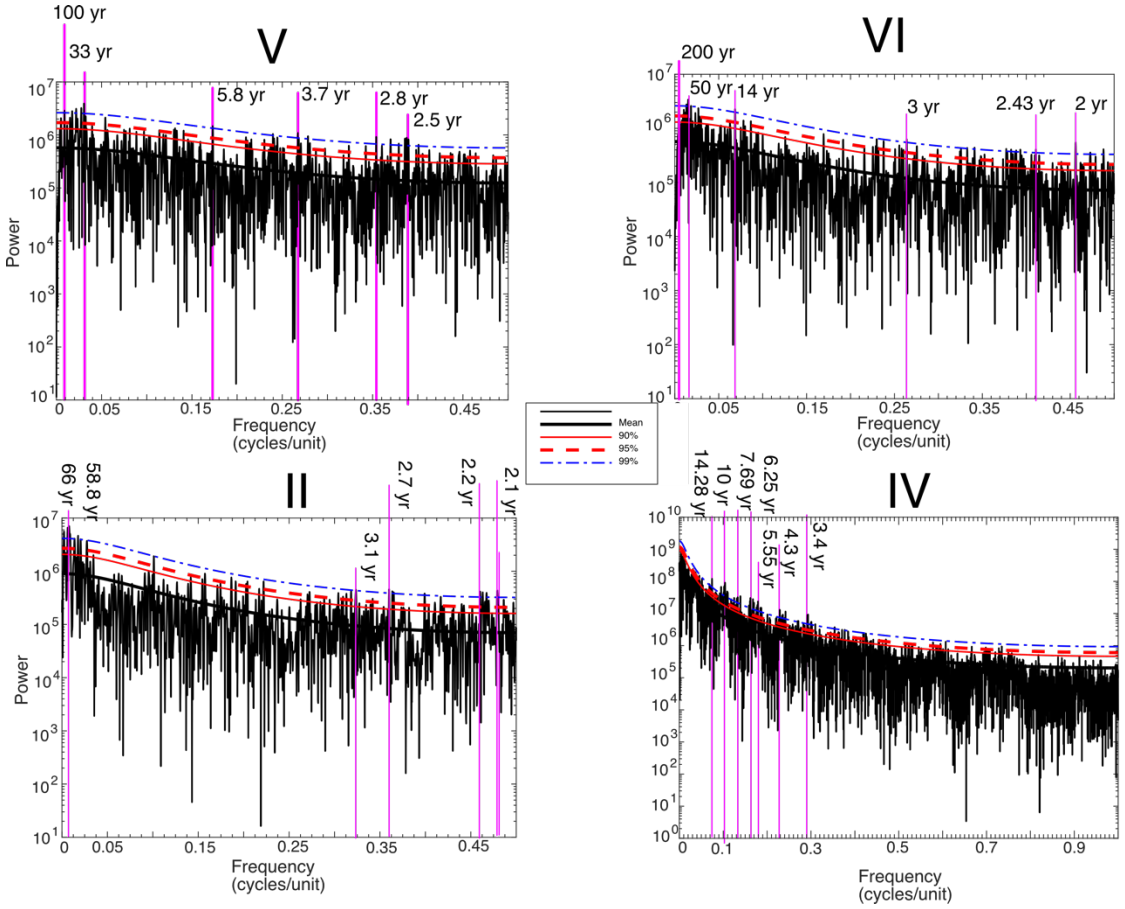

Figure 5.4- Periodogram analysis of stages VI, V, IV, and II. The solid purple lines indicate significative periods with more of 99% confidential limit.

On shorter time scales, it has been shown that the variability in the SSTs of the Atlantic Basin is affected by the NAO with the positive phase increasing the strength of trade winds, reducing the SSTs, thus decreasing atmospheric moisture and the precipitation over the continental region (Giannini et al., 2000; Bhattacharya et al., 2017). Comparing the study record with the NAO index (Trouet et al., 2009) the generally positive state of the NAO between 1050 and 1350 CE yr corresponds with a reduction in NMF precipitation (Fig. 7). I hypothesize that a decrease in the SSTs resulted in a slowdown of AMOC and increase of trades wind strength. In consequence, a southward displacement of the ITCZ during extended drought conditions in the NMF occurred. Due to the mechanism previously described, the presence of the 60-50 yr cycle reinforce the hypothesis about the relevant role of the Atlantic oscillations during this stage. The spectral analysis also reveals the presence of 128-year solar cycle (Fig. 5.3).

5.1.5-Summary and conclusions

La Alberca maar lake sediments provide a high-resolution record of paleoclimate and paleoenvironmental conditions in the Northern Mesoamerican Frontier during the last 6700 yr. The results reveal that the sedimentation process is related to paleoclimate and anthropogenic activity. The summer monsoon strength in the last 6700 yr BP seems to have been dominated by major climatic forcings like the variability in the Position of Intertropical Convergence Zone, El Niño Southern Oscillation activity, orbital precession cycles and SSTs of Atlantic Basin. In the Prehistory period I concluded, two main points:

1. The end of the Early-Holocene peak insolation period is well represented in our record around 5600 yr BP, by a drastic change in the stratigraphy from massive to well-laminated facies and a decrease of terrigenous input. After this period, a decrease in monsoon strength is interpreted by the increase of carbonate laminae, and by the enrichment of $\delta^{18}O$ and which is in agreement with other local and regional records.

2. More variable hydrological conditions start around 4400 yr BP as suggested by the decrease of lamination preservation and the increase of detrital input, which is coeval with a latitudinal variation of the Intertropical Convergence Zone position and the onset of El Niño Southern Oscillation.

The rise and intensification of agricultural activities by the Chupicuaro culture are interpreted to occur around ~ 225 BCE- 340 CE. This paleoclimate reconstruction supports Armillas´s (1969) theory that a major drought period played an essential role in the social and geographic displacement of Northern Mesoamerican Frontier around 700-880 CE in the Epiclassic period. However, the study record reveals the existence of two consecutive dry periods around ~700-790 CE and ~810-880, interrupted by a short humid phase. The pluvial period interpreted around 1400 to 1500 CE indicates that the rise of the Tarascan society in the Northern Mesoamerica Frontier happened under favorable climatic conditions. Finally, I argue that the changes in SSTs the Atlantic Basin played a major role in the modulation of climatic patterns in Mesoamerica Northern Frontier during the last 1300 yr.

This work highlights the important relationship between culture-climatic-environmental relations in the Northern Mesoamerican Frontier and shows that high-resolution studies of laminated sediments offer an excellent opportunity to decipher these complex relationships.

5.2-Paleoclimate and paleoenvironmental magnetism study during the Mid-Holocene and its cultural implications in Mesoamerica.

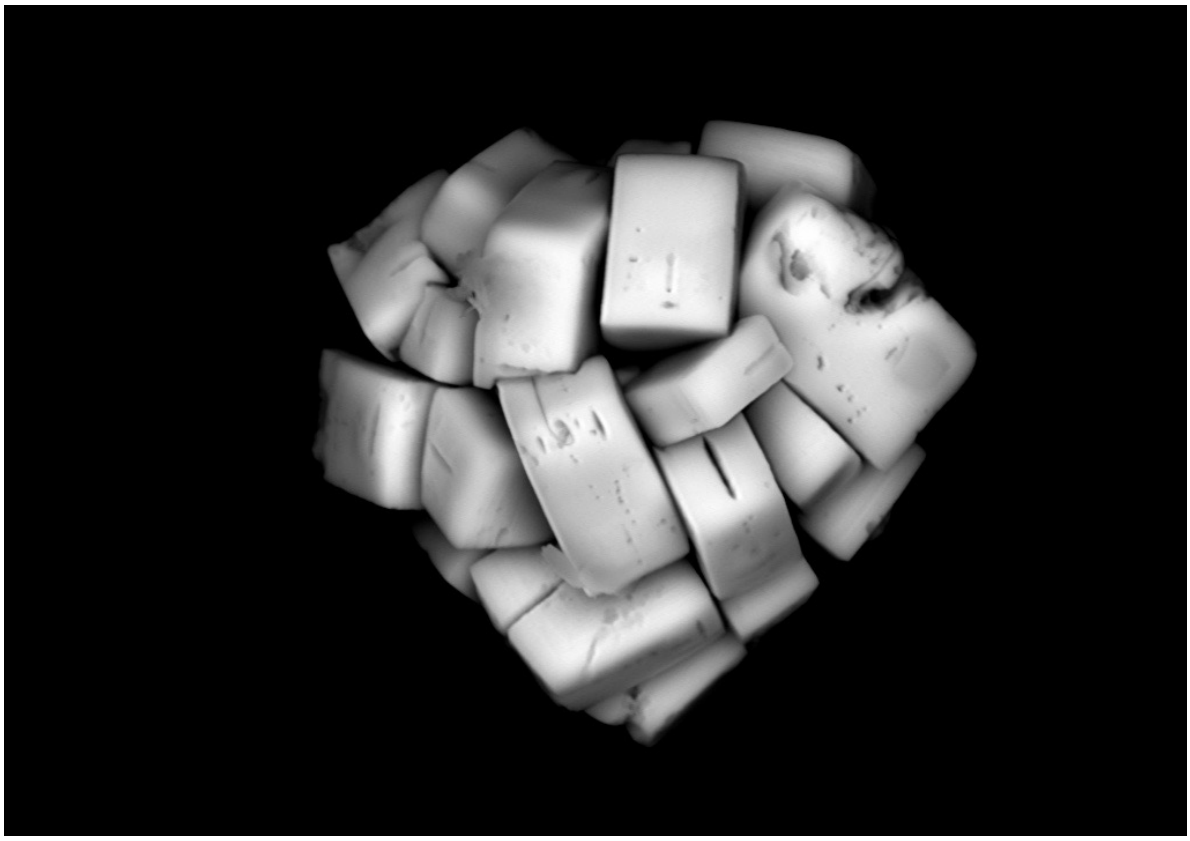

Framboidal pyrite extracted from La Alberca lake sediments by Kurt Wogau and Norbert Nowaczyk

5.2.1-Sources and genesis of magnetic minerals and its relationship with the NAM oscillations during the Mid-Holocene.

Although the magnetic fraction variability of all the record is discussed in this chapter, I focus my environmental and paleoclimatic interpretation in the time window of stage IV (4400-2200 yr cal BP). A detailed paleoclimatic interpretation of the entire record can be found in the previous sub-chapter (5.1).

On the basis of the rock magnetic results and SEM analysis, I identified iron oxides such as (titano-) magnetites, (titano-) maghemite, ilmenite, hematites, iron sulfides (mostly pyrite) and iron-carbonate (mostly siderite) (Fig. 4.11,4.12,4.13,4.14). Besides their original source (magmatic, pedogenic, authigenic, biogenic) and transport mechanism (eolian, runoff), the formation and preservation of those minerals depends on diverse natural factors such as the amount of organic matter in the sediments, change between oxic and anoxic stages in the water-sediment interphase, and water chemistry among others.

Post-depositional dissolution of the magnetic detrital fraction in lake sediments is common, especially in organic-rich sediments (e.g., Snowball, 1993; Nowaczyk et al., 2002; 2013) and the establishment of a sulfidic zone in the water/sediment interphase occur. This process is controlled by the proportion of organic matter and reactive iron (Roberts, 2015). Under anoxic conditions, Fe^{2+} is released from iron-bearing minerals reacting with H_2S produced by the reduction process, generating iron sulfides such as pyrite (Roberts, 1995, 2015; Roberts et al., 2011). When the Fe^{2+} exceeds the proportion of H_2S, intermediate iron sulfides can be formed like mackinawite and ferrimagnetic greigite (Roberts, 2015). Two typical indicators of sulphidic states in the magnetic mineralogy are the reduction of the magnetization and the removal of the fine-grains (SP and SD); the latter which implies an increase in the proportion of coarse-grains (MD and PSD).

The changes in magnetic mineralogy between peak stages (IV, III and II) and background stages (VI, V and II), can be well explained by dissolution processes, affecting the primary assemblage (Fig. 4.8, 5.5). Post-depositional dissolution of detrital minerals in “La Alberca” during stages VI, V and II is inferred from several indicators. First, low magnetic susceptibility and low magnetization evidenced by the k, kARM and IRM parameters (Fig. 5.5). Second, grain size indicators such as kARM, kARM/k_{LF} and ARM/SIRM increase, indicating the dominance of PSD-MD particles (Fig. 4.8, 5.5). Third, cubic pyrite, framboidal pyrite, skeletal grains composed of ilmenite in a magnetite structure and authigenic carbonate like siderite are the main minerals observed in these stages (Fig.

4.12 A,B, 4.13). Besides, the presence of well-preserved laminated sections in stage V, high percent off organic C, and increase of the Mn/Fe, ratio (Fig. 5.5) also supports the idea of the prevalence of anoxic conditions. This interpreted to be the result from reduced or even absent mixing states in the lake. In turn, this implies reduced wind stress or increased biologic activity.

During stage IV (4400-2200 yr cal BP), the S-ratio displays a gradual increase, indicating the relative contribution from a ferrimagnetic mineral fraction increases. This rise is accompanied by an increase in concentration parameters *(k)* and an increase in the kARM ratio as well (Fig. 5.5). This indicates that fine magnetite preserves and arrives into the lake in greater amounts. The PCA 1, which is coeval with ferrimagnetic concentration parameters (k and S-ratio), supports a detrital origin for the coarse magnetite. The Mn/Fe ratio during stage IV indicates a decrease in anoxic conditions, which is also evidenced by the low magnetic fraction preservation. These observations may be explained by the occurrence of major but sporadic rainfall events represented by massive dark layers (Fig. 5.5 and 5.6). These high fluctuations in paleoprecipitation are also supported by the high amplitude centennial-scale variability observed in $\delta^{18}O$ (sensitive to evaporation/precipitation conditions) (Fig. 5.5).

The effects of major rainfall events in the Alchichica saline lake have been previously studied. This lake shares similarities with La Alberca lake. Both lakes are depth crater maars, with a close system, classified as an alkaline (~pH=9.0), water chemistry dominated by sodium-magnesium and chloride-bicarbonate ions (Armienta et al.,2008). From 8 to 9 October of 1999, the effects of one single rainfall event was measured. An unusual reduction in the temperature and salinity occurred near to the surface of the water column around 5 to 10 m. The nutrients concentrations and distribution remain undisturbed and small variation in the percent of saturation of dissolved oxygen occurred. After this event, smaller rainfalls and wind currents (around 5 m s-1) resulted in the epilimnion mixing (Alcocer et al., 2007). The effects of ENSO event between 1998-1999 in the limnological conditions of the lake (temperature, dissolved oxygen, phytoplankton biomass) were evaluated as well. The results revealed a narrower and slightly colder hypolimnion than average values, a pronounced thermal change along thermocline, shallower thermocline, thinner hypolimnetic anoxic layer and a modest spring cyanobacteria bloom (Alcocer et al., 2003).

The age model indicates that the massive dark layers span between 10 or 20 years, which longer lasting than the previous events described in the Alchichica lake. I hypothesized that the constant input of fresh water during these decadal wet events, resulted in the decrease of thermal and density contrast in the water column, narrowing the hypolimnion, thus increasing the oxygenation of the lake bottom. This interpretation is supported by

high detrital input, high preservation of magnetic mineralogy and low values of Mn/Fe described in this period (Fig 5.6).

I infer that major changes in production, preservation and input of magnetic mineralogy follow up variability of anoxic or oxic conditions of the Alberca lake, mainly controlled by monsoon oscillation on the Mesoamerica region between 4400 to 2200 yr cal BP. Consequently, La Aberca record do not reveals an imprint of the 4.2 ka single dry event described by the isotopic signature of Red Sea sediments, the speleothem record of Mawmluh Cave (India), and the rise on dust content in ice core from Kilimanjaro (Africa) (Thompson et al.,2002; Arz et al.,2006; Berkelhammer et al., 2012)(Fig. 5.5). Instead of this, the record shows an increase of more variability of rainfall regime, causing continuous ventilation of the lake bottom starting at 4300 yr BP that reached its maximal expression around 2200 yr BP. Diverse records reveal the rise of hydrological variability or increase in dry conditions during the Mid-Holocene in Mesoamerica (Bernal et al., 2011; Lozano-Garcia et al., 2013; Jones et al., 2015; Davies et al., 2018).

This pattern is consistent with the onset of the high latitudinal variability of ITCZ displayed in the Cariaco basin record in Venezuela (Haug et al., 2001) (Fig. 5.5). The increase of ENSO activity and PDO oscillation have been proposed for explaining the mechanism behind the rise of ITCZ variability (Conroy et al., 2008; Bernal et al., 2011; Lozano-Garcia et al., 2013; Jones et al., 2015; Davies et al., 2018). In agreement with this interpretation, the RedFit spectral analysis reveals the dominance of high-frequency cycles of 3,4,5,6,7, yrs interpreted as an increase of ENSO forcing. The PDO is an ocean-atmosphere variability that occurs on decadal to interdecadal time (Linsley et al., 2000). Wavelet analysis of the detrital input parameter (Ti) reveals periodic variations of 30,20,16 and 10 yrs (Fig. 5.6). This observation raised the possibility that dominant multidecadal or interdecadal forcings being like PDO oscillation influenced the strength of the NAM system. During cool PDO states, increase of precipitation occurs in the Mesoamerican area. These conditions are prompted by the northward displacement of the intertropical convergence zone (ITCZ) due to the zone of warm waters moves northward caused by the wind- driven upwelling in the east Pacific cold tongue (Lachniet et al., 2017). I conclude that the Pacific forces such as ENSO and PDO started to influence the monsoon strength between about 4300 yr cal BP.

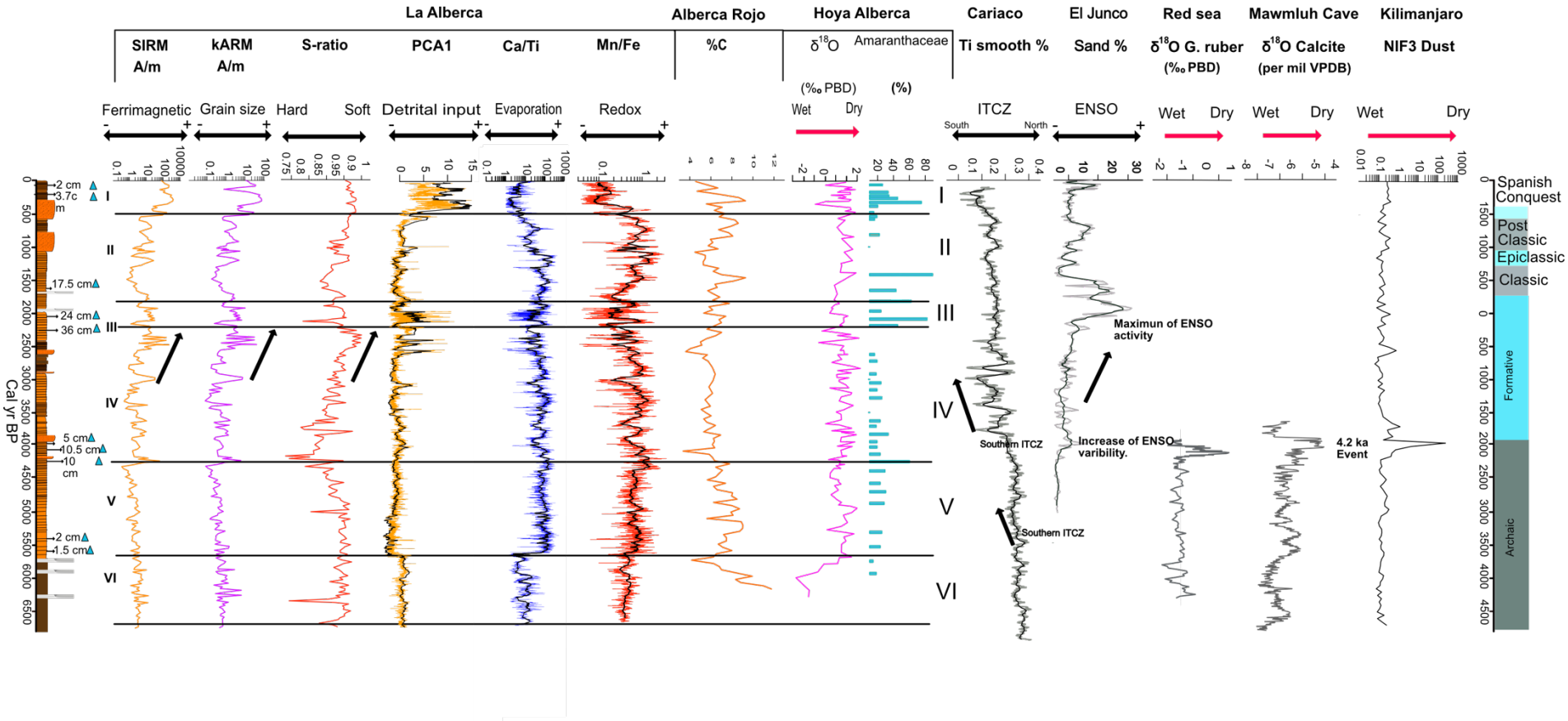

Figure 5.5- Comparison between selected magnetics (SIRM,kARM, S-ratio), chemistry (PCA 1, Ca/Ti, Mn/Fe), % C , pollen and δ18O parameters with regional and global paleoclimate records. Black arrows on magnetics parameters indicate the increase in oxic conditions. Ti record from Juanacatlan Basin sensitive to NAM variations (Metcalfe et al., 2010). Ti record of Cariaco Basin. This record is influenced by the position of ITCZ (Haug et al., 2001). Percent of sand of El Junco record sensitive of ENSO frequency (Conroy et al.,2008). δ18O record on G. ruber on Red Sea is sensitive to increase or reduction of monsoon strength (Arz et al., 2006). Mawmluh δ18O speleothem record provides information about the tropical monsoon strength (Berkelhammer et al.,2015). Dust history from Kilimanjaro ice core sensitive to dry conditions (Thompson et al., 2002). Grey and blue bars represent the principal archeological subdivision of the Mesoamerica history.

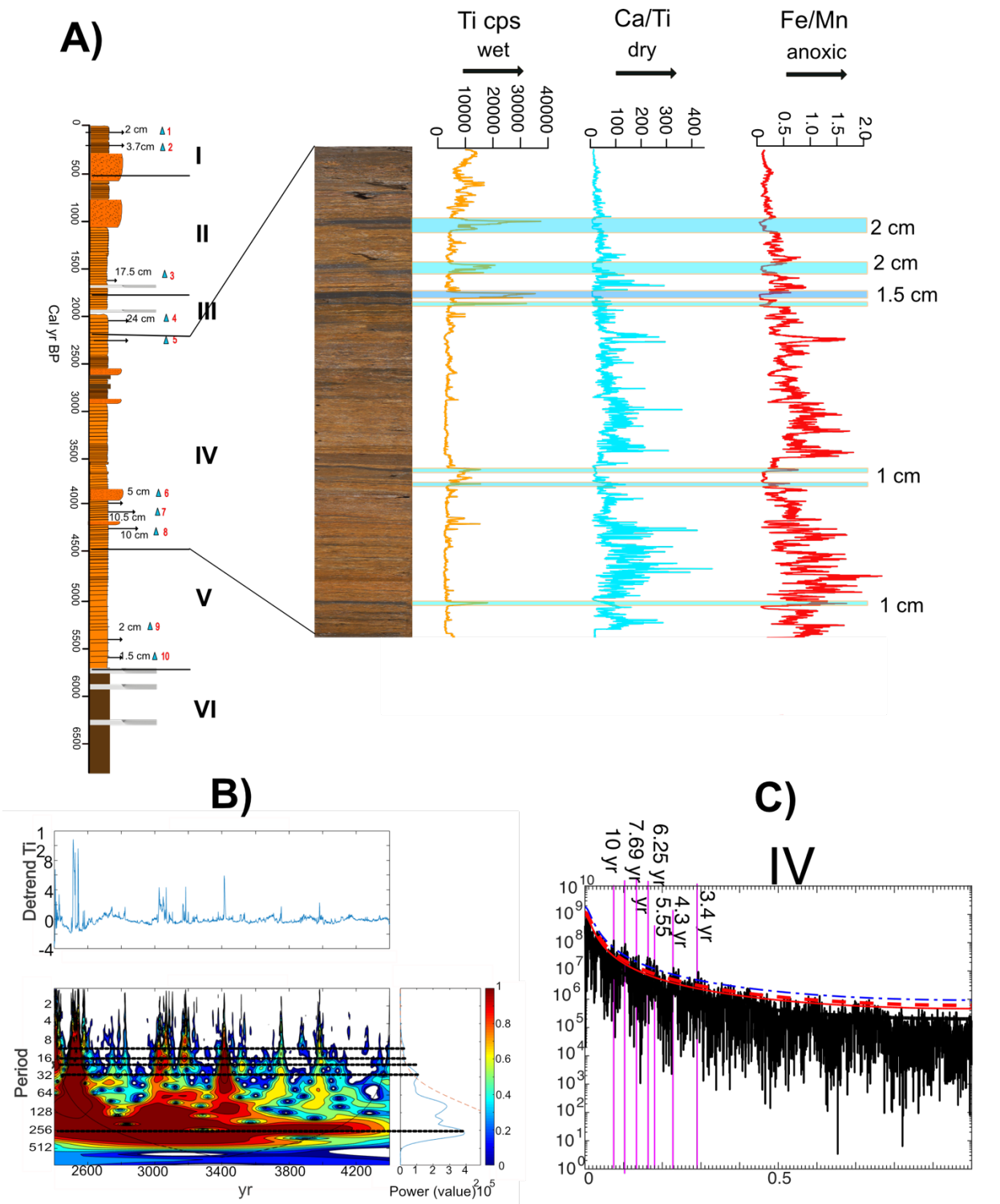

Fig 5.6- A) Detail core section of stage IV. Chemistry parameters and ratios sensitive to detrital input (Ti) carbonate precipitation (Ca/Ti) and redox conditions (Fe/Mn). Their respective interpretation is indicated at the top. The blue shading areas represent wet events with its respective thickness B) Wavelet analysis of stage IV displaying significative periods of 256,32 and 20 years C) Redfit analysis of stage IV revealing significative periods of 10, 7,6,5,3 and 3 years.

5.2.2-Anthropogenic imprint in the magnetic fraction and social implications of the hydrological variability during the Mid-Holocene in Mesoamerica.

Peak stages III (2200 cal yr BP-1725 cal yr BP) and I (450 cal yr BP- present) reveal well-preserved titano-magnetite with idiomorphic cubic-octahedral shapes, broken shapes and combinations of diverse grain sizes. I suggest that broken shapes are due mechanical transportation process, indicating a detrital origin of these crystals. In both stages, the detrital input and magnetite concentration describe an increase in lithogenic particles, which is synchronous with the rise in *Amaranthaceae* percent (Fig. 5.5).

The occupation period of the Chupicuaro culture in the region is constrained between 600 BCE-300 CE (Gorenstein, 1985), mainly coinciding with the timing of stage II (~ 250 BCE-225 CE). The arrival of European around the year 1500 CE is agreement with the time frame of stage I. The potential sources of detrital (titano-) magnetite in these stages are the crater wall volcaniclastic sediments, pre-maar lava fragments and soils from around the catchment area, and eolian input. High similarity between stages III and I magnetic properties (such as thermomagnetic curves, FORC diagrams and hysteresis curves) and magnetic properties of lavas, deposits and soils in the crater interior seem to corroborate the hypothesis. On the other hand, the observed high coercivity phase (interpreted as hematite) at the base of the stage IV and during stage III may have two sources. One is soil surrounding the crater, where samples are characterized by high coercivity components, and the crater wall tephra in which hematite was observed in the SEM analyses.

The transition from Archaic to Preclassic period is encompassed by fundamental social and technological changes, such as an increase in food production, reduced residential mobility, production of first ceramic artifacts and increased of social stratification. Rosenswig (2015) theory points out that the Archaic-Preclassic transition occurred after the end of the 4.2 ka event (2200 BCE), described as a global dry event reflected in proxy records from North America, Middle East, China and Antartica (Mayewski et al., 2004; Staubwasser & Weiss, 2006). This climatic event has been associated with the collapse of important ancient societies like the Akkadian empire, the Old Egyptian kingdom and the Harappan culture in the Indus Valley (Walker, 2012; Weiss, 2016)

In this regard, this paleoclimate and paleoenvironmental data do not support Rosenswig (2015) hypothesis. The study record reveals the establishment of highly variable hydrological conditions between 2350 BCE to 250 BCE rather than a single dry event. These conditions hindered the adaptation to the natural environment and resources in Mesoamerica, stressing agricultural production due to the availability of water resources,

which is a key-resources in semi-arid region for cultural development (Flohr et al., 2016). Thus, just after around 1200 yrs of an adaptive process to the severe environmental and climate conditions, from the start of the Pre-Classic (2200 BCE) to Middle Pre-Classic (1000 BCE), stagnant low social development ended. This is evidenced by the appearance of ceramic vessels, intensification of food production, (mainly maize), the beginning of monumental art and the first socially stratified culture raised on the south-east sector of Mesoamerica, the Olmecs. Around 600 BCE the Chupicuaro culture started to dominate the central region of NMF possible favored by the start of wetter conditions.

5.2.3-Concluding Remarks

The study of diverse magnetic parameters in combination geochemical proxies describes that during stage IV (~ 4400 to 2200 cal yr BP), high hydrological variability produced a gradual rise of oxic conditions in the lake, reaching its maximum expression in the final part of the stage. These oxic conditions are suggested by an increase of the ferrimagnetic fraction and its preservation as indicated by *k,* SIRM, S-ratio and kARM parameters. SEM analysis reveals the presence of well-preserved titanomagnetites with diverse shapes and grain sizes. I argue that the increase of oxic conditions responded to major sporadic rainfall events. These constant inputs of freshwater produced a decrease of thermal and density contrast in the water column, narrowing the hypolimnion, thus increasing the oxygenation of the lake bottom. The high variability of the position of ITCZ, the rise of ENSO and PDO forcings during the Mid-Holocene were suggested as the potential drivers to explain the hydrological variability register in La Alberca record.

In peak stages, III (2200 cal yr BP-1725 cal yr BP) and I (450 cal yr BP- present) the high input and preservation of magnetic detrital fraction are related to the start of agricultural activities by Chupicuaro culture (600 BCE-300 CE) and in the colonial period. I also propose that the 4.2 ka global dry event is not revealed in La Alberca record. Instead of this, the establishment of highly variable hydrological conditions between 4300 to 2200 cal yr BP is interpreted. In this way, this work does not support Rosenswig (2015) hypothesis that the transition between the Archaic to Pre-classic period is marked by the onset of a major single climatic event.

I propose that the hydrological variability interpreted in the record hindered the adaptation to the natural environment and resources of early Preclassic Mesoamerica cultures. These paleoclimatic conditions ended at about 250 BCE marking the end of pre-ceramic cultures and the rise of the first highly develop Mesoamerica society, the Olmecs in the south-east sector of Mesoamerica and the Chupicuaro culture in the central sector of NMF.

5.3-Paleoenvironmental and paleoclimatic study of the Late Preclassic period in the Northern Mesoamerican frontier

Crater maar La Alberca by Kurt Wogau

5.3-Varve formation

Under specific conditions, certain succession laminae can represent an annual cycle of sedimentation. These sedimentary structures are called varves. The varve formation is driven by the lakes respond to the seasonal climate cycle, geology, and anthropogenic factors (Zolitschka et al.,2015). The climate and geology shape the formation and evolution of soils and vegetation. Together, these factors influenced the sediment deposition in the lake and controlled the water chemistry and biological activity as well. The rise of erosion by anthropogenic practices (e.g., agriculture) and the increase of nutrients to the lake heavily influence the sedimentation process of the lake. Kienel et al. (2009) describe the formation of varve structures for the AD 1852–1973 time period, in the sedimentary sequence of La Alberca maar lake.

In this chapter, I describe the principals natural and anthropogenic processes involved in the formation and preservation of the varved sequence of La Alberca maar lake during the final part of the Pre-Classic archeological period. Furthermore, I correlate the paleoenvironmental and paleoclimatic findings with archeological data of the Late phase and Mixtlan phase of the Chupicuaro culture (Darras and Faugere, 2007). This comparison aims to understand the timing of occupation periods by the Chupicuaro culture in the study area in view of the background climate variability. Moreover, I intend to explain how human activities modified the environment in the Valle the Santiago region.

5.3.1-Varve interpretation

Two lamination patterns are observed denominated Type 1 (DOL-AL) and Type 2 (DOL-OS-AS).

Type 1(DOL-AL)

The origin of DOL describes a combination of mechanical and biological processes. First, the mechanical process is interpreted by the ocurrence of reworked detrital lithics-crystals, broken diatoms valves, amorphous organics matter, and basal contacts. I interpreted that this layer as deposited during the rainy season of the year, between May and October (Fig. 5.7), generating surface runoff that carries detritus and organic material into the lake. Second, with the onset of the rainy season, sediment influx increases the content of nutrients raising the productivity in the lake (e.g., Wetzel, 2001), thus producing a diatom bloom. This diatom bloom forms the organic debris settling down together with the larger detrital particles and plants remais.

During the final part of the dry season, when maximum temperatures are registered (March to May), strong evaporation raises the saturation of carbonates in the lake and the precipitation of these minerals occurs as soon as its solubility limit is reached (Zolitschka et al.,2015) (See more details about calcium carbonate precipitation in sub-chapter 5.1, section 5.1.3).

The rain water isotopic values of Valle the Santiago are between -11 to -7.7 %. Kienel et al. (2009) argue that the oxygen isotopic composition of the carbonates fraction during 1852–1973 AD in La Alberca lake are enriched to values around +1.6%, and conclude that precipitation of the carbonate sublayer is mainly ruled by the evaporation process.
In the study section, oxygen isotopic values are around +1.1%, confirming that the evaporation is the main processes for the precipitation of the AL. However, the biological processes, like diatom blooms may also be involved, consuming CO_2 and increasing the pH and thus reducing the solubility of carbonates (Stabel, 1986).

Type 2 (DOL-OL-AL)

The formation of DOL follows the same mechanism proposed for lamination pattern Type 1. However, I argue that the observed increase of detrital input displayed by PCA 1 in sub-stages III.c and III.f is strongly related to the increasing of soil erosion (Table 5.1), leaching high amounts of nutrients and thus resulting in eutrophic conditions in the lake (e.g., Striewski et al., 2009). In the fall season, with the arriving of first polar fronts (See description of polar fronts in chapter 2, section 2.3), the mixing of the water column occurred in the lake, recycling the high amount of nutrients stored in the hypolimnion and transferring to the photic zone. This process triggered a second algae bloom forming the OL, that is exclusively formed by *post-mortem* diatom frustules (Fig. 5.7).

Table 5.1- Mean thickness of detrital organic layers, aragonite layers and varves. Percent of distribution of varve Type 1, varve Type 2 and massive layers.

Sediment unit	Depth (cm)	Mean thickness DOL layer (mm)	Mean thickness OL layer (mm)	Mean thickness AL layer (mm)	Total varve thickness (DOL+OL+AL)	% Varve type 1	% Varve type 2
IIIa	236-227.5	0.49	0.44	0.3	1.23	89.4	1.51
IIIb	227.5-217	0.71	0.24	0.28	1.23	78.95	0
IIIc	217-192.6	0.65	0.55	0.36	1.56	39.39	46.22
IIId	192.6-183.1	0.66	0.49	0.34	1.49	69.4	12.28
IIIe	183.1-175.5	0.63	0.2	0.30	1.13	60	0
IIIf	175.5-168.1	0.88	0.61	0.31	1.8	53.13	40.62

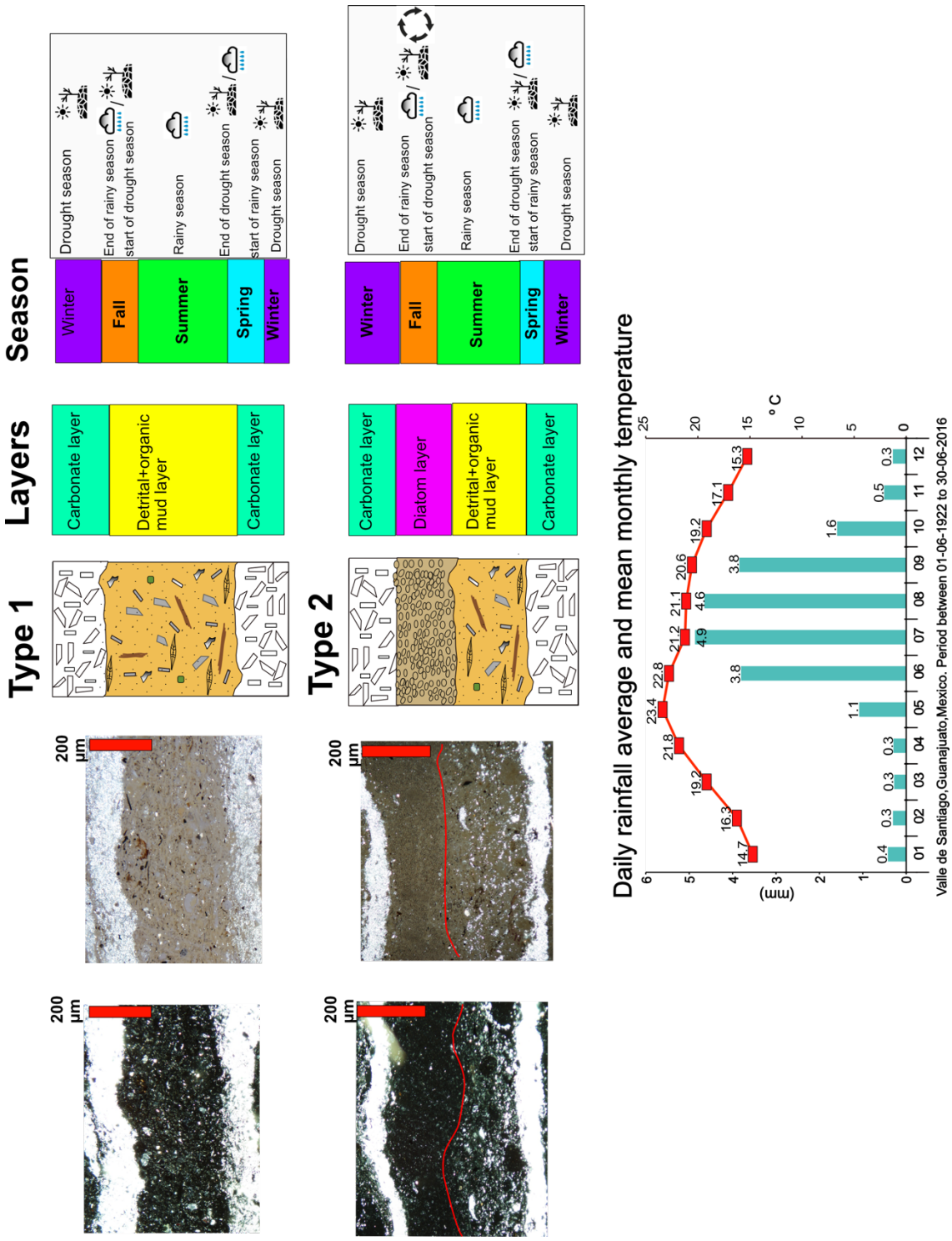

Figure 5.7- Thin section photos with crossed and parallel nichols, layer distribution and interpretation of varve Type 1 and Type 2. Daily rainfall average and monthly temperature from Valle the Santiago region between 1922 to 2016.

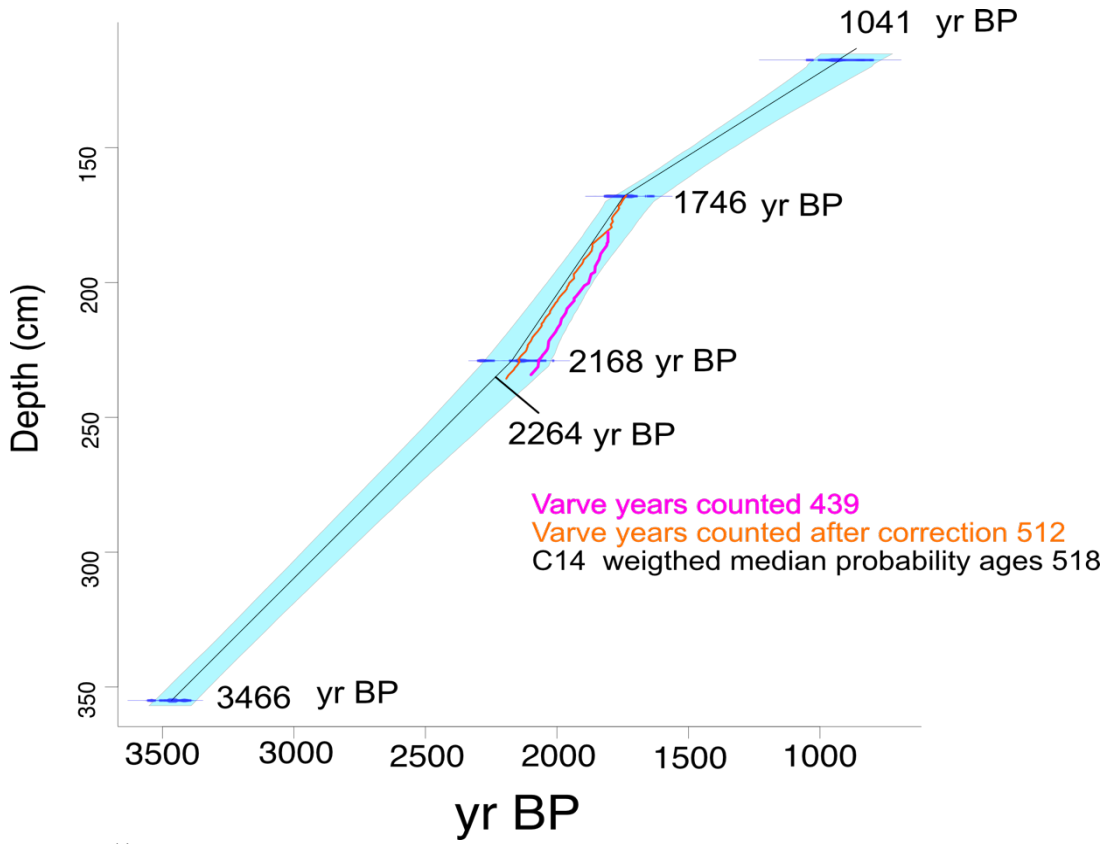

Figure 5.8-A) ^{14}C age model of la Alberca lake B) Chronology of study section anchored by two calibrate ^{14}C ages and one interpolated age. The solid purple line represents varve counts and the black solid line displays varve count after calculation of estimated age of massive layers, inferring sedimentation rates from neighboring varve.

I conclude that the formation of each lamination pattern (Type 1 and Type 2) represents an annual climate cycle, however, the formation of Type 2 is also influenced by the onset of anthropogenic activity in the study area (see discussion below). The verification of varve counts by an independent chronology method is needed due to diverse inconsistencies (e.g., hiatus) that the sequence can present (Ojala et al., 2012). The two weighted mean ages that anchor the floating study section lies between 1746 ± 183 cal yr BP and 2264 ± 243 cal yr BP covering a time interval of 518 years (Fig. 5.8). The average of the triple counts resulted in a deviation of 79 varve years or 15.25 %. The varve counts seem to be systematic younger than ^{14}C age model. Nearly all the varve counts reflect minimum chronologies, due to diverse processes that can affect the preservation of varve sequences such as bioturbation, erosion of the varve surface or complete erosion of the varve (Mingram et al., 2018). The presence of massive layers or turbites could be responsible for this divergence. The turbidites were removed from the section and a correction factor was applied in the massive layers. This factor was estimated by inferring sedimentation rates from the nearest neighboring varve. The corrected varve counting resulted in deviations of 6 years or 1.1 %.

5.3.2-Human and paleoclimate imprint in La Alberca sedimentary sequence during the Late Pre-Classical period

Previous results from La Alberca sedimentary sequence reveal an increase in anthropogenic activity during the late part of the Pre-Classical archeological period (~ 250 BCE-225 CE) (Fig 5.9). The start of anthropogenic activity is suggested by an increase in detrital flux, the rise in sedimentation rate and the high percentage of *Amaranthaceae* pollen (See discussion chapter 5.1). This interpretation is in agreement with the rise of the Chupicuaro culture in the region, during the Late Chupicuaro and Mixtlan occupation phases (Zepeda and Barrales, 2008). The main scope of this discussion is to study the timing of the occupation periods by the Chupicuaro culture (see chapter 2, section 2.5), its possible relationship with climate variability and how human activites (e.g. agriculture) modified the landscape in Valle de Santiago.

A climatic signal can be interpreted for sub-stages III.a, III.b, III.d and III. e. Sub-stage III.a (309-218 BCE) is characterized by well-preserved Type 1 varves, a constant input of detrital fraction indicated by the PCA 1 and *k* parameters, continuous calcium carbonate precipitation, a constant anoxic state indicated by the Mn/Fe ratio, and the small thickness of massive layers. The predominant Type 1 varves, the uniform input of detrital terrigenous and constant anoxic conditions indicates a relatively stable and stratified water column. Based on these observations, I interpret the dominance of moist conditions during this sub-stage. Additionally, the good preservation in Type 1 varves reflects a strong seasonal contrast (Fig. 5.9).

The substage III.b (time) is described by the decrease in the preservation of Type 1 varves, the reduction of detrital flux, low sedimentation rates (Table 5.1), the rise of carbonate concentration and the increase of anoxic or suboxic conditions. I interpreted a constant lake level reduction due to strong evaporation conditions. The strong evaporative conditions in the lake resulted in a high concentration of dissolved carbonates in the hypolimnion. The drop in the lake level, thus produced an unstable stratification and establishing suboxic to anoxic conditions in the water column (Anderson et al.,1985). This interpretation is strongly supported by increasing oscillations Mn/Fe and Ca/Ti ratios.

The sub-stages III.c (~137 BCE-37 CE) reveals the increase of detrital input (PCA 1 and *k*), the highest sedimentary rates in all the study section (Table 5.1), and a change between varve Type 1 varve and Type 2 varves. Therefore, I argue that the rise in the sedimentary clastic input, mean varve thickness 1.56, increased the nutrient-loading in the lake. In consequence, with the overload of nutrients, a rise of primary production occurs during the mixing state of the lake during the autumn season via the recycling of nutrients. This high productivity is represented by the OL that is mainly formed

by *Nitzschia paleacea* (Type 2 Varve), a diatom species tolerant to high nutrient availability (Voigt et al., 2008). This assumption is supported by paleo and modern limnological studies (e.g., Voigt et al., 2008; Urrea and Sabater, 2009).

The sub-stage III.d (time) displays a decrease in varve preservation, a decrease in input indicated by the PCA1 and magnetic susceptibility (*k).* The rise of calcium carbonate dominates the substage. Together these characteristics are interpreted as a dominant dry condition. A notable feature occurs in the lower part of the stage. The varve Type 2 still prevalence. Diatoms quickly react with the increase of nutrients in the lake systems; however, these changes can permanent modified the diatom community. I interpreted that modification in the nutrients budget of the lake system remained years after the high erosion described in sub-stage III.c resulting in the prevalence of diatoms bloom.

Sub-stage III.e (~87-155 CE) is characterized by the alternation of massive detrital layers and well preserved varves. Massive layers may occur during high detrital fluxes to the catchment area, during short humid periods increasing the oxic conditions and thus reducing the varve preservation (Zolitschka et al.,2015). This is in agreement with short periods of high detrital input described by the PCA 1 parameter, which coincides with the decreasing of anoxic conditions revealed by the Mn/Fe ratio. Together these observations are interpreted as oscillations between oxic and anoxic conditions in the lake, due to a highly variable precipitation regime. A detail discussion about the effects of wetter periods on the lake stratification can be found in the previous chapter.

The substage III.f (time) reveals a high preserved varve section, an increase in catchment input indicated by PCA1 and magnetic susceptibility and the highest mean varve thickness in all the record (Table 5.1). The presence of varve Type 2 predominates over varve Type 1. I interpreted that the increase of erosion enhanced the nutrient availability to the lake system, producing diatoms bloom reflected in the predominance of varve Type II. In addition, it is important to note that the substages III.c and III.f lies during the archeological Mixtlan phase (Darras and Faugere, 2007). The archeological evidence reveals the expansion of human settlements and the increase of the social organization by the Chupicuarto culture in the study area (Darras and Faugere, 2007). I propose that the increase of erosion and the subsequent eutrophication interpreted in both sub-stages reflects a strong human impact via the intensification of agricultural practices in the area. The increment of nutrients and the eutrophication of the lake, due to high detrital input during strong rainy seasons is also possible. I argue, however, that the agreement between anthropogenic indicators, like the rise in pollen percent of *Amaranthaceae*, and archeological evidence, such as occupation phases of the Chupicuaro culture (Fig. 5.9) are backing our interpretation that stages III.IV and III. I represent the first clear signal of human occupation in the Valle de Santiago region.

5.3.3-The record of human dynamics in Northern Mesoamerican Frontier and its relationship with climatic oscillations

The onset of ancient agriculture practices varied across different sectors of Mesoamerica. Based on the pollen record of the Aljojuca lake, in the Oriental Mesoamerica sector, Bhattacharya and Byrne (2016) argued that the rise of human landscape modification was around 1700 BCE. In the central Mesoamerica region, an increase in the human disturbance was described in the Chalco lake after 2000 BCE (Lozano-Garcia et al., 1993). Landscape disturbance by agricultural activities in the Northern Mesoamerica region is interpreted from the Patzcuaro, Hoya San Nicolas, Zacapu lakes and Upper Lerma river between 1500 BCE to 500 CE (Metcalfe et al., 1989). In Valle the Santiago, which lies in the NMF, the onset of small-scale agricultural activities was found in the pollen record of San Nicolas and Parangueo at 3700 BCE (Park et al., 2010). In the same region, a previous pollen study of La Alberca sediments revealed the imprint of ancient agricultural activities between 400 BCE-150 CE which was attributed to the Chupicuaro culture (Conserva, 2003).

The late Pre-Classic is a critical historical phase for understanding the expansion of cultures that came from the Acambaro Valley into the northern sector of Mesoamerica and the possible correlation between cultural history, and environmental and climatic changes. Conserva, (2003) describes a long occupation period between 400 BCE-150 CE in the Valle de Santiago area. However, based on the study of sedimentation rate over the last 4 000 years of twenty-one cores from Patzcuaro lake, O'Hara et al, (1994) suggested that long term agriculture in the NMF was not possible, due to high climate variability.

Radiocarbon analysis is the most widely technique used for constraint and dating ancient social events during the Holocene. Two potential sources can affect the precision of the method, such as an analytical error during the ^{14}C measurement and error related with the calendar year calibration. This last error occurs due to variability in ^{14}C production over time and lies typically in the range of 100-200 years (Wright, 2017). This issue hampers the correct interpretation of social changes in the archeological context. For example, the presence of plateaus or flatline during historical milestones in the radiocarbon calibration curve (Ramsey, 2001) hinders the possibility to systematically constrain the onset of European colonization, depopulation in the west of Africa and the rise of agricultural activities in Mesoamerican after 1620 CE. According to the age model, the study section has an average error of ±205 years. For this reason, the reader is to become aware of the level of uncertainty during the discussion of social events.

La Alberca record indicates that at least two periods of anthropogenic accelerated erosion (137 +/- 171 BCE- 37+/- 168 CE and 155 +/- 172 - 220 +/- 183 CE) occurred during the Late-Preclassic potentially due to anthropogenic activities in the lakes surrounding. In this regard, I suggest that the arrival of ancient agricultural societies to Valle the Santiago was around 137+/- 171 BCE, thus producing a high land degradation by the establishment of agricultural activities and in consequence modifying the limnology conditions of La Alberca.

Archeological data indicates a continuous migration period of the Chupicuaro culture from the Acambaro Valley to the northern region following the Laja and Lerma rivers during 250 BCE-100 CE (Zepeda and Barrales, 2008) (Fig 5.9). I hypothesized two short occupation periods interpreted from the study record (137 +/- 171 BCE - 37+/- 168 CE and 155 +/- 172 - 220 +/- 183 CE) are preceded by dry and hydrological variable climate conditions. In addition, the actual climate conditions in the NFM are marginal for agriculture practices (Kienel et al., 2009). This raises the possibility that anomalous wetter conditions occurred during the two interpreted occupation periods. Anomalous short wet periods were described during stage IV (see discussion section 5.2) due to the occurrence of a cool PDO state. One possibility is that the continuity of the influence of Pacific forcings, such as cool PDO state, could be the mechanism responsible for allowing paleoclimatic conditions (wetter periods) suitable for agriculture practices during stage III (2200 -1725 cay yr BP). A prominent wetter period is described by the Juxtlahuaca record between 0-200 CE (Lachniet et al., 2017), partly similar to the period of agriculture expansion described in this record.

These suggest, that climatic variability plays an important role, in the population dynamics of Chupicuaro and other cultures in the NMF, resulting in scarcity of vital resources for agricultural practices and thus reducing the chances of longer occupation periods. In other words, these characteristics provokes constant population migrations in order to find better places for agricultural practices, thus producing a high dynamic NMF.

In this regard, Armillas's theory, based on archeological evidence, describes the northward expansion of NMF during ~200 CE with a subsequent southward retraction around ~900 CE (Armillas, 1969). I hypothesize the occurrence of multiple migrations during the Late-Preclassic period, producing a subsequent retraction and expansion of NMF, before the period described by Armillas (1969). This hypothesis needs to be strongly tested using high-resolution paleoclimate records, paleoenvironmental records, specially varved records, along to NMF.

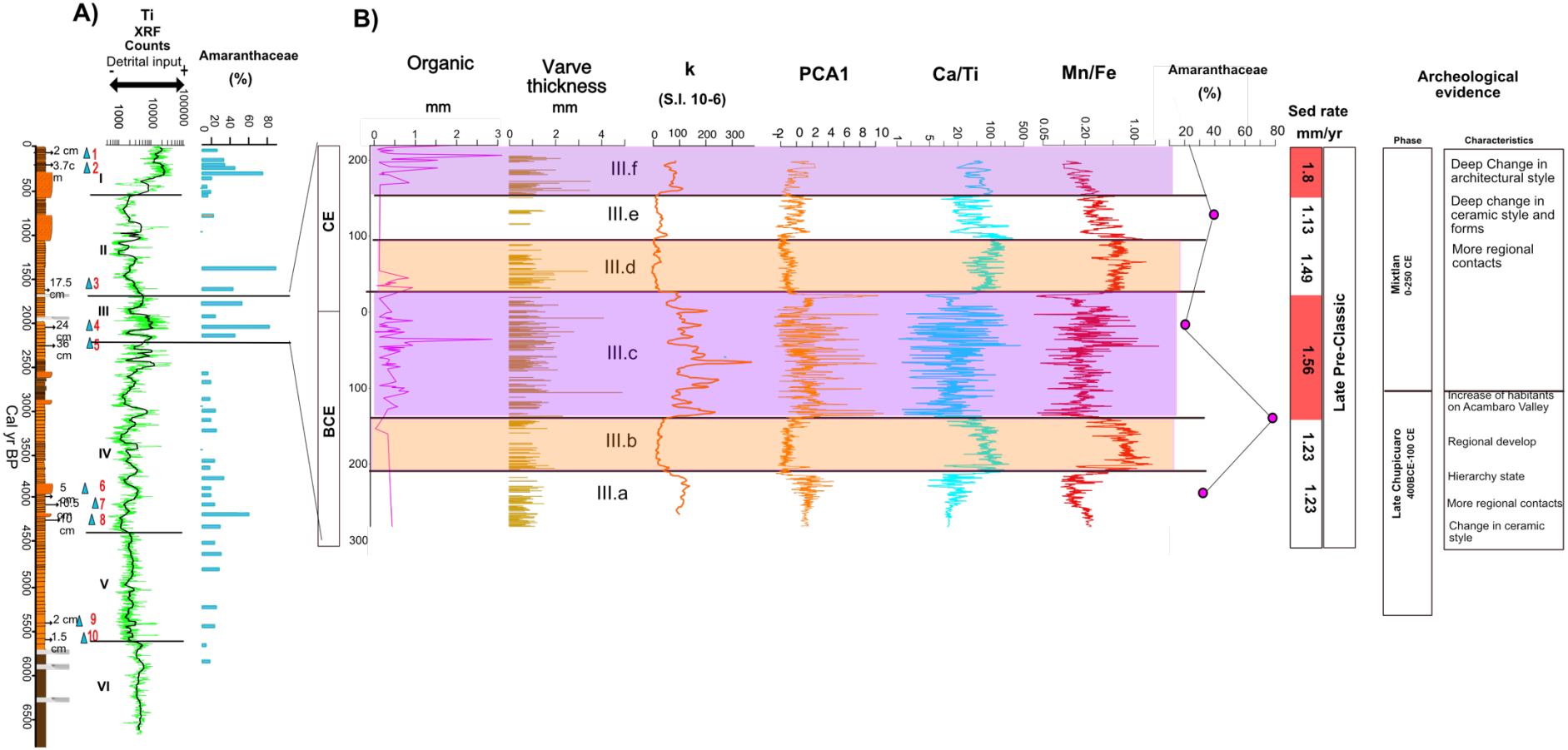

Figure 5.9- A) Comparison between stratigraphic section and Ti, $\delta^{18}O$ and *Amaranthaceae* records of La Alberca lake. B) Detailed varve analysis of stage III for the late Pre-Classic period. I compare varve results, with XRF results, sedimentation rates, pollen samples and archeological evidence (Darras and Faugere 2007). Orange bars represents interpreted as drought periods and purple bars represent periods with intensification in anthropogenic land use

5.3.4-Concluding remarks

Varve analysis from La Alberca lake reveals a complex history between anthropogenic land use by ancient agriculturists, and climatic fluctuations during the late Pre-Classic period in the Northern Mesoamerica frontier.

In the study section, I interpret the presence of two types of varves. Type 1 varves are comprised by the alternation of detrital organic layers and aragonite layers. Type 2 varves are composed by an alternation of detrital organic layer with an organic layer which is exclusively formed by post-mortem diatom frustules and aragonite layers. I conclude that formation of both varve types represents an annual hydrological cycle, however, the formation of Type 2 is also influenced by the rise of anthropogenic activities.

The anthropogenic signal in Type 2 varves is interpreted by the rise in sedimentation rate, increase in terrigenous input and the presence of organic layer mainly formed by *Nitzschia paleacea*, a diatom species tolerant to high nutrient availability. I propose that the increase of detrital input raised the nutrient loading and eutrophication in the lake occurs. Eutrophication is linked with the establishment of ancient agriculture activities in the Valle the Santiago. This interpretation is also supported high percent in *Amaranthaceae* pollen and archeological evidence related to the occupation phases of the Chupicuaro culture.

I hypothesize two periods of anthropogenic erosion (137 +/- 171 BCE- 37+/- 168 CE and 155 +/- 172 - 220 +/- 183 CE) both presiding by dry and hydrological variable climate conditions. Based on these interpretations and in combination with archeological evidence I conclude:

1-The actual climatic conditions in the NMF indicate that this region is marginal for agricultural practices. Thus the occurrence of anomalous wetter periods is proposed for explaining rise the of landscape degradation by anthropogenic activities. I propose that the continues influence of cool PDO states still occurring during stage III.

2-I propose that high climate variability conditions played an important role in the population dynamics of Chupicuaro and other ancient cultures in the Northern Mesoamerica frontier.

3-I hypothesize the occurrence of multiple population migrations during the Late-Preclassic period, producing a subsequence retraction and expansion of NMF, earlier than the period described by Armillas during the Epiclassic.

Chapter 6

General conclusions

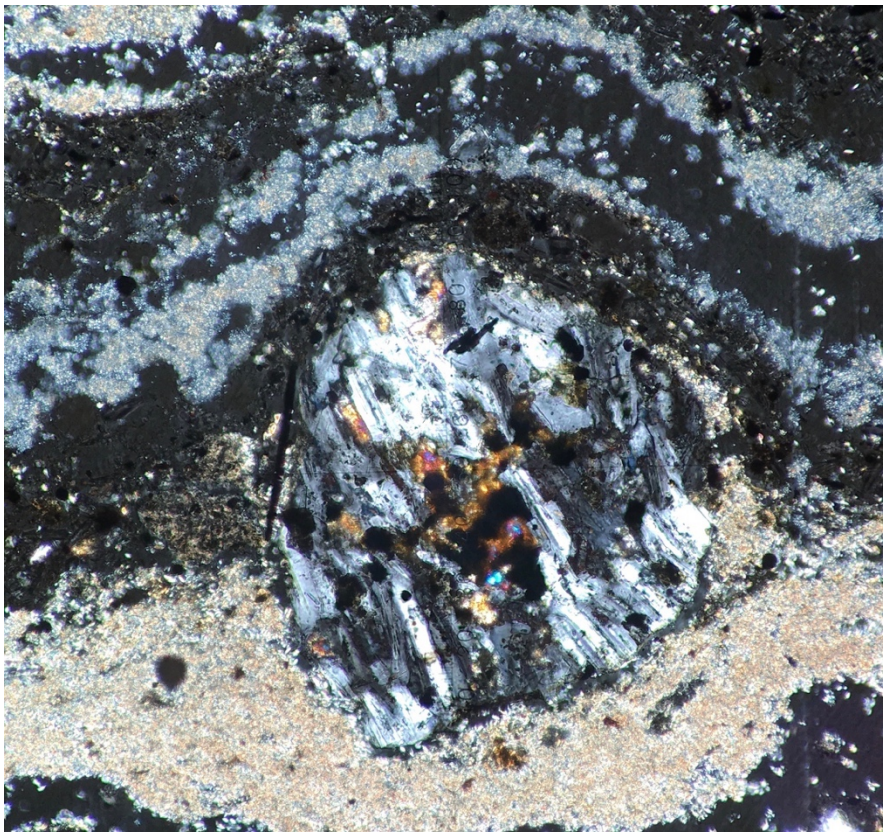

Andesitic lithic by Kurt Wogau

General conclusions

This thesis aims to provide a high-resolution data of paleoclimate and paleoenvironmental conditions in the Northern Mesoamerican Frontier, using the varved sediments of La Alberca maar lake. Besides, I study the link between climate change and environmental degradation with the evolution of Pre-Hispanics cultures in the Northern Mesoamerican Frontier. For these purposes, I used environmental magnetism, XRF, microfacies analysis and radiocarbon dating as principal techniques. In conclusion this study:

1. **Defines the paleoclimatic characteristics and timing of the end of Early-Holocene peak insolation period in the Northern Mesoamerican Frontier.**
   The end of Early Holocene peak insolation period is revealed around 5600 yr BP by a drastic shift in the stratigraphic characteristics of the record, changing from a massive layer to well-laminated facies, enrichment of $\delta^{18}O$ and decrease of detrital input revealed by the PCA 1 record. Those characteristics are interpreted as a reduction of monsoon strength.

2. **The rise of variable hydrological conditions around 4300 yrs and its possible correlation with the onset of ENSO activity and PDP in the Northern Mesoamerican Frontier.**
   Variable hydrological conditions are interpreted from a worsening preservation of lamination, an increase of detrital input, which correlates with the latitudinal displacements of the ITCZ register in the Cariaco record and the rise of El Niño Southern Oscillation and PDO

3. Hydrological variability is also observed in the magnetic mineralogy. In stage IV (~ 4400-2200 yr BP) a gradual rise of oxic conditions is suggested by the increase of concentration and preservation of ferrimagnetic fraction revealed by *k*, SIRM, S-ratio and kARM parameters. SEM displays well-preserved titanomagnetite crystals in this stage. The rising of oxic conditions was motivated by the enhanced mixing states of the lake. Strong variability of ITCZ position and onset of El Niño Southern Oscillation are proposed as the main mechanism of mixing states.

4. I interpret that the variable climate conditions during the first part of the Pre-Classic period hindered the adaptation Mesoamerican cultures, thus resulting in a delay of social, political and cultural evolution.

5. **Using varve analysis, two periods of agricultural intensification by the Chupicuaro culture were interpreted between 309 BCE- 225 CE.**
   Type 2 varves reveal an anthropogenic disturbances in the lake. This interpretation is supported by the rise of sedimentation rate, increase in terrigenous input and the presence of organic sublayers mainly formed by *Nitzschia paleacea*, a diatom species tolerant to high nutrient availability. The rise of agricultural activities increased the erosion and amount of nutrients coming to the lake, producing eutrophication.

6. Based on this interpretation, two periods of anthropogenic erosion were interpreted (137 +/- 171 BCE- 37+/- 168 CE and 155 +/- 172 - 220 +/- 183 CE). Both periods were preceded by dry and hydrological variable conditions. This interpretation describes multiple occupation periods during the Late Preclassic in the Valle de Santiago region.

7. **A severe drought period during the Epiclassic played an important role in the retraction of Northern Mesoamerican Frontier.**
   The Ca/Ti ratio reveals two subsequent drought periods during the Epiclassic around 700-790 CE and ~810-880 CE. This interpretation is in agreement with the Juxtlahuca speleothem record. I support Armillas´ theory that climatic change played an important role in the diverse geographic and social oscillation of the Northern Mesoamerican Frontier. However, I would like to mention that this is not a deterministic interpretation. I agree that climatic factors resulted in the stress of natural resources vital for the social and political evolution of Northern Mesoamerican cultures. In other words, the combination of all these important elements motivated the rise and fall of human settlements in the northern sector of Mesoamerica.

8. **The intrusion of Toltec culture and rise of Tarascan in the Northern Mesoamerican frontier under favorable climatic conditions.**
   This study reveals that the excursion of Toltec culture in the Northern Mesoamerican frontier was accompanied by the pluvial period between 900-1050 CE. The Aztec pluvial period between 1400-1500 CE is in agreement with the establishment of the Tarascan culture in the zone.

9. **Land deterioration by agricultural activities during the colonial period.**
   Between 1500- 2000 CE high detrital input described by Ti parameter correlates with the increase of *Amaranthaceae*. The start of agricultural activities in colonial times is interpreted.

10. **SSTs of the Atlantic basin as the principal driver of Mesoamerican Monsoon.**
    This study suggests that that variability in the SSTs of Atlantic basin can modify the strength of the Mesoamerican monsoon. With low(high) SSTs temperatures the Atlantic Meridional Overturning Circulation decreases (increases), moving southward (northward) the tropical rain belt. Another atmospheric mechanism proposed is related with the North Atlantic Oscillation. Positive NAO increases the trade winds intensity, thus reducing the SSTs. This process slows down the AMOC and shifts southward the ITCZ occurred, resulting in drought conditions in the Northern Mesoamerican Frontier.

This work highlights the potential of the varved records for the reconstruction of paleoclimate and paleoenvironmental variability with a centennial or decadal resolution. Additionally, La Alberca record shows a high correlation between climatic and environmental changes and the historical evolution of Northern Mesoamerican Frontier.

Outlook

Armillas´ (1964, 1969) theory argues that climate change in the Northern Mesoamerican Frontier played a fundamental role in its social dynamics. Brown (1984) rejected this hypothesis, suggesting that intense anthropogenic pressure ruled the sedimentation process in diverse lakes located along the Northern Mesoamerican Frontier, about 1100 CE (Post-Classical period). The pollen study of Conserva (2008) suggests a climate change during the Epiclassic period, which resulted in population displacement, retraction of the Northern Mesoamerican Frontier toward the southern position, due to scarcity of vital resources.

This dissertation presents a high-resolution paleoclimatic-paleoenvironmental record for the last 6700 yrs from the Northern Mesoamerican Frontier. Diverse methods were employed in order to solve one central question: Did climate-environmental changes play a major role in the social oscillations in the Northern Mesoamerican Frontier? I suggest that climate change indeed played an essential role. However, this was not the only factor. Climatic changes were the trigger process amplified by social and political disruptions. The combination of these processes provoked the collapse or reductions of the complex social structures.

This thesis sheds light on another interesting aspect: the response of Mesoamerican societies to gradual and rapid climate changes. Whereas, high hydroclimate variability between 4300 yr BP to 2500 yr BP just resulted in a delay in the developing of complex Mesoamerican societies, a drastic climate change (e.g., Epiclassic drought) culminated in a social crisis. Although these ancient societies possessed a high knowledge of their natural resources, dramatic climate changes could not be faced in some cases. The varve analysis describes a multiple short periods of land scape transformations. This describes the Northern Mesoamerican Frontier as a region, with constants social migrations where its inhabits lived in a constant searching of natural resources.

The naturality of drastic climate changes is not well understood. Several ocean-atmospheric mechanisms and external forces have been proposed in order to explain it. The La Alberca record describes a complex interaction between SST oscillations in the Atlantic, the rise of ENSO forcing on the Pacific side, oscillations in tropical circulation such as the ITCZ, and the possibility that solar cycles played a role in the monsoon variations. To improve the knowledge of this topic, high-resolution records have to be studied in all the Mesoamerica area and the use of novel techniques such as varve analysis have to be mandatorily implemented, especially for the possible improvement of ages models of the study records. Just in this way, in the near future, we can be able to produce high-quality mathematical climate models and climate predictions with less

dating uncertainty. Last but not least, many archeological enigmas and questions still buried in the past and waiting. We need to take advantage of all these new high-resolution techniques in order to solve it.

References

Alcocer, J., & Bernal-Brooks, F. W. (2010). Limnology in Mexico. *Hydrobiologia*, 644(1), 1-54.

Alcocer, J., & Filonov, A. E. (2007). A note on the effects of an individual large rainfall event on saline Lake Alchichica, Mexico. *Environmental Geology*, 53(4), 777-783.

Alcocer, J., & Lugo, A. (2003). Effects of El Niño on the dynamics of Lake Alchichica, central Mexico. *Geofísica Internacional*, 42(3), 523-528.

Alcocer, J., & Hammer, U. T. (1998). Saline lake ecosystems of Mexico. *Aquatic Ecosystem Health & Management*, 1(3-4), 291-315.

Alcocer, J., Escobar, E., & Lugo, A. (2000). Water use (and abuse) and its effects on the crater-lakes of Valle de Santiago, Mexico. *Lakes & Reservoirs: Research & Management*, 5(3), 145-149.

Alley, R. B., Marotzke, J., Nordhaus, W. D., Overpeck, J. T., Peteet, D. M., Pielke, R. A., & Wallace, J. M. (2003). Abrupt climate change. *science*, 299(5615), 2005-2010.

Anderson, R. Y. (1985). *Meromictic lakes and varved lake sediments in North America* (No. 1607). US Government Printing Office.

Aranda-Gómez, J. J. (2014). Structural analysis of subsidence-related deformation at the bottom of Rincón de Parangueo maar, México. *In Proceedings IAVCEI-5th International Maar Conference* (pp. 174-175). Centro de Geociencias, UNAM Querétaro.

Aranda-Gómez, J. J., & Carrasco-Nuñez, G. (2014, November). The Valle de Santiago Maars, México: The Record of Magma–Water Fluctuations during the Formation of a Basaltic Maar (La Alberca) and Active Post-Desiccation Subsidence at the Bottom of a Maar Lake (Rincón de Parangueo): Intra-conference Field Trip Guidebook. *In Field Guide for Intra-conference Fieldtrip (20 November 2014) 5th International Maar Conference (5IMC-IAVCEI)* (Vol. 17, p. 22).

Aranda-Gómez, J. J., Levresse, G., Martínez, J. P., Ramos-Leal, J. A., Carrasco-Núñez, G., Chacón-Baca, E., & Noyola-Medrano, C. (2013). Active sinking at the bottom of the Rincón de Parangueo Maar (Guanajuato, México) and its probable relation with subsidence faults at Salamanca and Celaya. *Boletín de la Sociedad Geológica Mexicana*, *65*(1), 169-188.

Arbuszewski, J. A., Cléroux, C., Bradtmiller, L., & Mix, A. (2013). Meridional shifts of the Atlantic intertropical convergence zone since the Last Glacial Maximum. *Nature Geoscience*, 6(11), 959-962.

Armienta, M. A., Vilaclara, G., De la Cruz-Reyna, S., Ramos, S., Ceniceros, N., Cruz, O., & Arcega-Cabrera, F. (2008). Water chemistry of lakes related to active and inactive Mexican volcanoes. *Journal of Volcanology and Geothermal Research*, 178(2), 249–258. https://doi.org/10.1016/j.jvolgeores.2008.06.019

Armillas, P. (1964). Condiciones ambientales y movimientos de pueblos en la frontera septentrional de Mesoamérica. *Homenaje a Fernando Márquez-Miranda*, 62-82.

Armillas, P. (1969). Section of anthropology: The arid frontier of Mexican civilization. *Transactions of the New York Academy of Sciences*, 31(6 Series II), 697-704.

Armillas, P. (1991). El norte de Mesoamérica. Pedro Armillas. Vida y obra, 2, 155-206.

Arz, H. W., Lamy, F., & Pätzold, J. (2006). A pronounced dry event recorded around 4.2 ka in brine sediments from the northern Red Sea. *Quaternary Research*, 66(3), 432-441.

Arz, H. W., Lamy, F., Pätzold, J., Müller, P. J., & Prins, M. (2003). Mediterranean moisture source for an early-Holocene humid period in the northern Red Sea. *Science*, 300(5616), 118-121.

Barron, J.A., Metcalfe, S.E., & Addison, J.A., (2012). Response of the North American monsoon to regional changes in ocean surface temperature. *Paleoceanography* 27, PA3206. http://dx.doi.org/10.1029/2011PA002235

Berger, A., & Loutre, M. F. (1991). Insolation values for the climate of the last 10 million years. *Quaternary Science Reviews*, 10(4), 297-317.

Berkelhammer, M., Sinha, A., Stott, L., Cheng, H., Pausata, F. S., & Yoshimura, K. (2012). An abrupt shift in the Indian monsoon 4000 years ago. *Geophys. Monogr. Ser*, *198*, 75-87.

Bernal, J. P., Lachniet, M., McCulloch, M., Mortimer, G., Morales, P., & Cienfuegos, E. (2011). A speleothem record of Holocene climate variability from southwestern Mexico. *Quaternary Research*, 75(1), 104-113.

Bernardino (de Sahagún), Anderson, A. J., & Dibble, C. E. (2012). Florentine codex: general history of the things of New Spain. University of Utah Press

Bhattacharya, T., & Byrne, R. (2016). Late Holocene anthropogenic and climatic influences on the regional vegetation of Mexico's Cuenca Oriental. *Global and Planetary Change*, 138, 56–69.https://doi.org/10.1016/j.gloplacha.2015.12.005

Bhattacharya, T., Byrne, R., Böhnel, H., Wogau, K., Kienel, U., Ingram, B. L., & Zimmerman, S. (2015). Cultural implications of late Holocene climate change in the Cuenca Oriental, Mexico. *Proceedings of the National Academy of Sciences*, 112(6), 1693–1698.https://doi.org/10.1073/pnas.1405653112

Bhattacharya, T., & Chiang, J. C. (2014). Spatial variability and mechanisms underlying El Niño-induced droughts in Mexico. *Climate dynamics*, *43*(12), 3309-3326.

Bhattacharya, T., Chiang, J. C., & Cheng, W. (2017). Ocean-atmosphere dynamics linked to 800–1050 CE drying in Mesoamerica. *Quaternary Science Reviews*, 169, 263-277.

Blaauw, M. (2010). Methods and code for "classical" age-modelling of radiocarbon sequences. *Quaternary Geochronology*, 5(5), 512–518. https://doi.org/10.1016/j.quageo.2010.01.002

Bloemendal, J., King, J. W., Hall, F. R., & Doh, S. J. (1992). Rock magnetism of Late Neogene and Pleistocene deep-sea sediments: Relationship to sediment source, diagenetic processes, and sediment lithology. *Journal of Geophysical Research: Solid Earth*, *97*(B4), 4361-4375.

Bond, G., Kromer, B., Beer, J., Muscheler, R., Evans, M. N., Showers, W., & Bonani, G. (2001). Persistent solar influence on North Atlantic climate during the Holocene. *Science*, 294(5549), 2130-2136.

Braniff, B. (1998). Morales, Guanajuato y la tradición Chupícuaro. Instituto Nacional de Antropología e Historia. (Vol. 373).

Braniff, B. (2000). A summary of the archaeology of north-central Mesoamerica: Guanajuato, Querétaro, and San Luis Potosí. *Greater Mesoamerica: The Archaeology of West and Northwest Mexico*. University of Utah Press, Salt Lake City, 35-42.

Brauer, A., & Casanova, J. (2001). Chronology and depositional processes of the laminated sediment record from Lac d'Annecy, French Alps. *Journal of Paleolimnology*, 25(2), 163-177.

Brown, R. B. (1984). The paleoecology of the Northern Frontier of Mesomaerica (Pollen, Mexico, Archeology) (Published doctoral dissertation). The University of Arizona. Arizona, New Mexico, USA.

Brown, R.B., (1992). Arqueología y Paleoecología del Norcentro de México. Instituto Nacional de Antropología e Historia, Mexico City.

Butzer, K. W., & Butzer, E. K. (1997). The 'natural'vegetation of the Mexican Bajío: Archival documentation of a 16th-century savanna environment. *Quaternary International*, 43, 161-172.

Butzer, K. W. (2012). Collapse, environment, and society. *Proceedings of the National Academy of Sciences*, 201114845.

Cardenas, G.E.(1999). El bajio y su definicion territorail y cultural. El Colegio de Michoacán A.C., Centro INAH Michoacán.

Cavazos, T., Turrent, C., & Lettenmaier, D. P. (2008). Extreme precipitation trends associated with tropical cyclones in the core of the North American monsoon. *Geophysical Research Letters*, *35*(21).

Chiang, J. C. H., Cheng, W., & Bitz, C. M. (2008). Fast teleconnections to the tropical Atlantic sector from Atlantic thermohaline adjustment. *Geophysical Research Letters*, 35(7), 1–5. https://doi.org/10.1029/2008GL033292

Chiang, J.C., & Friedman, A.R., (2012). Extratropical cooling, interhemispheric thermal gradients, and tropical climate change. Annu. Rev. *Earth Planet. Sci*. 40 (1), 383.

Clark, J. E., Pye, M. E., & Gosser, D. C. (2007). Thermolithics and corn dependency in Mesoamerica. In Lowe, L. S., and Pye, M. E. (eds.), *Archaeology, Art, and Ethnogenesis in Mesoamerican Prehistory: Papers in Honor of Gareth W. Lowe*, Papers 68, New World Archaeological Foundation, Brigham Young University, Provo, pp. 23–42.

Conroy, J. L., Overpeck, J. T., Cole, J. E., Shanahan, T. M., & Steinitz-Kannan, M. (2008). Holocene changes in eastern tropical Pacific climate inferred from a Galápagos lake sediment record. *Quaternary Science Reviews*, 27(11-12), 1166-1180.

Conserva, M. E. (2003). Climate and vegetation change in Central Mexico: Implications for Mesoamerican Prehistory (Published doctoral dissertation). UC Berkeley. California, USA.

Croudace, I. W., Rindby, A., & Rothwell, R. G. (2006). ITRAX: description and evaluation of a new multi-function X-ray core scanner. *Geological Society, London, Special Publications*, 267(1), 51-63.

Curtis, J. H., Hodell, D. A., & Brenner, M. (1996). Climate variability on the Yucatan Peninsula (Mexico) during the past 3500 years, and implications for Maya cultural evolution. *Quaternary Research*, 46(1), 37-47.

Darras, V., Faugère B., (2007). Chupícuaro, entre el Occidente y el Altiplano central. Un balance de los conocimientos y las nuevas aportaciones. CEMCA-Colegio de Michoacan, México. *Dinámicas culturales entre el Occidente, el Centro-Norte y la Cuenca de México del Preclásico al Epiclásico*. pp.51-84,

Davies, S. J., Lamb, H. F., & Roberts, S. J. (2015). Micro-XRF core scanning in palaeolimnology: recent developments. *In Micro-XRF studies of sediment cores* (pp. 189-226). Springer, Dordrecht.

Davies, S. J., Metcalfe, S. E., Aston, B. J., Byrne, A. R., Champagne, M. R., Jones, M. D., & Noren, A. (2018). A 6,000-year record of environmental change from the eastern Pacific margin of central Mexico. *Quaternary Science Reviews*, 202, 211–224. https://doi.org/10.1016/J.QUASCIREV.2018.11.008

De Boer, C. B., & Dekkers, M. J. (1998). Thermomagnetic behaviour of haematite and goethite as a function of grain size in various non-saturating magnetic fields. *Geophysical Journal International*, 133(3), 541-552.

deMenocal, P. B. (2001). Cultural Responses to Climate Change During the Late Holocene. [Review]. *Science Paleoclimate*, 292(5517), 667–673. https://doi.org/10.1126/science.1059287

Dixit, Y., Hodell, D. A., & Petrie, C. A. (2014). Abrupt weakening of the summer monsoon in northwest India~ 4100 yr ago. *Geology*, *42*(4), 339-342.

Donohoe, A., Marshall, J., Ferreira, D., & Mcgee, D. (2013). The relationship between ITCZ location and cross-equatorial atmospheric heat transport: From the seasonal cycle to the Last Glacial Maximum. *Journal of Climate*, 26(11), 3597-3618.

Dräger, N., Theuerkauf, M., Szeroczyńska, K., Wulf, S., Tjallingii, R., Plessen, B., & Brauer, A. (2017). Varve microfacies and varve preservation record of climate change and human impact for the last 6000 years at Lake Tiefer See (NE Germany). *The Holocene*, *27*(3), 450-464.

Douglas, M. W., Maddox, R. A., Howard, K., & Reyes, S. (1993). The mexican monsoon. *Journal of Climate*, 6(8), 1665-1677.

Dueñas,M.(2017). La frontera septentrional de Mesoamérica durante el Epiclásico (600-900 A.D.). Una Mirada a través de la teoría de sistemas mundo de la arqueología en Aguascalientes, México. (Master degree dissertation). Universidad Autónoma de San Luis, San Luis Potosi, México.

Dunlop, D. J., Özdemir, Ö., & Schmidt, P. W. (1997). Paleomagnetism and paleothermometry of the Sydney Basin 2. Origin of anomalously high unblocking temperatures. *Journal of Geophysical Research:* Solid Earth, 102(B12), 27285-27295.

Dyer, T. G. J. (1979). Rainfall along the east coast of southern Africa, the Southern Oscillation, and the latitude of the subtropical high-pressure belt. *Quarterly Journal of the Royal Meteorological Society*, 105(444), 445-451.

Elliot, M. (2012). An anthropological approach to understanding Late Classic period cultural collapse in Mesoamerica's northwestern frontier. *Wood and Charcoal Evidence for Human and Natural History*, 217-226.

Elliott, M., Fisher, C. T., Nelson, B. A., Garza, R. S. M., Collins, S. K., & Pearsall, D. M. (2010). Climate, agriculture, and cycles of human occupation over the last 4000 yr in southern Zacatecas, Mexico. *Quaternary Research*, 74(1), 26-35.

EarthNow Team. National Oceanic and Atmospheric Administration https://sphere.ssec.wisc.edu/

Evans, S. T. (2008). Ancient Mexico and Central America: archaeology and culture history. New York: Thames & Hudson.

Faegri, K., & Iversen, J. (1989). Textbook of Pollen Analysis (4th edn by Faegri, K., Kaland, PE & Krzywinski, K.).

Fenoglio,F., Fonseca, E., & Hinojosa, I. (2008)."El Epiclásico en el Marques, Quéretaro. *Un grano de arena. Tiempo Y Región, Estudios Históricos y Sociales,* Vol 2. Municipio de Querétaro,INAH,UAQ, México.

Ferrari, L. (2000). Avances en el conocimiento de la Faja Volcánica Transmexicana durante la última década. *Boletín de la Sociedad Geológica Mexicana*, 53(1), 84-92.

Flannery, K. V., Marcus, J., & Kowalewski, S. A. (1981). The Preceramic and Formative of the Valley of Oaxaca. In Sabloff, J. (ed.), Supplement 1 to the *Handbook of Middle American Indians*, University of Texas Press, Austin, pp. 48–93

Flohr, P., Fleitmann, D., Matthews, R., Matthews, W., & Black, S. (2016). Evidence of resilience to past climate change in Southwest Asia: Early farming communities and the 9.2 and 8.2 ka events. *Quaternary Science Reviews*, 136, 23-39.

Florance, C. A. (2000). The Late and Terminal Preclassic in southeastern Guanajuato: Heartland or periphery. Greater Mesoamerica: *The Archaeology of West and Northwest Mexico, University of Utah Press, Salt Lake City*, 21-33.

Frederick, C. D. (1995). "Fluvial Response to Late Quaternary Climate Change and Land Use in Central Mexico." (Unpublished Ph.D. Dissertation thesis), University of Texas, Austin.

Giannini, A., Kushnir, Y., & Cane, M. A. (2000). Interannual variability of Caribbean rainfall, ENSO, and the Atlantic Ocean. *Journal of Climate*, 13(2), 297-311.

Glenn CR, & Kelts K (1991). Sedimentary rhythms in lake deposits. In: Einsele G, Ricken W, Seilacher A (eds*) Cycles and Events in stratigraphy*. Springer, Berlin, pp 188–221

Gochis, D. J., Watts, C. J., Garatuza-Payan, J., & Cesar-Rodriguez, J. (2007). Spatial and temporal patterns of precipitation intensity as observed by the NAME event rain gauge network from 2002 to 2004. *Journal of Climate*, *20*(9), 1734-1750.

Gorenstein, S. (1985). Acambaro: Frontier Settlement on the Tarascan-Aztec Border *Vanderbilt University Publications in Anthropology* (Vol. 32).

Gray, S. T., Graumlich, L. J., Betancourt, J. L., & Pederson, G. T. (2004). A tree-ring based reconstruction of the Atlantic Multidecadal Oscillation since 1567 AD. *Geophysical Research Letters*, 31(12).

Grossman, E. L., & Ku, T. L. (1986). Oxygen and carbon isotope fractionation in biogenic aragonite: temperature effects. *Chemical Geology: Isotope Geoscience Section*, 59, 59-74.

Grove, D. C. (1997). Olmec archaeology: A half century of research and its accomplishments. *Journal of World Prehistory*, 11(1), 51-101.

Harrison, S. P. A., Kutzbach, J. E., Liu, Z., Bartlein, P. J., Otto-Bliesner, B., Muhs, D., & Thompson, R. S. (2003). Mid-Holocene climates of the Americas: a dynamical response to changed seasonality. *Climate Dynamics*, *20*(7-8), 663-688.

Haug, G. H., Hughen, K. A., Sigman, D. M., Peterson, L. C., & Röhl, U. (2001). Southward migration of the intertropical convergence zone through the Holocene. *Science*, *293*(5533), 1304-1308.

Henry, W. K. (1979). Some aspects of the fate of cold fronts in the Gulf of Mexico. *Monthly Weather Review*, 107(8), 1078-1082.

Heslop, D. (2009), On the statistical analysis of the rock magnetic S-ratio*, Geophys. J. Int.,* 178, 159–161, doi:10.1111/j.1365-246X. 2009.04175.x

Heslop, D., Dekkers, M. J., Kruiver, P. P., & van Oorschot, I. H. M. (2002). Analysis of isothermal remanent magnetization acquisition curves using the expectation-maximization algorithm. *Geophysical Journal International*, 148(1), 58–64.https://doi.org/10.1046/j.0956-540x.2001.01558.x

Hidalgo, H. G., Durán-Quesada, A. M., Amador, J. A., & Alfaro, E. J. (2015). The Caribbean low-level jet, the inter-tropical convergence zone and precipitation patterns in the intra-Americas sea: A proposed dynamical mechanism. *Geografiska Annaler: Series A, Physical Geography*, 97(1), 41-59.

Higgins, R. W., Yao, Y., & Wang, X. L. (1997). Influence of the North American monsoon system on the US summer precipitation regime. *Journal of Climate*, *10*(10), 2600-2622.

Hodell, D. a., Brenner, M., & Curtis, J. H. (2005). Terminal Classic drought in the northern Maya lowlands inferred from multiple sediment cores in Lake Chichancanab (Mexico). *Quaternary Science Reviews*, 24(12–13), 1413–1427.

Hodell, D. A., Curtis, J. H., & Brenner, M. (1995). Possible role of climate in the collapse of Classic Maya civilization. *Nature*, 375(6530), 391.

Hodell, D. A., Curtis, J. H., Jones, G. A., Higuera-Gundy, A., Brenner, M., Binford, M. W., & Dorsey, K. T. (1991). Reconstruction of Caribbean climate change over the past 10,500 years. *Nature*, *352*(6338), 790.

Holmes, J. A., Metcalfe, S. E., Jones, H. L., & Marshall, J. D. (2016). Climatic variability over the last 30 000 years recorded in La Piscina de Yuriria, a Central Mexican crater lake. *Journal of Quaternary Science*, 31(4), 310-324.

Jones, M. D., Metcalfe, S. E., Davies, S. J., & Noren, A. (2015). Late Holocene climate reorganisation and the north American monsoon. *Quaternary Science Reviews*, *124*, 290-295.

Joyce, R. A., & Henderson, J. S. (2007). From feasting to cuisine: Implications of archaeological research in an early Honduran village. *American Anthropologist* 109: 642–653

Kennett, D. J. (2012). Archaic-period foragers and farmers in Mesoamerica. In Nichols, D. L., and Pool, C. A. (eds.), The Oxford Handbook of Mesoamerican Archaeology, Oxford University Press, New York, pp. 141–150.

Kienel, U., Bowen, S. W., Byrne, R., Park, J., Böhnel, H., Dulski, P., & Negendank, J. F. W. (2009). First lacustrine varve chronologies from Mexico: Impact of droughts, ENSO and human activity since AD 1840 as recorded in maar sediments from Valle de Santiago. *Journal of Paleolimnology*, 42(4), 587–609.https://doi.org/10.1007/s10933-009-9307-x

Kienel, U., Dulski, P., Ott, F., Lorenz, S., & Brauer, A. (2013). Recently induced anoxia leading to the preservation of seasonal laminae in two NE-German lakes. *Journal of Paleolimnology*, 50(4), 535–544.https://doi.org/10.1007/s10933-013-9745-3

King, J., Banerjee, S. K., Marvin, J., & Özdemir, Ö. (1982). A comparison of different magnetic methods for determining the relative grain size of magnetite in natural materials: some results from lake sediments. *Earth and Planetary Science Letters*, *59*(2), 404-419.

Lachniet, M. S., Asmerom, Y., Polyak, V., & Bernal, J. P. (2017). Two millennia of Mesoamerican monsoon variability driven by Pacific and Atlantic synergistic forcing. *Quaternary Science Reviews*, 155, 100–113. https://doi.org/10.1016/j.quascirev.2016.11.012

Lachniet, M. S., Bernal, J. P., Asmerom, Y., Polyak, V., & Piperno, D. (2012). A 2400 yr Mesoamerican rainfall reconstruction links climate and cultural change. *Geology*, 40(3), 259-262.

Leng, M. J., & Marshall, J. D. (2004). Palaeoclimate interpretation of stable isotope data from lake sediment archives. *Quaternary Science Reviews*, 23(7-8), 811-831.

Lewis Jr, W. M. (1983). A revised classification of lakes based on mixing. *Canadian Journal of Fisheries and Aquatic Sciences*, 40(10), 1779-1787.

Li, H. C., & Ku, T. L. (1997). $\delta^{13}C$–$\delta^{18}C$ covariance as a paleohydrological indicator for closed-basin lakes. *Palaeogeography, Palaeoclimatology, Palaeoecology*, *133*(1-2), 69-80.

Li, M., Hinnov, L., & Kump, L. (2019). Acycle: Time-series analysis software for paleoclimate research and education. *Computers & geosciences*, 127, 12-22.

Linsley, B. K., Wellington, G. M., & Schrag, D. P. (2000). Decadal sea surface temperature variability in the subtropical South Pacific from 1726 to 1997 AD. *Science*, 290(5494), 1145-1148

Liu, Q., Roberts, A. P., Larrasoana, J. C., Banerjee, S. K., Guyodo, Y., Tauxe, L., & Oldfield, F. (2012). Environmental magnetism: principles and applications. *Reviews of Geophysics*, *50*(4).

Long, A., Benz, B. F., Donahue, D. J., Jull, A. T., & Toolin, L. J. (1989). First direct AMS dates on early maize from Tehuacán, Mexico. *Radiocarbon*, *31*(3), 1035-1040.

Lozano-García, M. S., Ortega-Guerrero, B., Caballero-Miranda, M., & Urrutia-Fucugauchi, J. (1993). Late Pleistocene and Holocene paleoenvironments of Chalco lake, central Mexico. *Quaternary Research*, 40(3), 332-342.

Lozano-García, S., Torres-Rodríguez, E., Ortega, B., Vázquez, G., & Caballero, M. (2013). Ecosystem responses to climate and disturbances in western central Mexico during the late Pleistocene and Holocene. *Palaeogeography, Palaeoclimatology, Palaeoecology*, *370*, 184-195.

Luhr, J. F., Kimberly, P., Siebert, L., Aranda-Gómez, J. J., Housh, T. B., & Mattietti, G. K. (2006). México's Quaternary volcanic rocks: Insights from the MEXPET petrological and geochemical database. *Geological Society of America Special Papers*, *402*, 1-44.

Magaña, V. O., Vázquez, J. L., Pérez, J. L., & Pérez, J. B. (2003). Impact of El Niño on precipitation in Mexico. *Geofísica internacional*, 42(3), 313-330.

Marchetto, A., Ariztegui, D., Brauer, A., Lami, A., Mercuri, A. M., Sadori, L., & Guilizzoni, P. (2015). Volcanic lake sediments as sensitive archives of climate and environmental change. In *Volcanic Lakes* (pp. 379-399). Springer, Berlin, Heidelberg.

Maxbauer, D. P., Feinberg, J. M., & Fox, D. L. (2016). MAX UnMix: A web application for unmixing magnetic coercivity distributions. *Computers & Geosciences*, *95*, 140-145.

Mayewski, P. A., Rohling, E. E., Stager, J. C., Karlén, W., Maasch, K. A., Meeker, L. D., & Lee-Thorp, J. (2004). Holocene climate variability. *Quaternary research*, *62*(3), 243-255.

McGee, D., Donohoe, A., Marshall, J., & Ferreira, D. (2014). Changes in ITCZ location and cross-equatorial heat transport at the Last Glacial Maximum, Heinrich Stadial 1, and the mid-Holocene. *Earth and Planetary Science Letters*, 390, 69-79.

Metcalfe, S. E., Barron, J. A., & Davies, S. J. (2015). The Holocene history of the North American Monsoon: 'known knowns' and 'known unknowns' in understanding its spatial and temporal complexity. *Quaternary Science Reviews*, 120, 1-27.

Metcalfe, S. E., Jones, M. D., Davies, S. J., Noren, A., & MacKenzie, A. (2010). Climate variability over the last two millennia in the North American Monsoon region, recorded in laminated lake sediments from Laguna de Juanacatlán, Mexico. *The Holocene*, *20*(8), 1195-1206

Metcalfe, S. E., Street-Perrott, F. A., Brown, R. B., Hales, P. E., Perrott, R. A., & Steininger, F. M. (1989). Late Holocene human impact on lake basins in Central Mexico. *Geoarchaeology*, 4(2), 119-141.

Mingram, J., Stebich, M., Schettler, G., Hu, Y., Rioual, P., Nowaczyk, N., Liu, J. (2018). Millennial-scale East Asian monsoon variability of the last glacial deduced from annually laminated sediments from Lake Sihailongwan, N.E. China. *Quaternary Science Reviews*, 201, 57–76. https://doi.org/10.1016/J.QUASCIREV.2018.09.023

Minobe, S. (1999). Resonance in bidecadal and pentadecadal climate oscillations over the North Pacific: Role in climatic regime shifts. *Geophysical Research Letters*, 26(7), 855-858.

Mitchell, D. L., Ivanova, D., Rabin, R., Brown, T. J., & Redmond, K. (2002). Gulf of California sea surface temperatures and the North American monsoon: Mechanistic implications from observations. *Journal of Climate*, 15(17), 2261-2281.

Mohtadi, M., Prange, M., & Steinke, S. (2016). Palaeoclimatic insights into forcing and response of monsoon rainfall. *Nature*, 533(7602), 191.

Murphy GP (1986). The chronology, pyroclastic stratigraphy and petrology of the Valle de Santiago Maar Field. Central Mexico. University of California, Berkeley

Muxworthy, A. R., & Roberts, A. P. (2007). Muxworthy, A R, Roberts, A P, First-order reversal curve (FORC) diagrams, In: Gubbins, D and Herrero-Bervera, E, editor, Encyclopedia of Geomagnetism and Paleomagnetism, Springer, 2007, Pages: 266 - 272

Nowaczyk, N. R. (2011). Dissolution of titanomagnetite and sulphidization in sediments from Lake Kinneret, Israel. *Geophysical Journal International*, 187(1), 34-44.

Nowaczyk, N. R., Haltia, E. M., Ulbricht, D., Wennrich, V., Sauerbrey, M. A., Rosén, P., Vogel, H., Francke, A., MeyerJacob, C., Andreev, A. A., & Lozhkin, A. V. (2011) Chronology of Lake El'gygytgyn sediments a combined magnetostratigraphic, palaeoclimatic and orbital tuning study based on multiparameter analyses, Clim. Past, 9, 2413–2432

Nowaczyk, N. R., Minyuk, P., Melles, M., Brigham-Grette, J., Glushkova, O., Nolan, & M.,Forman, S. L. (2002). Magnetostratigraphic results from impact crater Lake El'gygytgyn, northeastern Siberia: a 300 kyr long high-resolution terrestrial palaeoclimatic record from the Arctic. Geophysical Journal International, 150(1), 109–126. https://doi.org/10.1046/j.1365-246X.2002.01625.x

O'Hara, S. L., Metcalfe, S. E., & Street-Perrott, F. A. (1994). On the arid margin: the relationship between climate, humans and the environment. A review of evidence from the highlands of central Mexico. *Chemosphere*, 29(5), 965-981.

O'Hara, S. L., Street-Perrott, F. A., & Burt, T. P. (1993). Accelerated soil erosion around a Mexican highland lake caused by prehispanic agriculture. *Nature*, 362(6415), 48.

Ojala, a. E. K., Francus, P., Zolitschka, B., Besonen, M., & Lamoureux, S. F. (2012). Characteristics of sedimentary varve chronologies - *A review. Quaternary Science Reviews*, 43, 45–60.https://doi.org/10.1016/j.quascirev.2012.04.006

Orozco, F., & Madinaveitia, A. (1941). Estudio químico de los lagos alcalinos. *An. Inst. Biol. Univ. Nal. Autón. Méx*, *12*, 429-438.

Overpeck, J. T., & Cole, J. E. (2006). Abrupt change in Earth's climate system. *Annu. Rev. Environ. Resour.*, *31*, 1-31.

Özdemir, Ö., & Dunlop, D. J. (1997). Effect of crystal defects and internal stress on the domain structure and magnetic properties of magnetite. *Journal of Geophysical Research: Solid Earth,* 102(B9), 20211-20224

Park, J. J. (2005). Holocene environmental change and human impact in Hoya Rincon de Parangueo, Guanajuato, Mexico. *The Korean Journal of Ecology*, 28(5), 245-254.

Park, J., Byrne, R., Böhnel, H., Garza, R. M., & Conserva, M. (2010). Holocene climate change and human impact, central Mexico: a record based on maar lake pollen and sediment chemistry. *Quaternary Science Reviews*, 29(5-6), 618-632.

Park, J., Byrne, R., & Böhnel, H. (2019). Late Holocene Climate Change in Central Mexico and the Decline of Teotihuacan. *Annals of the American Association of Geographers*, 109(1), 104-120.

Peterson LC, Haug GH, Hughen KA, R.hl U (2000) Rapid changes in the hydrologic cycle of the tropical Atlantic during the last glacial. *Science* 290:1947–1951. doi:10.1126/science. 290.5498.1947

Peterson, L. C., & Haug, G. H. (2006). Variability in the mean latitude of the Atlantic Intertropical Convergence Zone as recorded by riverine input of sediments to the Cariaco Basin (Venezuela). *Palaeogeography, Palaeoclimatology, Palaeoecology*, 234(1), 97-113.

Philippsen, B., & Heinemeier, J. (2013). Freshwater reservoir effect variability in northern Germany. *Radiocarbon*, 55(3), 1085-1101.

Piperno, D. R., Moreno, J. E., Iriarte, J., Holst, I., Lachniet, M., Jones, J. G., Ranere, A. J., & Castanzo, R. (2007). Late Pleistocene and Holocene environmental history of the Iguala Valley, central Balsas watershed of Mexico. *Proceedings of the National Academy of Sciences* 104: 11874–11881

Piperno, D. R., Ranere, A. J., Holst, I., Iriarte, J., & Dickauc, R. (2009). Starch grain and phytolith evidence for early ninth millennium BP maize from the central Balsas River valley, Mexico. *Proceedings of the National Academy of Sciences of the United States of America* 106: 5019–5024.

Pollard, H. P. (2000). Tarascan external relationships. Greater Mesoamerica. The Archaeology of West and Northwest Mexico, University of Utah Press, Salt Lake City, 71-80.

Poore, R., Dowsett, H., Verardo, S., Quinn, T., (2003).Millennial- to century-scale variability in Gulf of Mexico Holocene climate records. *Paleoceanography* 18, 1048

Pope, K. O., Pohl, M. E., Jones, J. G., Lentz, D. L., Von Nagy, C., Vega, F. J., & Quitmyer, I. R. (2001). Origin and environmental setting of ancient agriculture in the lowlands of Mesoamerica. *Science,* 292(5520), 1370-1373.

Porter, M. N. (1956). Excavations at Chupícuaro, Guanajuato, Mexico. *Transactions of the American Philosophical Society*, 515-637.

R Development Core Team (2010). R: A Language and Environment for Statis- tical Computing. R Foundation for Statistical Computing, Vienna, Austria, ISBN 3-900051-07-0. http://www.R-project.org.

Ramsey, C. B. (2001). Development of the radiocarbon calibration program. *Radiocarbon*, 43(2A), 355-363.

Rasmussen, S. O., Bigler, M., Blockley, S. P., Blunier, T., Buchardt, S. L., Clausen, H. B., & Gkinis, V. (2014). A stratigraphic framework for abrupt climatic changes during the Last Glacial period based on three synchronized Greenland ice-core records: refining and extending the INTIMATE event stratigraphy. *Quaternary Science Reviews*, *106*, 14-28.

Reimer, P. J., Bard, E., Bayliss, A., Beck, J. W., Blackwell, P. G., Bronk Ramsey, C., Grootes, P. M., Guilderson, T. P., Haflidason, H., Hajdas, I., HattŽ, C., Heaton, T. J., Hoffmann, D. L., Hogg, A. G., Hughen, K. A., Kaiser, K. F., Kromer, B., Manning, S. W., Niu, M., Reimer, R. W., Richards, D. A., Scott, E. M., Southon, J. R., Staff, R. A., Turney, C. S. M., & van der Plicht, J. (2013). IntCal13 and Marine13 Radiocarbon Age Calibration Curves 0-50,000 Years cal BP. *Radiocarbon*, 55(4).

Rincón, N., 2005, Estratigrafía del cráter de explosión Hoya La Alberca. Ciudad Madero, Tamaulipas, México, Instituto Tecnológico de Ciudad Madero, tesis ingeniero geólogo, 78 p.

Roberts, A. P. (2015). Earth-Science Reviews Magnetic mineral diagenesis. *Earth Science Reviews*, 151, 1–47. https://doi.org/10.1016/j.earscirev.2015.09.010

Roberts, A.P., Chang, L., Rowan, C.J., Horng, C.S., Florindo, F., (2011). Magnetic properties of sedimentary greigite (Fe_3S_4): an update. *Rev. Geophys*. 49, RG1002.

Roberts, A. P., Cui, Y., & Verosub, K. L. (1995). Wasp-waisted hysteresis loops: Mineral magnetic characteristics and discrimination of components in mixed magnetic systems. *Journal of Geophysical Research: Solid Earth*, 100(B9), 17909-17924.

Roberts, N. (2013). The Holocene: an environmental history. John Wiley & Sons

Rosenswig, R. M. (2015). A Mosaic of Adaptation: The Archaeological Record for Mesoamerica's Archaic Period. *Journal of Archaeological Research*, 23(2), 115–162. https://doi.org/10.1007/s10814-014-9080-x

Rosenswig, R. M. (2015). A mosaic of adaptation: The archaeological record for Mesoamerica's archaic period. *Journal of Archaeological Research*, 23(2), 115-162.

Saint-Charles Zetina, J. C., Anzures, C. V., & Limón, F. F. (2010). Tiempo y Región. Estudios Históricos y Sociales. Estudios Históricos y Sociales, Vol 1. Municipio de Querétaro,INAH,UAQ, México

Saint-Charles, J. C. (2007). "La trinidad: un emplazamiento defensivo del Epiclásico en Tequisquiapan". Tiempo Y Región, Estudios Históricos y Sociales, Vol 1. Municipio de Querétaro,INAH,UAQ, México. 19-59

Saint-Charles, J. C., Viramontes, C., & Fenoglio,F. (2010). "El Rosario, Querétaro: un enclave teotihucano en el Centro Norte". Tiempo Y Región, Estudios Históricos y Sociales, Vol 4. Municipio de Querétaro, INAH, UAQ, México. 7-13

Sanders, W.T., Parsons, J.R., & Santley, R.S., (1979). The Basin of Mexico: Ecological Processes in the Evolution of a Civilization. Academic Press, New York, p. 561.

Sauer, C. O. (1941). Foreword to historical geography. *Annals of the Association of American Geographers*, 31(1), 1-24.

Schneider, T., Bischoff, T., & Haug, G. H. (2014). Migrations and dynamics of the intertropical convergence zone. *Nature*, 513(7516), 45.

Servicio Meteorológico Nacional Comisión Nacional del Agua del Servicio Meteorológico Nacional, http://smn.cna.gob. mx/productos/normales/estacion/normales

Shlens, J. (2014). A tutorial on principal component analysis. arXiv preprint arXiv:1404.1100.

Sluijs, A., Schouten, S., Pagani, M., Woltering, M., Brinkhuis, H., Damsté, J. S. S.,& Matthiessen, J. (2006). Subtropical Arctic Ocean temperatures during the Palaeocene/Eocene thermal maximum. *Nature*, *441*(7093), 610.

Small, E. E. (2001). The influence of soil moisture anomalies on variability of the North American monsoon system. *Geophysical research letters*, *28*(1), 139-142

Snowball, I. F. (1993). Geochemical control of magnetite dissolution in subarctic lake sediments and the implications for environmental magnetism. *Journal of Quaternary Science*, 8(4), 339-346.

Stabel, H. H. (1986). Calcite precipitation in Lake Constance: Chemica equilibrium, sedimentation, and nucleation by algae 1. *Limnology and Oceanography*, 31(5), 1081-1094.

Stahle, D. W., Burnette, D. J., Díaz, J. V., Heim, R. R., Fye, F. K., Paredes, J. C., & Cleaveland, M. K. (2012). Pacific and Atlantic influences on Mesoamerican climate over the past millennium. Climate Dynamics, 39(6), 1431-1446.

Stahle, D. W., Diaz, J. V., Burnette, D. J., Paredes, J. C., Heim, R. R., Fye, F. K., & Stahle, D. K. (2011). Major Mesoamerican droughts of the past. *Geophys. Res*. Lett., 38, L05703, doi:10.1020/2010GL046472.

Stanley, J. D., Krom, M. D., Cliff, R. A., & Woodward, J. C. (2003). Short contribution: Nile flow failure at the end of the Old Kingdom, Egypt: strontium isotopic and petrologic evidence. *Geoarchaeology*, *18*(3), 395-402.

Staubwasser, M., & Weiss, H. (2006). Holocene climate and cultural evolution in late prehistoric–early historic West Asia. *Quaternary Research*, 66(3), 372-387.

Staubwasser, M., Sirocko, F., Grootes, P. M., & Segl, M. (2003). Climate change at the 4.2 ka BP termination of the Indus valley civilization and Holocene south Asian monsoon variability. *Geophysical Research Letters*, 30(8).

Steinhilber, F., Beer, J., & Fröhlich, C. (2009). Total solar irradiance during the Holocene. *Geophysical Research Letters*, 36(19).

Striewski, B., Mayr, C., Flenley, J., Naumann, R., Turner, G., & Lücke, A. (2009). Multi-proxy evidence of late Holocene human-induced environmental changes at Lake Pupuke, Auckland (New Zealand). *Quaternary International*, 202(1-2), 69-93.

Super, John C. (1988). Food, conquest, and colonization in sixteenth-century Spanish America. Albuquerque: University of New Mexico Press.

Thompson, L. G., Mosley-Thompson, E., Davis, M. E., Henderson, K. A., Brecher, H. H., Zagorodnov, V. S.& Beer, J. (2002). Kilimanjaro ice core records: evidence of Holocene climate change in tropical Africa. *Science,* 298(5593), 589-593.

Ting, M., Kushnir, Y., Seager, R., & Li, C. (2011). Robust features of Atlantic multi-decadal variability and its climate impacts. *Geophysical Research Letters*, *38*(17).

Trombold, C. D., & Israde-Alcantara, I. (2005). Paleoenvironment and plant cultivation on terraces at La Quemada, Zacatecas, Mexico: the pollen, phytolith and diatom evidence. *Journal of Archaeological Science*, 32(3), 341-353.

Trouet, V., Esper, J., Graham, N. E., Baker, A., Scourse, J. D., & Frank, D. C. (2009). Persistent positive North Atlantic Oscillation mode dominated the medieval climate anomaly. *Science*, 324(5923), 78-80

Urrea, G., & Sabater, S. (2009). Epilithic diatom assemblages and their relationship to environmental characteristics in an agricultural watershed (Guadiana River, SW Spain). *Ecological Indicators*, 9(4), 693-703.

Usoskin, I. G., Gallet, Y., Lopes, F., Kovaltsov, G. A., & Hulot, G. (2016). Solar activity during the Holocene: the Hallstatt cycle and its consequence for grand minima and maxima. Astronomy & Astrophysics, 587, A150.

Viramontes A. (2008). El Centro Norte de México en el contexto mesoamericano. Tiempo y Región, Volumen II, 13-24.

Voigt, R., Grüger, E., Baier, J., & Meischner, D. (2008). Seasonal variability of Holocene climate: a palaeolimnological study on varved sediments in Lake Jues (Harz Mountains, Germany). *Journal of Paleolimnology*, 40(4), 1021-1052.

Wahl, D., Hansen, R. D., Byrne, R., Anderson, L., & Schreiner, T. (2016). Holocene climate variability and anthropogenic impacts from Lago Paixban, a perennial wetland in Peten, Guatemala*. Global and Planetary Change*, 138, 70-81.

Walker, M. J. C., Berkelhammer, M., Björck, S., Cwynar, L. C., Fisher, D. A., Long, A. J.,Weiss, H. (2012). Formal subdivision of the Holocene Series/Epoch: A Discussion Paper by a Working Group of INTIMATE (Integration of ice-core, marine and terrestrial

records) and the Subcommission on Quaternary Stratigraphy (International Commission on Stratigraphy). *Journal of Quaternary Science*, 27(7), 649–659.

Wanner, H., Beer, J., Bütikofer, J., Crowley, T. J., Cubasch, U., Flückiger, J., & Küttel, M. (2008). Mid-to Late Holocene climate change: an overview. *Quaternary Science Reviews,* 27(19-20), 1791-1828.

Warren, J. B. (1971). Fray Jerónimo de Alcalá: author of the Relación de Michoacán?. *The Americas*, 27(3), 307-32.

Weiss, H. (2016). Global megadrought, societal collapse and resilience at 4 . 2-3 . 9 ka BP across the Mediterranean and west Asia, 24(2), 4–5.https://doi.org/10.22498/pages.24.2.62

Weiss, H., Courty, M. A., Wetterstrom, W., Guichard, F., Senior, L., Meadow, R., & Curnow, A. (1993). The Genesis and Collase of Third Millenium North Mesopotamian Civilization. *Science*, 261(August), 995–1004.https://doi.org/10.1126/science.261.5124.995

Wetzel, R. G. (2001). Limnology: lake and river ecosystems. gulf professional publishing.

Whitmore, T. M., & Turner, B. L. (1992). Landscapes of cultivation in Mesoamerica on the eve of the conquest. *Annals of the Association of American Geographers,* 82(3), 402-425.

Winter, A., Miller, T., Kushnir, Y., Sinha, A., Timmermann, A., Jury, M. R., & Edwards, R. L. (2011). Evidence for 800 years of North Atlantic multi-decadal variability from a Puerto Rican speleothem. *Earth and Planetary Science Letters*, 308(1-2), 23-28.

Wright, D. K. (2017). Accuracy vs. precision: Understanding potential errors from radiocarbon dating on African landscapes. *African Archaeological Review*, 34(3), 303-319.

Wurtzel, J. B., Black, D. E., Thunell, R. C., Peterson, L. C., Tappa, E. J., & Rahman, S. (2013). Mechanisms of southern Caribbean SST variability over the last two millennia. *Geophysical Research Letters*, 40(22), 5954-5958.

Xie, S. P., & Carton, J. A. (2004). Tropical Atlantic variability: Patterns, mechanisms, and impacts. *Earth Climate: The Ocean-Atmosphere Interaction, Geophys. Monogr*, *147*, 121-142.

Zamora Ayala, V. (2004). Asentamientos prehispánicos en el Estado de Guanajuato. Acta Universitaria, 14(2), 25-44.

Zepeda Garcia, G., Barrales D. (2008). Arqueología e identidad en Cañada de la Virgen, Guanajuato. Tiempo y Región, Volumen II, 215-238.

Zhao, X., Heslop, D., & Roberts, A. P. (2015). A protocol for variable-resolution first-order reversal curve measurements. *Geochemistry, Geophysics, Geosystems*, 16(5), 1364-1377.

Zolitschka, B., Francus, P., Ojala, A. E. K., & Schimmelmann, A. (2015). Varves in lake sediments e a review. *Quaternary Science Reviews*, 117, 1–41. https://doi.org/10.1016/j.quascirev.2015.03.019

Appendix

Appendix 1- Water chemistry composition of La Alberca lake (Alcocer and Bernal-Brooks, 2010).

Lake Name	Na^{+}	K^{+}	Ca^{2+}	Mg^{2+}	SO^{2-}_{4}	Cl^{-}	B	SiO_2	CO^{2-}_{3}	HCO^{-}_{3}	Bal %
La Alberca	3102	530	1.7	100	536	2400	13	11.3	2913	1185	-10.9

Appendix 2- Saturated and oversaturate mineral in the lake water (Alcocer and Bernal-Brooks, 2010).

Lake Name	Chaldony	Cristobalite	Quartz	Silica gel	SiO_2
La Alberca	0.79	0.81	1.19	0.26	-0.03

Appendix 3- Phytoplankton, chlorophyll, and primary production (Alcocer and Bernal-Brooks, 2010).

Lake Name	Dominant Taxa
La Alberca	Oscillatoria sp, Actinastrum sp

Appendix 4- Zooplankton density and composition (Alcocer and Bernal-Brooks, 2010).

Lake Name	Dominant Taxa
La Alberca	Diaptomus alburquerquensis, Hexarthra polyodonta, Brachionus inermis Alona

Appendix 5- Benthic macroinvertebrates (Alcocer and Bernal-Brooks, 2010).

Lake Name	Dominating organisms
La Alberca	Chaoborus sp. Lumbriculus

Appendix 6- Fish fauna (Alcocer and Bernal-Brooks, 2010).

Lake Name	Dominant taxa
La Alberca	Alloophorus robustus, Goodea atripinnis, Chirostoma bartoni, Oreochromis mossambicus

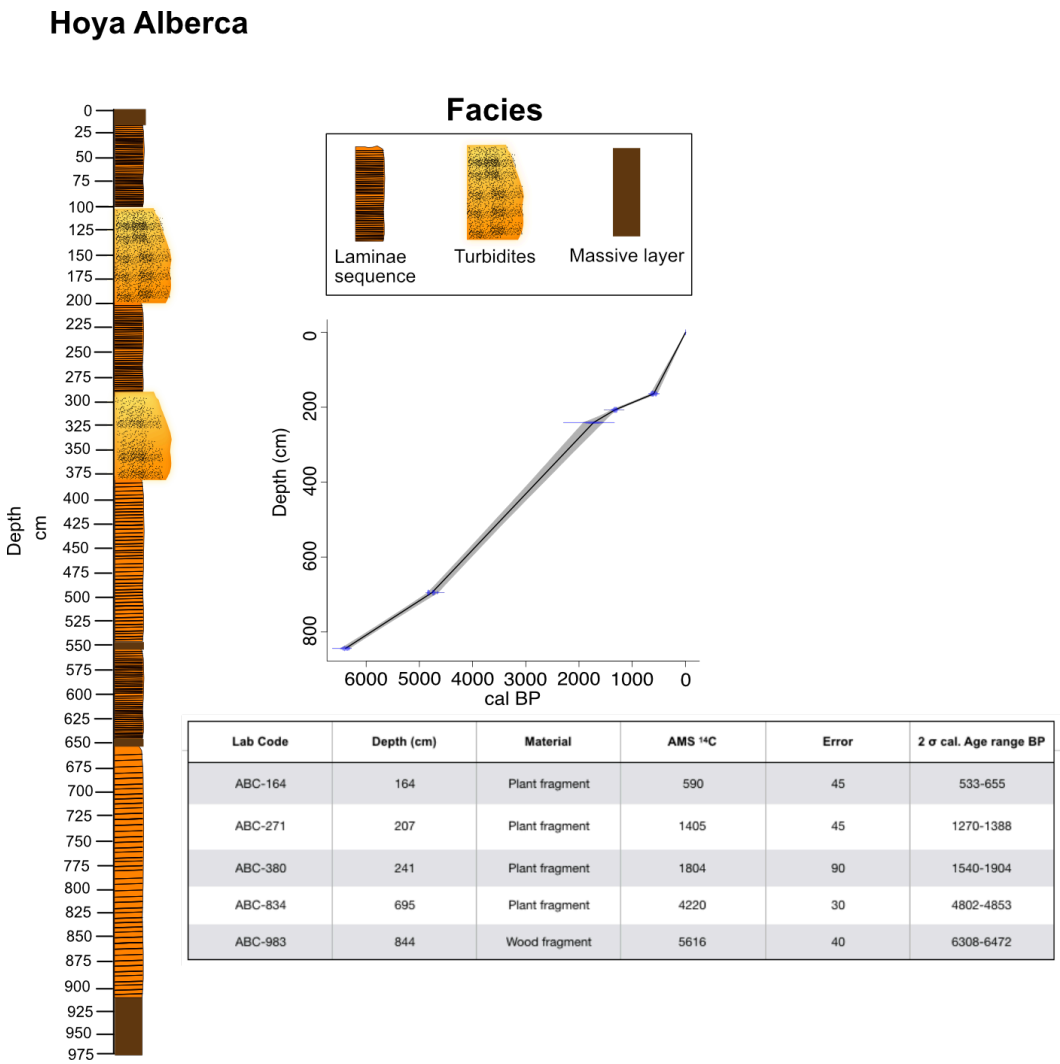

Lab Code	Depth (cm)	Material	AMS ^{14}C	Error	2 σ cal. Age range BP
ABC-164	164	Plant fragment	590	45	533-655
ABC-271	207	Plant fragment	1405	45	1270-1388
ABC-380	241	Plant fragment	1804	90	1540-1904
ABC-834	695	Plant fragment	4220	30	4802-4853
ABC-983	844	Wood fragment	5616	40	6308-6472

Appendix 7- Stratigraphic column of the Hoya Alberca core, main sedimentary facies, age model and five AMS ^{14}C data acquired from terrestrial plants and fragments of wood.

Appendix 8- AMS ^{14}C ages from core Alberca Rojo and its respective equivalent depth on core Alberca Azul with turbidites and without turbidites.

Core	Sample	Sample depth (cm)	Equivalent depth on master core (AZ)	Equivalent depth on master core (AZ) without turbidites
Rojo	A-1b2-1	150.1	192	168
	A-1b2-7	214	276	229
	A-2b2-3	401.6	438	355

Appendix 9- XRD data for different depths from La Alberca maar lake core (AZ).

	Depth (cm)	8	80	158	166	191	234	268	311	334	435	496	592	643	792
Alberca minerals															
Aragonite		X	X	X	X	X	X	X	X	X	X	X	x	x	x
Anorthite		X		X		X			X	X				x	
Anorthoclase		X							X						
Albite				X	X	X		X		X		X		x	x
Monohydrocalcite		X													
Dolomite			X												
Cristobalite							X								
Ankerite			X												
Natrite			X												
Margarite					x		x	x				x			x

Appendix 10- Stratigraphic position and thickness of the ten turbidites removed from the master core Alberca Azul.

Turbidite number	Depth From (cm)	To (cm)	Thickness (cm)
1	22.5	25.3	2.8
2	44.3	48	3.7
3	170	187.5	17.5
4	218	241	23
5	285	321	36
6	479.5	484.5	5
7	486.5	497	10.5
8	509	519	10
9	622	624	2
10	633	634.5	1.5